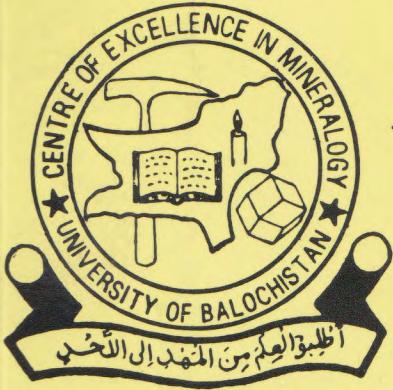


ISSN 0257 - 3660



ACTA MINERALOGICA PAKISTANICA

Volume 7

1993



**NATIONAL CENTRE OF EXCELLENCE IN MINERALOGY
(UNIVERSITY OF BALOCHISTAN), QUETTA, PAKISTAN**

ACTA MINERALOGICA PAKISTANICA

VOLUME 7, 1993

PATRON: D. K. RIAZ BALOCH

EDITOR: ABDUL HAQUE

ASSISTANT EDITORS: JAWED AHMAD
M. A. FAROOQI
KHALID MEHMOOD
MEHRAB KHAN

REFEREES FOR THE THIS VOLUME:

ABDUL FARAH, ISLAMABAD, PAKISTAN.
ABDUL HAQUE, NEC MINERALOGY, QUETTA, PAKISTAN.
AFTAB AHMAD BUTT, PUNJAB UNIVERSITY, LAHORE, PAKISTAN.
ANTHONY HALL, R.H.B., NEW COLLEGE, LONDON UNIVERSITY, UK.
DUANE M MOOR, ILLINOIS STATE GEOLOGICAL SURVEY, USA.
FAIZ AHMAD SHAMS, PUNJAB UNIVERSITY, LAHORE, PAKISTAN.
FAZAL UR REHMAN, P.A.E., MINERALS CENTRE, LAHORE, PAKISTAN.
GEORGE R. McCORMIC, IOWA UNIVERSITY, USA.
KHALIL A. MALLICK, KARACHI UNIVERSITY, PAKISTAN.
M. AZAM MALIK, O.G.D.C., ISLAMABAD, PAKISTAN.
MUBARIK ALI, QUAID-I-AZAM UNIVERSITY, ISLAMABAD, PAKISTAN.
MUHAMMAD ASHRAF, AJK UNIVERSITY, PAKISTAN.
MUHAMMAD TAHIR SHAH, NEC GEOLOGY, PESHAWAR, PAKISTAN.
MUMTAZUDDIN, QUETTA, PAKISTAN.
R. A. HOWIE, LONDON, UK.
R. A. KHAN TAHIRKHELI, PESHAWAR UNIVERSITY, PAKISTAN.
SHAMIM A. SIDDIQUI, BALOCHISTAN UNIVERSITY, QUETTA, PAKISTAN.
SHER BAHADUR, ESSO EXP. & PROD. PAK. Ltd. ISLAMABAD, PAKISTAN.
S. IQBAL MOHSIN, KARACHI UNIVERSITY, PAKISTAN.

ISSN 0257 — 3660

PRICE:

PREPAID ORDERS FROM PAKISTAN: RS. 100
OTHER COUNTRIES: U.S. \$ 12.00 OR U.K. £ 8.00
This price includes postage and handling charges.

Published in December each year.

Printed at **KASHMIR OFFSET PRESS, QUETTA, PAKISTAN.**

ACTA MINERALOGICA PAKISTANICA VOLUME 7, 1993

CONTENTS

- I. Strom generated turbidites of the lower Ludlow group (Late Silurian), Llangollen area, north Wales, United Kingdom.
ABDUL SALAM KHAN 3
- II. Proposed lithostratigraphic subdivision of Chilton limestone, Quetta District, Balochistan, Pakistan.
JAWED AHMAD, ABDUL HAQUE & MIAN HASSAN AHMAD 11
- III. Major metallic minerals of Sindh, Pakistan.
SYED AFZAL AHMAD 15
- IV. Petrology of different dykes of Sra-Salwat area, Muslim Bagh, District Qila-saifullah, Balochistan, Pakistan.
ABDUL HAQUE & MASOOD AQBAL 20
- V. Earthquakes and risks management in Pakistan.
MUBARAK ALI & ZULFIQAR AHMAD 24
- VI. Preparation of oriented clay mineral samples for X-ray diffraction analyses.
JAWED AHMAD & ABDUL HAQUE 35
- VII. Petrographic comments on Khewra trap, the Salt Range, Pakistan.
S. M. SHUAIB, SHAMIM A. SHEIKH & SHAHID NASEEM 38
- VIII. Dolomite reservoirs within Chilton range, south of Quetta District, Balochistan, Pakistan.
ABDUL HAQUE, JAWED AHMAD & MIAN HASSAN AHMAD 47
- IX. Measurement of spectral induced polarization on rock samples containing sulphide minerals.
S. W. H. NAQVI 49
- X. Clay minerals of Ghazig Formation from a section taken in Deghari valley, Mastung District, Balochistan, Pakistan.
JAWED AHMAD & ABDUL HAQUE 64
- XI. Skarization of the massive sulfide ores and associated rocks of the Pazang group in Besham area at the northern margin of Indo-Pakistan plate.
MUHAMMAD TAHIR SHAN 68
- XII. Petrology of the lava flow of Koh-i-Sultan, Chagai District, Balochistan, Pakistan.
MASOOD IQBAL, ABDUL HAQUE & KARAM KHAN 79
- XIII. A note on the chalcopyrite disease in sphalerite in the volcanic-hosted copper mineralization in Dir area, northern Pakistan.
MOHAMMAD TAHIR SHAH 82

PHOTOGRAPHS ON THE OUTSIDE COVER

Top: Field photograph (grid ref. 915072) taken on the western cliff of "Kargaz Peak" (▲ 5556), situated in the north-west of Ghot Shafi Muhammad (central south portion of teposheet No. 351/6), near 30 miles to the south-west of Khuzdar. Petrographic studies of the area where such photograph is taken by C.E.M, M.Phil student, Mr. Muhammad Ayub Baloch, Lecturer Geology Department, U.O.B, are still under investigation.

Bottom: Field photograph (grid ref. 912075) of "pillow lava" viewed on less altitude around the northern flank of Kargaz Peak (Top photo.).

STORM GENERATED TURBIDITES OF THE LOWER LUDLOW GROUP (LATE SILURIAN) LLANGOLLEN AREA, NORTH WALES, UNITED KINGDOM

ABDUL SALAM KHAN

Department of Geology, University of Balochistan, Quetta, Pakistan.

ABSTRACT: In the Llangollen are, the lower part of the Lower Ludlow Group comprises thin bedded siliciclastic (terrigenous) sandstone, siltstone, calcareous siltstone and mudstone. Four distinct facies are recognized on the basis of composition and grain size. Facies 1 is characterized by siliciclastic fine sandstones and silt stones that are almost entirely laminated matrix deficient and poorly graded, with rare intervening mudstone. Facies 2 is composed of calcareous siltstones, characterized by very fine lamination, sharp upper and lower boundaries, and laterally discontinuous, interbedded with facies 3 which is characterized by uniform mudstone. Facies 4 is characterized by thin bands of laminated hemipelagic mudstone. Proximal sequences are made up of facies 1 while distal sequences consist of facies 2, 3 and 4. Marked variations in composition, texture and sedimentary structures, lack of major slump bodies and paleogeographic position of these sequences indicate that storm and wind forced currents were important in the deposition of these sediments.

INTRODUCTION

In the Welsh Basin, the Wenlock-Ludlow (Middle to Late Silurian) succession is about 1500-3500m thick (Warren et al., 1984) and comprises sandstones, siltstones and mudstones with fine grained sediments dominant. Cummins (1957) proposed three subdivisions of the succession which are in ascending order: Denbigh Grits, Nantglyn Flags and Lower Ludlow Grits. The strata overlying Nantglyn Flags are here termed as the Lower Ludlow Group, broadly equivalent to the Lower Ludlow Grits of Cummins (1957). Here the term "Group" is preferred because the sequence is composed of different lithofacies ranging from sandstone dominated to mudstone dominated.

In the Llangollen area (Fig. 1a) the Lower Ludlow Group is about 900m thick and is in faulted contact with the Nantglyn Flags Group. Lithologically, the succession in this area differs from that of Denbigh Trough, being composed mainly of mudstone/siltstone with less sandstones. The lower part of the sequence is

characterized by thin beds of sandstone and siltstone with less common mudstone. It is about 225m thick and is exposed along the hillside near Tan y graig (SJ,14554042) 8km southeast of Llangollen. It constitutes upper part of the Glyn Dyfrdwy Group of Wills and Smith (1922). The sandstones contains calcareous cements which give buff "rottenstone" colour on weathering. Graptolites are very rare in these rocks, however *M. nilssoni* has been reported by Wills and Smith (1922). These beds are replaced by a sequence of calcareous siltstones and mudstones, Nant-y-Bache Group of Wills and Smith (1922). The contact between these lithofacies sequences is not exposed but it seems that this second sequence (calcareous siltstones and mudstones) may be the downcurrent equivalent of the first sequence (sandstone and siltstones) because both contain sand and detrital carbonate. The upper part of the Lower Ludlow Group in the Llangollen area is composed of siltstone/mudstone turbidites.

This paper discusses proximal to distal sedimentological changes in the Lower Ludlow Group sequences exposed in the west of

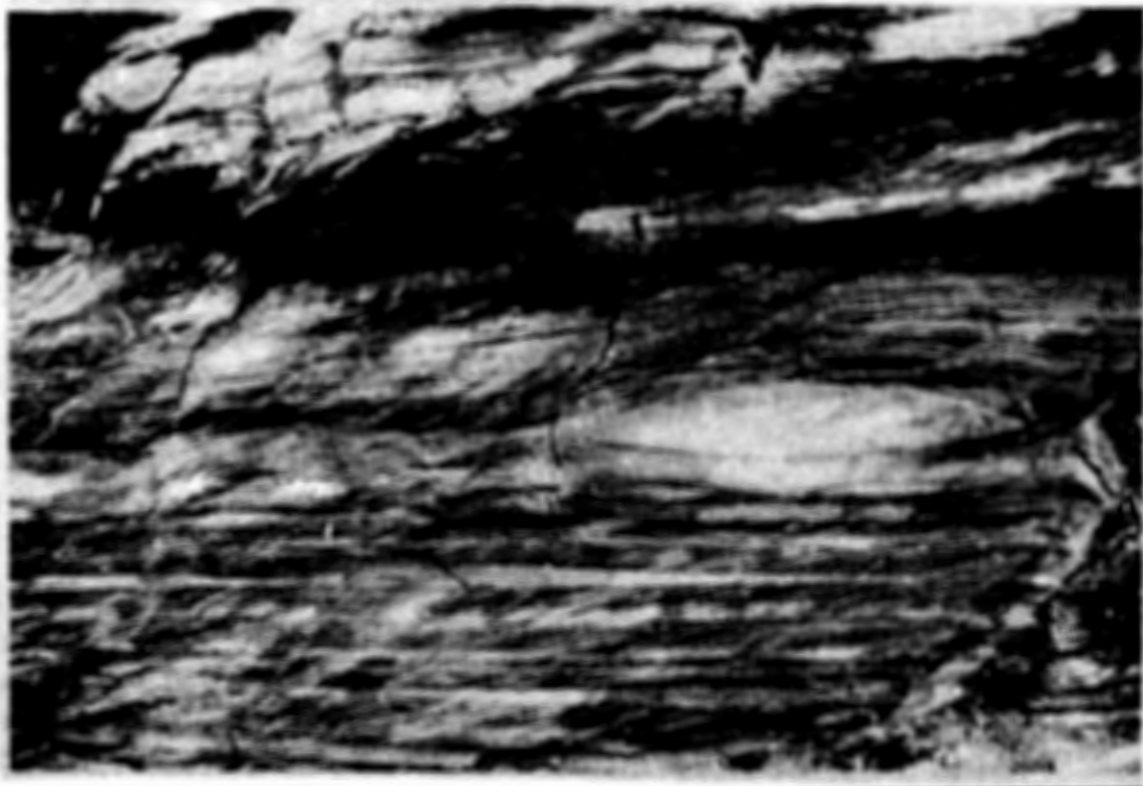


Plate 1. Field photograph of facies 1 (from proximal sequence) showing dome-shaped lens (internally low angle cross laminated), bounded by parallel laminated units (Lower Ludlow Group, 5km west of Llangollen, north Wales, SJ 14554044).



Plate 2. Field photograph showing lens-shaped, discontinuous and irregular calcareous bands (facies 2) interbedded with uniform mudstone (facies 3) (Lower Ludlow Group, 4km, west of Llangollen, North wales, SJ 18254374).

Llangollen, North Wales and determines depositional processes and environments of these sequences.

FACIES DESCRIPTIONS

Four facies are recognized in the Lower Ludlow Group of the Llangollen area. These are terrigenous sandstone/siltstone, calcareous siltstone, uniform mudstone, and laminated mudstone.

Facies 1 (Terrigenous sandstone)

This facies comprises siliciclastic sandstone beds with area interbedded mudstone (Fig.1b) and occurs in the proximal part of the sequence. It is composed of angular to subangular quartz and feldspar with some mica which generally are matrix free. Beds generally are bounded by parallel laminated units (similar to Bouma Tb division) at the bases and by slightly lenticular laminated units, draping them at the upper surface. Some times the overlying laminated unit extend down to the lower unit and makes it isolate from the next one (Plate 1). This looks like small hummocky stratification (Dot and Bourgeois, 1982). It consists of asymmetrical ripples internally cross laminated which are lenticular, irregular and undulose with sharp, erosive and flat bases. They range from less than 1cm to several centimetres in thickness and from few to tens of centimetres long. Some of the ripples seem to be climbing on one another. The angle of the foreset laminae is quite variable from few degrees to more than 25 degrees and generally are tangential to the lower boundry. In some cases, laminae of the stoss side have been eroded, only they are preserved on the less side indicating no net deposition. Parallel lamination (Plate 1) is very common in this facies and occurs both as isolated bed and in association with other units. Thickness of parallel laminated units vary from less than 1cm up to 10cm. This unit is similar to the laminated division of Bouma

(Tb and Td).

Facies 2 (Calcareous Siltstones)

This facies is present on both sides of Derwen palaeo-submarine high. It occurs interbedded with uniform mudstone (Fig. 1c) and is very common in the distal part of the sequence.

The most important, prominent and widespread feature of this is lens-shaped units ranging in size from 2cm to 25cm in length and 1cm to 8cm in thickness, separated from each other from few centimetres to 100cm both in horizontal and vertical distance that occur with irregular spacing in vertical sequence and are discontinuous laterally within a short distance. Individual beds can be seen to wedge out when traced few meters. This irregular, discontinuous and undulose nature of this facies produce conspicuous variations in bed thickness from place to place. The facies comprises very fine sand to silt size carbonate sediments that weathers to buff colour. They are internally laminated, generally showing low angle cross lamination, tangential to the lower boundry. The laminations are extremely fine which can rarely be seen in hand specimen, however they are quite clear in thin sections and X-radiographs and generally defined by thin streaks of opaque minerals. In some cases, there is segregated concentration of quartz and opaque minerals at the base of these calcareous lenses and show red staining, probably due to oxidation of pyrite.

Facies 3 (Uniform Mudstone)

This facies occurs in the distal part of the sequence interbedded with facies 2 (Calcareous Siltstone) and consists of thin to medium (from 2cm to 20cm) bedded mudstone. The bedding can only be distinguished by the intervening calcareous siltstone. Due to pinchingout and swelling up of the calcereous siltstone, beds are not constant in thickness laterally. Generally they have sharp boundries with the calcareous siltstone or very rapid

transition from calcareous siltstone to overlying mudstone. Generally in polish slabs, this facies is structureless and uniform, however faintly and vaguely lamination can be seen in X-radiograph and thin section. In some cases, this facies appears to be bioturbated which can only be seen in thin section and X-radiograph and this is represented by vague swirling and partially distortion of lamination. Under microscope, it is well sorted and ungraded to slightly graded.

Facies 4 (Laminated Mudstone)

This facies occurs only in the distal sequences and is interbedded with the facies 3 (uniform mudstone). It makes not more than 5% of the total sequence. The thickness of individual layers varies from millimeter scale to 5cm (Plate 2) which are laterally constant and show no obvious pinching out and swelling. It consists of very fine lamination averaging 2 to 4 laminae per millimeter (Khan & Kelling, 1992). Individual laminae can only be identified in X-radiograph. The origin of this facies has been discussed (Khan & Kelling, 1992).

DISCUSSION

In geological records, most of the turbidity currents seem to have been generated from large slumps (caused by rapid deposition of sediments on slope and/or instability of slope). The ingredients for such type of currents are slumps, slide and evidence of rapid deposition. All these ingredients are missing here. Density currents may also be generated by major storm activities (Hamblin and Walker, 1979).

The sedimentary structures, similar to that of Bouma (1962) Tbcd divisions, identified in these facies suggest deposition under waning flow conditions. Previously these sequence (throughout Wales) have been interpreted as turbidites (Cummins, 1959). Recently Tyler and Woodcock (1987) described, the coeval sequences from the central Wales (generally identical to this facies) as "distal storm deposits".

During this study, these rocks were studied throughout Wales, with special emphasize on the rocks of the Llangollen area, and marked variation in composition, bed thickness, type and sequence of sedimentary structures and grain size were observed from proximal to distal part of the sequence. All these variations are consistent with slump generated turbidity flow (Macdonald, 1986), and storm and wind-forced gravity flow (Kreisa, 1981; Brenchley, 1985), but if compared in detail, storm deposits are distinct from slump turbidites (Kreisa, 1981).

To evaluate the importance and dominance of these mechanisms in the deposition of these sequences, each feature is discussed in detailed.

Compositional variation: There is marked difference in composition from terrigenous rich sediments in the proximal part of the facies to carbonate rich sediments in the distal part. This segregation is more consistent with storm activity. During a storm period, sediments on the shoreface was resuspended and carried downslope under the influence of gravity. The terrigenous sediments (heavier) were settled after being transported for short distance. Under a turbulence flow, such compositional segregation is unlikely because it can carry the heavy sediments through its turbulence.

Lateral variation in sedimentary structures: Lateral variation in sedimentary structures can be seen within few metres distance. Beds with lateral persistent in sedimentary structures are also common, but many of them show lateral irregularity in sedimentary structures, merging into one another. This may be the result of local resedimentation and storm activity. Parallel lamination is not perfectly planar and thickens and thins slightly. Parallel laminated units, draping the lens-shaped structure (Plate 1) are broadly lenticular and undulatory.

Discontinuity and lateral variation in bed thickness: Turbidite deposits do show variation in bed thickness from proximal to distal part of

the sequence which is gradual and systematic. But, the calcareous siltstone facies is quite irregular in thickness and discontinuous laterally, showing abrupt pinching out and swelling up within one meter space (Plate 2) and this is a very common feature of this facies. Some of them just wedged out laterally.

Lag concentration: The lens-shaped calcareous units generally contain shell and opaque mineral concentration at the base showing no grading or very poorly graded, overlain by internally cross laminated units. This seems to be the bottom current reworking rather than fallout from waning density flow.

Relation with the mud-partings: The interbedded mud-partings are rarely preserved in the proximal part of the sequence (Fig. 1b), but in the distal part of the sequence, the calcareous siltstone facies is interbedded with thick bedded uniform mudstone facies. The boundaries between calcareous siltstone facies and uniform mudstone facies are generally sharp or show abrupt transition from the calcareous siltstone to overlying mudstone suggesting rapid deposition of calcareous siltstone, followed by slow suspension of sediments forming uniform mudstone beds. In case of turbidites, thin bedded fine grained deposits show very gradual continuity from basal coarser sediments to overlying finer sediments.

The absence of mud-parting in the proximal part of the sequence may indicate frequent events of storm stirring, or the next event having been powerful enough to remove the overlying mudstone. Due to no or very shallow scouring, the second interpretation is less probable. In case of turbidites, amalgamation in thin bedded deposits is unlikely.

Palaeogeographic position: As described above, these deposits occur along the slope on the both sides of the Derwen Hills which is thought to be palaeo-submerged ridge between Central and North Wales. In the geological records, most of the turbidity currents are related with slumps, in

which downslope moving flow accelerates and turn into turbulent flow (Hampton, 1972). The absence of associated slumped beds suggests that the palaeo-slope was too gentle to generate slump-generated density flows.

INTERPRETATIONS

All these features indicate that these sediments were deposited on a gentle and relatively shallow slope. It is suggested that storms were important in the formation of these deposits. Hamblin and Walker (1979) proposed that storm may generate density currents and suggested that there is "an intimate relationship between storms, generation of density currents, and the molding of density current deposits into hummocky cross stratification under the influence of continuing wave surge from the storms". It is believed that sediments on the lower shoreface of the Derwen palaeo-high were resuspended by storm surge or ebb mechanism (Brenchley, 1985). The coarser sediments (mainly terrigenous sand and silt) were settled down rapidly after moving a short distance near the shore, just below wave base producing thin laminated and graded beds without intervening mudstone (facies 1) and then reworked by currents generating rippled cross laminations. Frequently, either they were reworked by weak waves or strong currents, producing lens-shaped structures, showing curved laminae and internal truncation which give impression of small scale hummocky type stratification (Dott and Bourgeois, 1982). If these are a kind of micro-hummocky stratification, then they represent weak wave generated storm. The lens-shaped structures resemble starved ripples but probably are not because starved ripples are usually produced due to the scarcity of sediments (Stow and Bowen, 1980). Here these lens-shaped units are truncated and have been eroded by the overlying units. The finer suspended detritus, comprising calcareous silt and clay particles, slowly moved down the marginal slope, became decoupled into gravity flows, dominated by calcareous silt with subordinate siliclastic silt (facies 2) and suspended sediment clouds (clay particle),

deposits. The detached density flows (carrying calcareous silt particles) moving to areas of low gravitational potential and gained momentum from their excess density and behave as high velocity turbidity flows (Tyler and Woodcock, 1987), capable of scouring the underlying sediments as is evident from the erosive bases of the calcareous siltstone beds (facies 2). The slightly graded, faintly laminated and homogenous nature of the overlying mudstone (facies 3) suggest deposition from slowly moving, dilute could of density flow.

ACKNOWLEDGEMENTS

This paper is based on part of a Ph. D. thesis completed at Keele University, England under the supervision of Professor Gilbert Kelling under the tenure of a scholarship, sponsored by Ministry of Science and Technology, Government of Pakistan. ASK is grateful to the Ministry of Science and Technology, Government of Pakistan for awarding Postgraduate scholarship. Many thanks are due to Profeessor Gilbert Kelling for his supervision, guidance and help during this reserch and other staff members of the Department of geology, Keele University are also thanked for their help. The author is also thankful to the amonyous referee for his valuable comments.

REFERENCES

BOUMA, A. H (1962) Sedimentology of some Flysch deposits. Elsever, Amsterdam, P. 168.

BRENCHLEY, P. J. (1985) Storm influenced sandstone beds. *Modern Geology* 9, pp. 360-396.

CUMMINS, W. A. (1957) The Denbigh Grits: Wenlock greywackes in Wales. *Geol. Mag.* 94, pp. 433-451.

(1959) The lower Ludlow Grits in Wales, Liverpool and Manchester

Geol. Jour. 2, pp. 168-179

DOTT, R. H. & BOURGEIS, J. (1982) Hummocky stratification: significance of its variable bedding sequence. *Geol. Soc. Am. Bull.* 93, pp. 663-680

HAMBLIN, A. P. & WALKER, R. G. (1979) Storm dominated shallow marine deposits: The Fernei-Kootenay (Jurassic) transition, southern Rocky mountain *Can. J. Earth Sei.* 16, pp. 1673-2690.

HAMPTON, M. A. (1972) The role of subaqueous debris flow in generating turbidity currunt. *J. Sed. Pet.* 42, pp. 775-793.

KHAN, A. S. & KELLING. G. (1992) Discussion on laminated hemipelagic facies from the Wenlock and Ludlow of the Welsh Basin. *Jour. Geol. Soc. Lond.* 148. pp. 1145-1148.

KREISA, R. D. (1981) Storm -generated sedimentry structures in subtidal marine facies with examples from the Middle and Upper Ordovician of southwestern Virginia. *Jour. Sed. Petrol.* 51, pp. 823-848.

MACDONALD, D. I. M. (1986) Proximal to distal sedimentological variation in linear turbidite trough: implication for the fan model. *Sedimentology*, 33, pp. 243-259.

STOW, D. A. V. & BOWEN, A. J. (1980) Physical model for the transport and sorting of fine-grained sediments byturbidity currents *Sedimentology*, 27, pp. 31-46

TYLER, J. E. & WOODCOCK, N. H. (1987) Baily Hill Formation: Ludlow Series tubidites in the Welsh Borderland reinterpreted as distal storm deposit. *Geol. Jour.* 22. pp. 73-86

WARREN, P. T., PRICE, D., NUTT, M. I. J. & SMITH, E. G. (1984) Geology of the country around Rhyl and Denbig. British Geological Survey Sheet Memoir No. 95 & 107. Her Majesty's stationery office. 217p.

WILLS, L. J. & SMITH, B. (1922) The lower Paleozoic rocks of the Llangollen District with special reference to the tectonics. Quart. Jour. Geol. Soc. Lond. 78, pp. 176-226.

Manuscript received on 16.5.1994

Accepted for publication on 5.12.1994

PROPOSED LITHOSTATIGRAPHIC SUB-DIVISION OF CHILTON LIMESTONE, QUETTA DISTRICT, BALOCHISTAN, PAKISTAN.

JAWED AHMAD

Centre of Excellence in Mineralogy, University of Balochistan,
P.O. Box 43, Quetta, Pakistan.

ABDUL HAQUE

Centre of Excellence in Mineralogy, University of Balochistan,
P. O. Box 43, Quetta, Pakistan.

MIAN HASSAN AHMED

Geological Survey of Pakistan, P.O. Box 15, Quetta, Pakistan.

ABSTRACT: Chilton limestone of central Balochistan has already been classed into lower and upper parts. The lower part of Chilton limestone consists of thin to thick series of well developed reef facies, solutional caves and thin beds of black and rusty-brown chert and less amount of dolomite. Its upper portion constitutes lithologically massive to thick bedded limestone, dolomitic limestone and notable amount of dolomite itself.

In the present work, six types of Chilton limestone are recognized and proposed viz: oolitic limestone; reef limestone; dolomite limestone; compact limestone; sublithographic limestone, and micritic limestone.

INTRODUCTION

This present work has been carried out as a joint venture between Centre of Excellence in Mineralogy and Geological Survey of Pakistan Laboratories. The studied problem lies over the toposheets No.34 J/16 and 34 N/4.

The whole project comprises two well known and definite localities: Ziarat Nala, situated in the south of Chilton Range of the western flank of major anticline, and Gwani Nala, located SW of Murdar Ghar, the eastern limb of major syncline.

Ziarat Nala (34 J/16) is 2 kms. west of Lak-Pass and 17 kms. SW of Quetta near RCD national highway. Ziarat Nala is the faulted flank of major anticline of Chilton Range, of orientation NE-SW dips towards west. A high angle thrust fault dipping towards west brought, the western flank of anticline, up relative to the foot wall/hills of the Chilton Range. Thus, producing thrust faults imbrications and probably associated strike-slip faults.

Gwani Nala (34 N/4) is about 3 kms. NE of sub-Tehsil Spazant and nearly 17 kms. SE of Quetta over Quetta-Sukkar highway. Gwani Nala situated on the eastern limb of major syncline.

STRATIGRAPHY OF THE PROJECT AREAS

Though the stratigraphy of the area in question is beyond the scope of this present paper, it is succinctly given in the order of law of superposition as:

Shrinab Formation: (Hunting Survey Corporation, 1960): Early Jurassic. Oldest rock unit in central Balochistan, and has further subdivided by William (1959) as: Spingwar member (lower most); Loralai middle member, and Angira member (top most). The Angira member, in the Ziarat Nala, varies from thin to thick and massive limestone, interbedded with dark, black, khaki, olive, grey and calcareous shales.

Chilton Limestone: (Hunting Survey Corporation, 1960): Middle Jurassic, with maximum thickness in the project area (Ziarat Nala, Lak-Pass).

Sember Formation: (William, 1959): Late Jurassic. In the project area Sember Formation is mostly covered by sub-recent and scree deposits of Chilton and Dunghan limestones. Sember Formation is mainly soft olive-grey, greenish-grey shale which is only twelve meter thick.

Parh Limestone, (Vredenburg, 1909c): Cretaceous. 54 meters thick assemblage of limestone and shale plus marl, in the project area. Lower portion constitutes rusty-brown, khaki, greenish-grey, calcareous, fossiliferous flaky marl and shale. Middle part comprises limestone interbedded with marl and shale where in

belemnite can be seen and finally the upper portion contains thin-tabular (4-40cms.) fossiliferous, creamish, pink limestone. The upper contact with Dunghan limestone is unconformable.

Dunghan limestone: (Greisbach, 1881): Paleocene. 18 meters thick to massive, dark-brown buff, dark-grey limestone has seen in the project area, where in fragments of gastropods, bivalves, forams and algae can be easily traced out.

CHILTON LIMESTONE

The lower contact of Chilton limestone with the Angira member (Shrinab Formation) is transitional and being measured as 103.8 meters. Lenses of black-rusty chart, ferruginous breccia, and nodules are well developed near the upper contact with Sember Formation.

The name Chilton derived after the Chilton Range SW of Quetta. It extends NW and NE of Khuzdar, to E of Zhob and further E towards Dera Ismail Khan. It has its maximum width near Mastung, Ziarat Nala, Lak Pass and in Mangochar.

Apart from already existing literatures regarding the whole lithological description of Chilton limestone (Shah, 1977; Iqbal et al, 1980; Bagwa, 1981; Kazmi, 1981; Fatmi, 1984; etc.) which is beyond the scope of this project. The result of the present research work over the stratigraphic sections of Ziarat and Gwani Nalas has been proposed and the lithologic sub-division of Chilton limestone is summarized in Table 1.

Table:1 PROPOSED LITHOSTRATIGRAPHIC SUB-DIVISION OF CHILTON LIMESTONE

Units	Ziarat Nala (Total thickness 400 meters)	Thickness in cms.	Gwani Nala (Total thickness 300 meters)	Thickness in cms.
1.	Oolitic limestone	8-40		
2.	Reef limestone.	2-40	Micritic limestone	2-30
3.	Dolomitic limestone	2-250	Dolomitic limestone	80-150
4.	Compact limestone	80-135	Compact limestone.	4-80
5.	Lithographic limestone	100-280		

From table 1, we have the following units being described briefly as below.

Oolitic Limestone: thin to thick bedded (80-40cm.) bluish-grey, black-grey, fossiliferous, chert nodules are present.

Reef Limestone: light brown, grey, micritic, thin to thickly bedded, thin beds are more argillaceous having strong coals, sponges, alga, polyzoe, fragments of brachiopods, bivalves and belemite.

Dolomitic Limestone: brownish-black, rusty brown, very rough surface, feted small, thin to thick beds and massive (4 to 80 and 80 to 250 cms.). At some places carbonaceous material is predominant in the massive beds.

Compact limestone: rusty-brown, bluish-grey, black to dark-grey sublithographic, karst weathering, small solutional caves at some places, massive beds alternate with wavy argillaceous beds.

Lithographic Limestone: thick to massive (100-280 cms.) very fine grained rock composed of uniformly sized, thick beds of brownish-grey to blackish-grey, calcite veins are well developed, fossil fragments are filled with calcite, massive beds are ash-grey blackish-grey, chert nodules and veins, iron concretions at some places, marl and nodular limestone are present.

CONCLUSION

Chilton limestone as a whole is oolitic-oolitic, refoid and crystalline. Beds are regular to compact, internally massive, ranging from 3 to 250 cms. Some intervals are organic, bituminous, and give feted smell. Karst and caves are commonly seen. Stony corals and sponges are also common. Lenses of black rusty cherts, ferruginous breccia and nodules are well developed near the upper contact with Sember Formation.

The Chilton limestone has been divided

lithologically into five units on the basis of petrographic studies: oolitic limestone; reef limestone; dolomitic limestone; compact limestone; and lithographic limestone.

Within Chilton limestone a new locality of good and workable quantity of dolomite has been discovered, meanwhile previously reported site has been studied and then confirmed. Moreover, such high grade limestone and dolomite deposits are easily accessible and could be utilized as a basic raw material for the industrial development within Pakistan, especially in Balochistan.

REFERENCES

- BAJWA, S., & AHMED, H.** (1981) Geology of Chilton (Quadrangle 34 J/16) Quetta District, Balochistan. Geol. Surv. Pak. Inf. Rel. p.161.
- FATMI, A. N.** (1984) Stratigraphy and stratigraphic problems of Jurassic rocks of Pakistan. International symposium. Jurassic Stratigraphy, Erlangen (Germany) vol.3, pp. 653.
- GREISBACH, C.L.** (1881) Report on the geology of the section between the Bolan Pass in Balochistan and Girish in southern Afghanistan. India, Geol. Surv. Mem, vol. 18, pp. 1-60.
- HUNTING SURVEY CORPORATION, LTD.** (1960) Reconnaissance Geology of part of West Pakistan (Colombo plan co-operation Project): Canada Govt. Toronto.
- IQBAL, M.W.A., & SHAH, S.M.I.** (1980) A guide to the Stratigraphy of Pakistan. Rec. Geol. Surv. Pak. vol. 53.
- KAZMI, A.H.** (1981) Stratigraphy and sedimentation of the Jurassic in the North-Eastern Balochistan. Geol. Bull. Univ. Peshawar., vol. 14 pp. 193-198.

SHAH, S.M.I. (1977) Stratigraphy of Pakistan,
Mem. Geol. Surv. Pak. vol.12 pp. 35-64.

WILLIAM, M.D. (1959) Stratigraphy of Lower
Indus Basin, West Pakistan. World
Petroleum. Conf. 5th, N.Y., Sect. 1
paper, 19, pp. 377-390.

VREDENDURG, E.W. (1909c) Report on the
geology of Sarawan, Jhalawan, Mekran
and the state of Las Bela. India Geol.
Surv. Recs., vol. 38, pt.3, pp. 189-215.

Manuscript received on 15.2.1994.

Accepted for publication on 28.2.1994.

MAJOR METALLIC MINERALS OF SINDH, PAKISTAN.

SYED AFZAL AHMAD

Geological Survey of Pakistan, P. O. Box 15, Quetta, Pakistan.

ABSTRACT: The major metallic minerals found in Sindh Province, are celestite, laterite and ochre. Celestite deposit possesses a faint blue tinge, maybe white, yellow, green or reddish in colour, exposed in Laki Formation of Eocene age. Laterite containing concretions of iron oxide and interbedded sandy layers occurs above the Ranikot Formation of Paleocene age in the Lakhra anticline. The laterite band marks the regional unconformity in the area. Whereas, Ochre formed as sedimentary transported material mixed with shales and also occupies the same stratigraphic position as laterite.

INTRODUCTION

The major metallic minerals of Sindh are celestite and ochre. Celestite is one of the two strontium minerals used in the manufacture of strontium salts. Its chemical composition is strontium sulphate (SrSo4). It is usually pure but may contain small amounts of calcium, barium, iron and silica. The mineral crystallizes in orthorhombic system and commonly occurs as tabular or prismatic crystals; also in cleavable, granular, or fibrous masses. The laterite is 'red residual soil,' developed in humid tropical and sub-tropical regions of good drainage. It is leached off silica and contains concentrations particularly of iron and aluminum hydroxide. It may be ore of iron, aluminum, manganese or nickel. Ochre is a yellow, brown or reddish mixture of hematite, limonite, and clay. It is iron rich product of residual or lateritic weathering which can be derived only from iron rich rocks. It commonly occurs as sedimentary transported materials mixed with shales.

The purpose of this paper is to have some information regarding the metallic minerals found in Sindh Province.

The geological succession in the area is follows:-

<u>Formation</u>	<u>Lithology</u>	<u>age</u>
Recent Sediments.		Recent
Manchar Formation	Unconformity Sandstone & Conglomerate Unconformity	Pliocene
Tiyon Formation	Limestone & Shale	Eocene.
Laki Formation	Limestone & mart Uncomformity	
Rani Kot Formation	Limestone Shale & Sandstone	Paleocene

CELESTITE

The celestite deposits found in three separate areas, north, east, and south of Thano Bula Khan (Bogue, 1961, p.4). The lease east of Thano Bula Khan is being mined at present. The central lease area, covering 13 sq.km. is 10 km. to the east of Thano Bula Khan (Fig. 1) which is located at 104 km. to the north east of Karachi and is connected by a metalled road. It is also connected with Hyderabad which is 65 km. to the west. The other two leases of approximately 12 sq.km. are 14 km. to the northeast and 13 km. to the south of Thano Bula Khan. The nearest railhead is at Meting, about 38 km. from Thano Bula Khan.

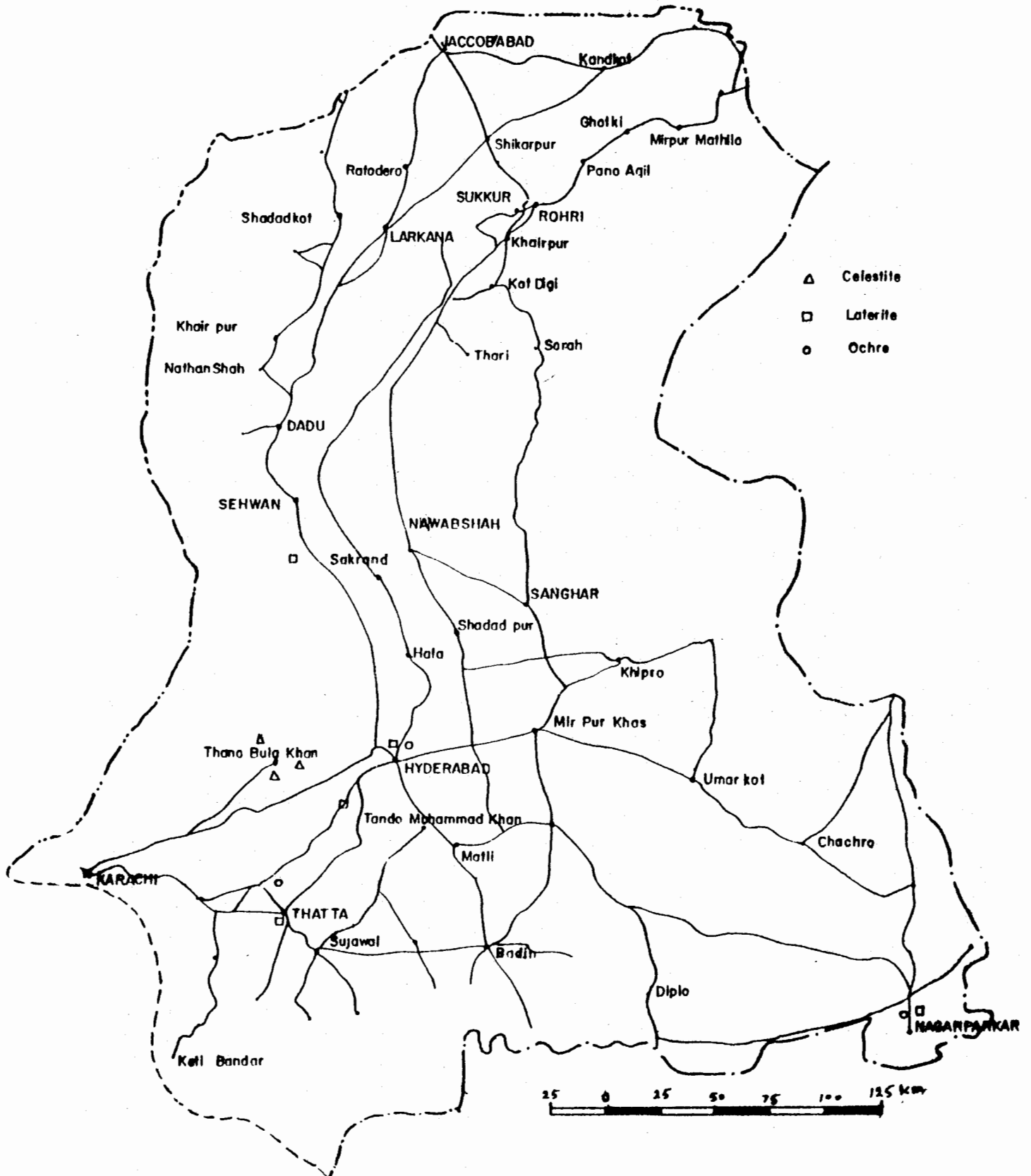


Fig. 1. Location map of metallic minerals of Sindh.

Geological Occurrences: Celestite occurs in two principal type of deposits: i) Disseminated as crystals or irregular grains in shales, limestone and dolomites. ii) In fracture and cavities within rocks of varying ages but principally of sedimentary origin. Most of the well known deposits of celestite are of this type.

The Laki limestone forms a big anticline. The limestone bed is low dipping and 5 to 6 meters thick near the deposit in the central lease area which has been examined in some details. The deposit after on a structural terrace on the western flank of a broad anticline.

On the western flank of the anticline, an open fissure mineralized extends at least for 34 km. Its strike follows with the strike of the limestone, N 20° E. The width of the mineralized fracture is from a few cm. to 40 cm. Foot an hanging walls of the deposit are regularly formed.

The central portion of the area has a developed mineralized zone. The celestite occurrence is traceable for about 2 kilometers. The average width of the mineralized fracture zone is about 0.5 meter. The exposed extension in depth is measured to 15 m. There are outcrops that have been worked in the valley and hill tops, more or less 15 meters apart from each other. The celestite occurs in crystals, cleavable and granular masses. In places crystals upto 0.3 meter long are present.

Gangue material is normally absent except for occasional gypsum or calcite. There are alternate zones of pure celestite and mixed celestite-limestone.

The southern part of the central lease is similar in geology and general outline to the deposit of the northern part. The fissure can be followed through outcrops upto the central part over a distance of about 3 km. The celestite outcrops can be traced for a distance of approximately 182 meters.

Uses: Powdered celestite is used as a filler in

white paint, as substitute for barite as rubber filler, and in oil drilling mud. Strontium and its compound are utilized in pyroelectrics, such as in tracer bullets, distress signal rockets and flares, military signal flares, transportation steel, and fireworks. Other uses include ceramics, chemicals, depilators, caustic soda refining desulphurizing steel, dielectrics, grease, luminous paint, plastics and welding rod coatings. Strontium salts are used also in desaccharizing beet-sugar molasses, and as a purifying flux in metallurgy.

Reserves: Based on the shallow open cuts, proved reserve have been calculated at 1,500 metric tons in the central areas. Indicated and inferred reserves of celestite have been estimated only on the ore which would be available between the outcrops on the ridges and the bottom of the valley. The difference in elevation between the ridges and valley is about 15 meters. The width of the fracture zone in which celestite veins occur was estimated at 0.5 meter in the central part and 0.3 meter in the southern part. (Jaffery and Ahmad, 1991). The estimates of indicated ore reserve is based partly on specific measurements and partly on project distance on geological evidence.

The celestite contains about 25 percent limestone fragments. The amount of available celestite, therefore, would be about 38376 metric tons. The mining loss and the ore dressing loss with the present method of hand-sorting is about 30 percent. This would reduce the amount of celestite for market to about 26570 metric tons. Celestite reserves: proved, 1974 metric tons; probable, 22632 metric tons and possible, 27552 metric tons.

LATERITE

The laterite deposits found in 5 different localities in Sindh. They are: i) Lakhra, Dadu District. (NW of Hyderabad) ii) Sehwan, Dadu District (30 km south of Sehwan); iii) Meting, Dadu District, (4km off Meting Railway Station); iv) Makli, Thatta District, (3km south of Thatta),

v) North of Nagarparkar, Thar District. (Fig. 1).

The deposits generally found above the Ranikot Formation of Paleocene age except in the Nagarparkar it is found in between the Eocene and Cretaceous rocks.

Geological Occurrences: In Lakhra it is highly ferruginous lateritic clay, containing concentration of iron oxide and interbedded sandy layers found above the Ranikot Formation of Paleocene age in the Lakhra anticline to the north west of Hyderabad.

In Meting it has the same stratigraphic position as in Lakhra but it is in lenticular form and also varies in thickness. In Makli hills and Sehwan it is found in thin lateritic layers interbedded with impure limestone overlies the same Ranikot Formation.

In Nagarparkar it is found as the lenses of lateritic clay between the Eocene and Cretaceous strata. The thickness of these lenses ranges between 1-3 meters. It also serves as marker bed for china clay in this particular area.

The chemical analysis of the samples in two different localities ranges as follow (after PMDC 1970) as:

	Lakhra		Nagarparkar	
Feo	37.7	15.8%	43.8	34.8%
Sio ₂	23.8	4.7%	22.3	11.9%
Al ₂ O ₃	44.7	23.6%	12.0	7.3%
CaO	6.1	0.8%	4.3	1.9%
MgO	1.8	0.8%	0.8	0.6%

Uses: Laterite may be used as an iron ore. If aluminum contents are higher then it is used in the manufacture of alum, bauxite bricks for furnaces, and the artificial abrasive called alundum.

OCHRE

The ochre deposits are mostly found as a sedimentary transported material with shales and

occupies the same stratigraphic position as lateritic bands in Sindh. It is pulverulent oxide, usually impure, brown and yellow ochre consist of limonite or goethite and red ochre of hematite.

The ochre deposits found in four different localities in Sindh. They are:- i) Lakhra, Dadu District; ii) Jhol Dhand, Dadu District; iii) Miharo bazar, Hyderabad District; iv) Nagarparkar, Tharparkar District.(Fig. 1).

In Lakhra the ochre bed occupies the same stratigraphic position as the lateritic band. It occurs as thin layers. In Jhol Dhand the ochre bed found in patches and streak of limonitic ochre and it is found in a poorly stratified clay bed. The thickness of this bed is about 15 to 25 cm. and reserves about 3500 metric tons (approx.). In Miharo bazar area it is found as a band about 15-25 cm. thick in the Shonari member of Laki Formation, the quality is variable and satisfactory. In Nagarparkar area the ochre is to be found to associated with laterite.

Uses: It is used as pigment in the manufacture of paints.

CONCLUSIONS

These are the metallic minerals discovered in Dadu and Thar Districts of Sindh Province.

The reserves of the celestite mineral is about 30,000 metric tons, whereas of laterite has not been estimated. Similarly the reserves for ochre had only been estimated for the Jhol Dhand deposit about 3,500 metric tons.

REFERENCES

AHMAD, Z. (1970) Mineral Directory of Pakistan. GSP Record vol. 15 part-3, p.8.

ASHRAF & SATTAR (1965) Mineral Resources of Sindh Province. (4th five year development programme WPIDC Mining Division Karachi, June 1970).

BOGUE, R.G. (1961) Celestite near Thana Bula Khan, Hyderabad. Mineral Information circular, Geol. Sur. Pak. 18 pp.

JAFFERY, S.S.A., & AHMAD S.A. (1991) Mineral Directory of Sindh. GSP. I.R. No. 506, pp. 3-12.

Manuscript received on 9.6.1994.

Accepted for publication on 22.10.1994.

PETROLOGY AND PETROGRAPHY OF DIFFERENT DYKES OF SRA - SALWAT AREA, MUSLIMBAGH, DISTRICT QILA-SAIFULLAH, BALOCHISTAN, PAKISTAN.

ABDUL HAQUE

Centre of Excellence in Mineralogy, University of Balochistan,
P.O. Box 43, Quetta, Pakistan.

MASOOD IQBAL

Geological Survey of Pakistan, P.O.Box 15, Quetta, Pakistan.

ABSTRACT: Sra Salwat area is the part of Zhob igneous complex and which has never been so far petrographically studied in detail. Dolerite, rodingite and pyroxenite dykes, part of the mapped area, studied petrographically is the subject of the present paper. The orientation of these dykes is NW to SE, almost subvertical and they cut ultramafic tectonites largely, and to some extent the associated sedimentary rocks, therefore, they show last and independent phase of igneous activity. On the basis of mineralogy and texture, the above classification of these dykes has done, wherein dolerite dykes occupy the lower stratigraphic level as compared to other categories.

INTRODUCTION

Three categories of dykes have been studied petrologically and petrographically in the Sra Salwat area. They are:

1) Dolerite dykes being the predominant and have been classed according to Bilgrami (1964) as: i) Normal dykes ii) Fine grained dolerite dykes iii) Quartz dolerite dykes and iv) Hornblende dolerite dykes.

2) Rodingite dykes which are few in numbers. The later one has been derived from the former one due to alteration (Bilgrami & Howie, 1960).

(3) The third and rare category are pyroxenite dykes, which are unmapable under such scale and have been sampled in the southeast of the studied area.

The petrographic studies of all the three

categories include their textures, mineralogical compositions, alterations. Through the study of model analyses, such classification had already given by Bilgrami (1964) now has been recognized and confirmed.

PETROLOGY AND PETROGRAPHY

DOLERITE DYKES:

These dark greenish grey, to medium grained dykes have been intruded in the serpentinized-harzburgite terrain. Some of them are highly altered and have both ophitic or prophyritic and intersertal textures. Common alteration minerals are chlorites, actinolite and epidote.

These dykes belong to Sra Salwat area classed into four categories and have been studied petrographically as below:

1. Fine grained dolerite dykes

With naked eyes, these dykes are grey to dark-grey, fine grained inequigranular, hypocrySTALLINE and porphyritic. Within aphanitic ground mass, with the help of hand lens, plagioclase laths and pyroxene crystals can be observed.

Microscopic Study: The following minerals have been microscopically identified in these fine grained dolerite dykes, namely: plagioclase, pyroxene, hornblende, chlorite, sericite, opaque iron-oxides. Plagioclase shows lath shaped-phenocrysts and microcrystalline groundmass of andesine and labradorite. Euhedral colourless pyroxene (diopside) crystals within plagioclase phenocrysts are seen. Microcrystalline ground mass are highly altered to sericite. The pyroxene crystals show zoning and undulose extinction. Pyroxene is highly altered to green hornblende and chlorite. Amongst the opaque minerals are ilmenite or magnetite which are anhedral, tiny-shot and disseminated in the rocks.

Sometimes the ground mass, sometimes the phenocrysts have been altered. Alteration products are hornblende, chlorite, sericite and calcite.

The assemblage of the existing minerals of these fine grained dolerite dykes show under the microscope well developed porphyritic and subophitic textures.

2. Normal dolerite dykes:

The fresh samples within hand show light grey to dark-grey, mottled white and greenish grey colours. The weathered surface is brownish black. Holocrystalline, phaneritic, fine to medium grained often show porphyritic texture.

Microscopic Study: Microscopically plagioclase (55-75%), pyroxene (15-30%), iron-oxide (2-8%), sometimes quartz (less than 2%) are observed by volume. Hornblende (4-6%) and chlorite (1-2%) are the alteration products.

Most of the plagioclase (50%) has been altered to sericite. Plagioclase is andesine to labradorite ($An_{45}-An_{55}$) having clear stouts with carlsbad twinning.

Non-pleochroic pyroxene is subordinate, anhedral to subhedral; clinopyroxene large grains defined by augite and diopside. These pyroxene are highly fractured and cleaved in one direction, also show undulatory extinction. Hornblende is developed by the expense of pyroxene which is evident by relict pyroxene. Pyroxene is also altered to acicular brown amphibole.

The interstitial anhedral quartz grains between plagioclase crystals show undulatory extinction and has well developed micropegmatitic intergrowth with plagioclase.

Brownish black, irregularly disseminated anhedral crystals of ilmenite as well as the stout plagioclase contains coffee brown, anhedral crystals of picotite represent the opaque iron-oxide minerals.

Pyroxene is partially to completely altered to hornblende and chlorite, whereas plagioclase into sericite. Sericite is dense, earthy brown in colour and from pseudomorphs after plagioclase.

Under the microscope, the association of different sizes and forms of minerals shows hypidiomorphic, granular medium-grained inequigranular, intergranular ophitic texture with pyroxene crystals surrounded by plagioclase laths. Micropegmatic intergrowth of quartz crystals randomly oriented with plagioclase laths have been observed.

3. Quartz dolerite dykes:

Weathered color of these dykes is brownish grey whereas, its fresh surface is mottled white and greenish grey. These rocks are holocrystalline, phaneritic and medium grained, with small vitreous quartz being seen by the help of a hand lense.

Microscopic study: Constitutes plagioclase (60-70%), pyroxene (15-20%), quartz plus micropegmatite upto 8% and the remainings are opaque iron-oxide. Chlorite and sericite are the alteration products.

Plagioclase is totally altered to sericite having subhedral to euhedral and lath shaped, being randomly oriented. This mineral has intergrown with quartz, thus forming plume shaped structure.

Subhedral to euhedral zoned and cleared pyroxene is represented by augite being partially replaced by chlorite.

Intergrowth quartz grains in the interstices of sericitized plagioclase are fine grained and euhedral, showing undulatory extinction.

Ilmenite in skeletal form, partially altered to dense brown isotropic material represents the opaque iron-oxide amongst the constituents. Texture point of view these dykes are hypidiomorphic intergranular, medium to coarse grained and show well developed micropegmatic intergrowth of quartz and altered plagioclase.

Sericitization is predominant. Along the margins, cracks and cleavages, pyroxene has been altered to fibrous, pale-green, weakly pleochroic chlorite, which proceeds towards the centres.

4. **Hornblende dolerite dykes:**

The weathered colour of these medium-grained dykes is black to brownish whereas the fresh colour is mottled white. They are holocrystalline, phaneritic and seems to be equigranular.

Microscopic study: Mineralogically composed of plagioclase (45-55%), hornblende (40-45%), pyroxene (2-6%) and opaque (2%).

Euhedral and lath shaped plagioclase is highly sericitized, and shows to some extent

foliation.

Subhedral to euhedral green hornblende crystals with well defined cleavage are developed in the interspaces of plagioclase laths.

Pyroxene is represented by colourless euhedral to subhedral augite in the remnants of core which are partially or wholly altered to hornblende and chlorite, along the periphery.

Subhedral ilmenite crystals represent opaque iron oxide being associated with hornblende and plagioclase.

Microscopically, these dykes are hypidiomorphic and intergranular and few of it exhibit foliated texture.

Alteration products are sericite from plagioclase, hornblende and chlorite from pyroxene. The rock as a whole is moderately to intensely altered.

RODINGITE DYKES:

Rodingite dykes are commonly calcium enriched gabbroic rocks with essential minerals like grossular garnet, diopside and dillage are very coarse crystals and fine grained carbonates. They are medium to coarse grained wherein prehnite chlorite or serpentine or both are the alteration products. Moreover, with quartz and augite they also define the accessory minerals.

These dykes having weathered surface brownish white and fresh surface white to white grey cut discordantly the serpentized-harzburgite terrain.

Microscopic study: Under the microscope the mineralogy of these dykes shows minerals like grossular-garnet, diopside, fine grained carbonates, augite, quartz, chlorite, prehnite.

Coarse and colourless crystals of grossular garnet having high relief is frequently

present (12% by volume) are partially altered to chlorite. Pale green to bright green, euhedral to subhedral diopside is also coarse grained and present 35-40% by volume. Fine grained carbonates range upto 25% by volume. Purplish brown and subhedral augite as a minor constituent of the rock in which zoning is observed in few grains.

Chlorite is the alteration product of grossular-garnet and is in accessory amount. Prehnite, in aggregates, is colourless and having sheathlike and show bow-tie structure. It is secondary mineral in these rocks.

PYROXENITE DYKE:

In the studied area, only one unmapable monomineralic pyroxenite subvertical dyke striking NE-SW in serpentized dunite terrain is observed. No chilling effects on the surrounding rocks has been observed. Such dyke is holocrystalline, coarse grained and bright green in colour. Clinopyroxene minerals can be seen with necked eyes.

Microscopic study: Under the microscope, the mineralogy of pyroxenite dykes shows mainly clinopyroxene (80-95%), with subordinate orthopyroxene (2-5%), olivine (1-2%) and less than 4% opaque minerals. Sometimes in few samples less than 2% plagioclase has been observed.

Amongst the predominant clinopyroxene, euhedral to subhedral diopside and subhedral to anhedral augite are observed. They are equidimensional with straight boundary and usually poikilitic containing small orthopyroxene crystals.

Orthopyroxene is mainly enstatite in rare quantity, usually in small grains within large grains of clinopyroxene. Enstatite shows one cleavage direction and sometimes being altered to serpentine. In olivine bearing varieties it shows irregular fractures due to shearing effects. Rare anhedral highly fractured olivine crystals are enclosed either within clinopyroxene or

orthopyroxene. Their fractures are refilled by red-brown iron oxides forming a mesh structure.

In few samples, rare plagioclase are represented by subhedral bytownite (An_{72}) being determined by Michel Levy's method.

Alteration product is very rare, sometimes serpentine and iron-oxide minerals are the alteration products of orthopyroxene and olivine. Some grains are pseudomorphs of serpentine after orthopyroxene.

The whole dyke rocks are hypidiomorphic, granular, coarse grained poikilitic texture.

REFERENCES

- BILGRAMI, S.A., & HOWIE, R.A.** (1960) The mineralogy and petrology of a rodingite dike, Hindu Bagh, Pakistan. *Amer. Mineralogist* 45, pp. 791-801.
- BILGRAMI, S.A.**, (1964) Serpentine-Limestone contact at Taleri Muhammad Jan, Zhob valley, West Pakistan. *Amer. Mineralogist* 45, pp. 1008-1019.

Manuscript received on 3.2.1994

Accepted for publication on 17.2.1994

EARTHQUAKES AND RISKS MANAGEMENT IN PAKISTAN

MUBARAK ALI AND ZULFIQAR AHMAD

Department of Earth Science, Quaid-i-Azam University, Islamabad, Pakistan.

ABSTRACT: Among natural calamities earthquakes are more disasterous. They have killed millions of people. The severity or potential for damage varies from harmless tremors to dreadful devastating jolts. Prediction of earthquakes is not yet successful. Prevention and preparedness are the dependable means to mitigate seismic hazards. Earthquake history of Pakistan has defined and signified the existence of heavy seismic risks in our social life.

INTRODUCTION

Earthquakes are a major threat to mankind. When they hit any area they cause destruction and death toll all-around. Hustle bustle towns are converted into heaps of rubbles and dust. Those houses which we consider our shelterer protection are changed into graves. Lovely kids, pretty faces, and elderly people, for whom we are ready to do every sort of sacrifice, leave the well wishers mourning. Their cries, their shouts for help remain unattended. For a long time the prevailing view was that the earthquakes came as punishment for man's failing. Whatsoever, the earthquakes are a dreadful havoc which reduce men to helplessness, break long human association in minutes, and spread socio-economic miseries around. Charles Darwin reflected his feelings on devastating earthquake of Chile (February 20, 1835).

"A bad earthquake at once destroys the oldest associations; the world, the every emblem of all that is solid, had moved beneath our feet like a crust over a fluid; one second of time has created in the mind a strong idea of insecurity, which hours of reflection would not have produced."

No one knows precisely how many times mankind became victim of earthquakes. However, from the documented earthquakes it appears that 2 million or more lives have been lost in the last two centuries, with an average loss of

10,000/year. The year 1976 is considered as the year of killer earthquakes (Bath 1979), because, as many as 100,000 people died in earthquakes of Guatemala (Feb. 4), Italy (May 6), China (July 28), West Iran (June 25), Philippine (August 16), and Turkey (Nov 6), Algerian earthquake of 1980 and Iranian earthquake of 1990 were even worse because more than 50,000 lives were lost, more were injured, and there were heavy property losses.

Earthquakes as a matter of fact are always around, but the devastating earthquakes of magnitude 8 are one to two per year for the earth as a whole. Proceeding towards lower magnitudes, the number increases exponentially. The estimated number of earthquakes of varied magnitude is given in Table-1.

Table 1 **Worldwide Earthquake per year**

MAGNITUDE Ms	AVERAGE NUMBER
8	2
7	20
6	100
5	3,000
4	15,000
3	More than 100,000

Geographical distribution of earthquakes

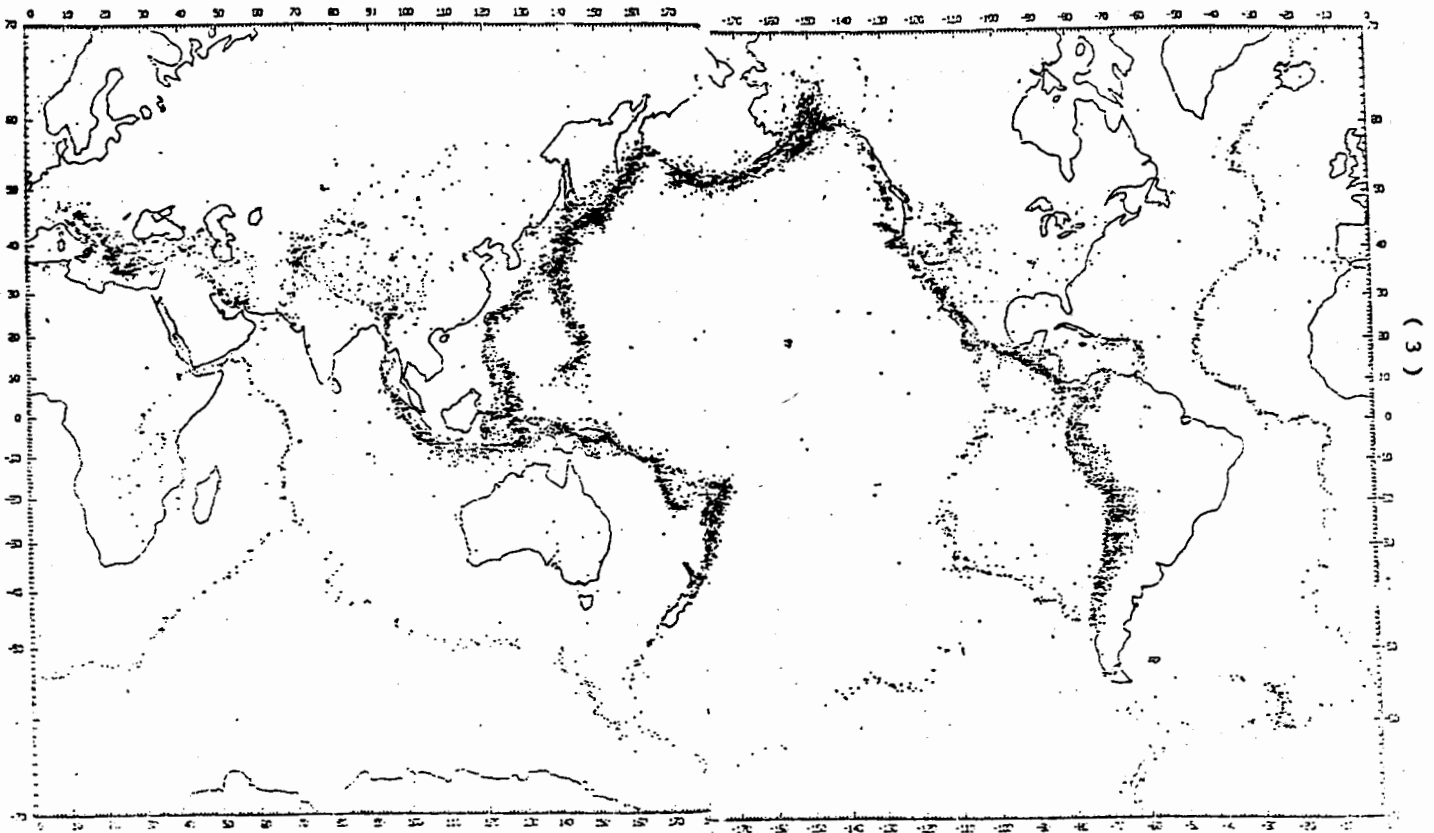


Fig. 1. Distribution of earthquakes around the world. Epicentre date 1961-67 (After Barazangi and Dorman, 1969).

Geographically, the earthquakes exhibit a striking distribution, and expose prominently the following three main belts (Fig.1) as the high seismicity areas of the world: 1) the circum - Pacific belt. 2) the mid - Atlantic to East African and Easter Island belt. 3) the Euro-Asian (Alpine) belt.

Circum - Pacific and Alpide (Alpine - Himalayan) belts include respectively 70% and 20% of the global earthquakes and define compression features developed by the

convergence of plates, whereas the mid-Atlantic - East African belt describes the ocean ridge extension features of plates divergence. The alpide belt that includes famous mountain ranges of the world, i.e., Atlas (Morocco), Alps (Mediterranean), Pontic and Taurus (Turkey), Elburz and Zogrös (Iran), Karakoram and Himalayas (Pakistan), and the Indian Himalayas, shows larger proportion of concentration of earthquakes in a latitudinal window between latitudes 20°N to 45°N, (Rikitake, 1976).

Seismicity of Pakistan

Pakistani areas are related to interaction of three lithospheric plates, i.e., Indian, Arabian, and the Eurasian plate (Fig. 2). In the north is the east-west trending Himalayan convergence zone formed by the collision of Indian plate with the Eurasian plate about 40 million years ago (Molnar and Tapponnier, 1975). In the southwest is the Makran convergence zone that is trending east-west and is formed by the subduction of oceanic lithosphere of the Arabian plate. These Makran and Himalayan convergence zones are linked by north-south trending Chaman-Ornach Nal transform fault zone (Farah et al, 1984) as shown in figure 3.

This active tectonic set-up of Pakistan is responsible for the accumulation of stresses and consequently the high seismicity ranging from micro-earthquakes to major earthquakes (Seeber et al., 1981). In this century about 1000 earthquakes of magnitude greater than 4 have been recorded, in which 4% are of magnitude higher than 6.9. Historical earthquakes which have been shaken severely Pakistani lands are mentioned in Table 2, and shown in figure 4. 40% of these events lie in northern part of the country, 40% in southwestern part, and the remaining 20% in the central part. If this distribution of seismicity is viewed in the context of that in the neighboring countries like India, China and Iran, it becomes obvious that Pakistan lies in a region of potentially heavy seismic risks.

Earthquake Hazard

The tectonic earthquakes, by mechanism, are related with the faults which become active through accumulation of stresses over geologic time. When these stresses in the fault zone overcome the frictional force, a displacement or rupturing takes place which constitutes the earthquake (Benioff 1964). Larger the frictional

Table 2 Documented earthquakes in Pakistan, Intensity more than 7.

DATE	INTENSITY	REGION	APPROX. IOC.
25 AD	9-10	TAXILA	33.7N, 72.9E
1669 JUN 23	8-9	ATTOCK	33.9N, 72.3E
1819 JUN 16	10+	RUN OF KUTCH	24.0N, 69.0E
1827 SEP 24	8-9	LAHORE	31.6N, 74.4E
1845 JUN 19	7-8	RUN OF KUTCH	23.9N, 68.8E
1852 JAN 24	8	MURREE BUGTI HILLS	29.3N, 68.9E
1868 AUG 11	7-8	PESHAWAR	34.0N, 71.6E
1868 NOV 10	7-8	BANNU	33.0N, 70.6E
1868 APR	7-8	PESHAWAR	34.0N, 71.6E
1869 DEC 20	7-8	CAMBELLPUR	33.8B, 72.3E
1821 MAY 22	7-8	GILGIT	35.9N, 74.3E
1878 MAR 02	7-8	KOHAT	33.6N, 71.4E
1878 MAR 02	7-8	PESHAWAR	34.6N, 71.6E
1888 DEC 28	8-9	QUETTA	30.2N, 67.0E
1889	8	KHUZDAR	27.8N, 67.2E
1892 DEC 20	8-9	CHAMAN	31.0N, 66.4E
1893 FEB 13	8-9	QUETTA	30.2N, 67.0E
1900	8	QUETTA	30.4N, 67.0E
1909 JUL 08	8-9	HINDUKUSH	36.5N, 70.5E
1909 JUL 08	7-8	KALAM (SAWAT)	35.4N, 70.5E
1909 OCT 21	8-9	KACHHI PLAIN	29.0N, 68.2E
1911 JUL 04	8-9	HINDUKUSH	36.0N, 70.5E
1921 NOV 15	8-9	HINDUKUSH	36.5N, 70.5E
1922 DEC 05		HINDUKUSH	36.8N, 69.5E
1931 AUG 27	7-8	NACH	29.9N, 67.3E
1935 MAY 30	9-1	QUETTA	28.9N, 66.4E
1937 SEP 09	7-8	KASHMIR	34.1N, 74.4E
1937 NOV 07	7-8	KASHMIR	34.7N, 73.1E
1941 SEP 29	8	QUETTA	30.2N, 67.0E
1945 NOV 27	10+	MAKRAN COAST	25.2N, 63.5E
1947 AUG 05	8	MAKRAN COAST	25.2N, 63.5E
1949 MAR 04	8	HINDUKUSH	36.0N, 70.5E
1955 FEB 18	7-8	QUETTA	30.4N, 67.0E
1956 MAY 13	8	FORT MUNRO	29.9N, 69.9E
1965 MAR 14	7-8	HINDUKUSH	36.3N, 70.7E
1966 AUG 01	7-8	LORALAI	30.1N, 68.6E
1972 SEP 03	6-8	HAMRAN-DAREL	35.9N, 73.3E
1974 JUL 30	6-8	HINDUKUSH	36.3N, 70.8E
1974 DEC 20	6-8	PATTAN	35.1N, 72.9E
1975 OCT 03		QUETTA	30.2N, 66.3E
1977 FEB 14	7	RAWALPINDI	
1981 SEP 12	6-8	DAREL VALLEY	

force is, major is the earthquake. Active faults and linements marked in Pakistan (Fig. 5) are more than 40, and some of them are considered seismically very active because the epicentres of many earthquakes have good alignment with them (Kazmi 1979). However, many epicentres do not appear to have any relation with the faults. This situation, thus seems to reflect the possibility of existence of discrete tectonic zones rather than the individual faults. The geological studies (Kazmi 1979), the seismotectonic results (Quittmeyer et

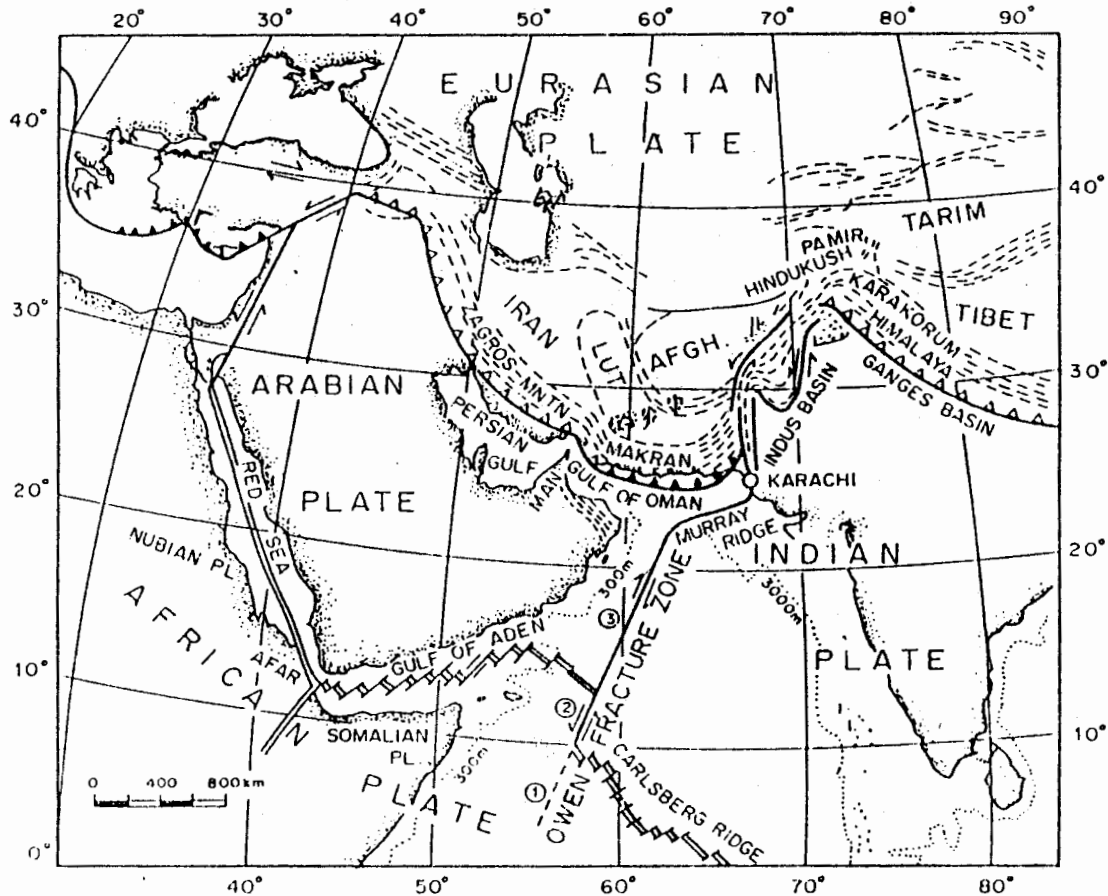


Fig. 2. Plate tectonic sketch map showing position of Arabian, Indian and Eurasian plates (After Jacob and Quidmeyer, 1979).

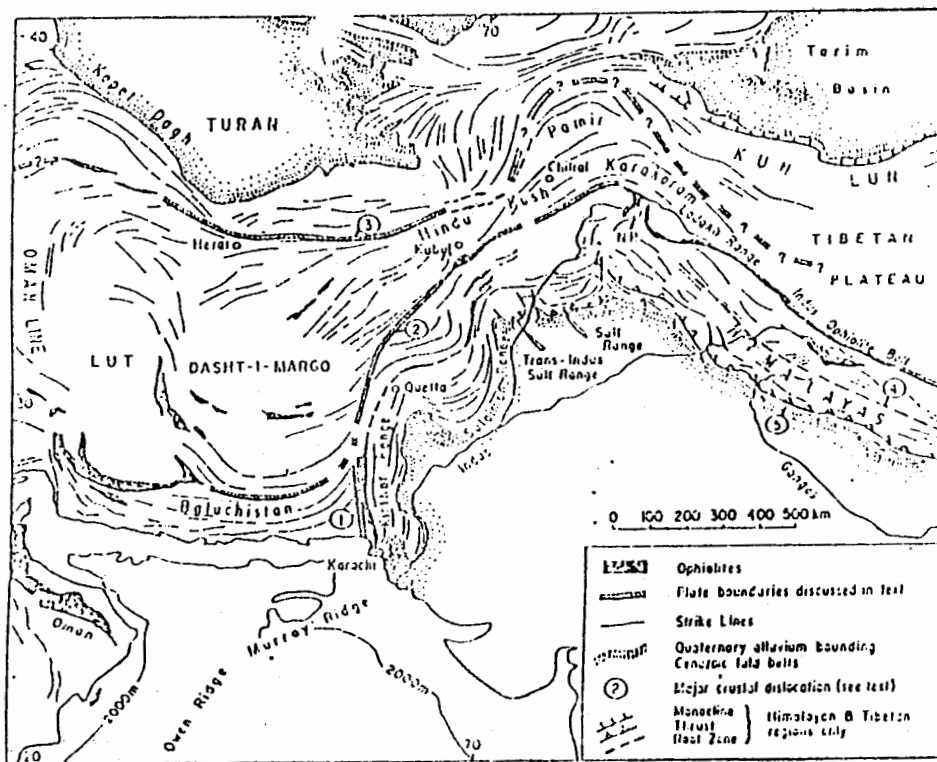


Fig. 3. Tectonic sketch map of Pakistan and adjacent regions 1. Ornach-Nal fault; 2. Chaman fault; 3. Herat Hindu Kush fault zone; 4. Himalayan Central Crystalline Axis, and 5. Himalayan Main Boundary fault (After Powell, 1979).

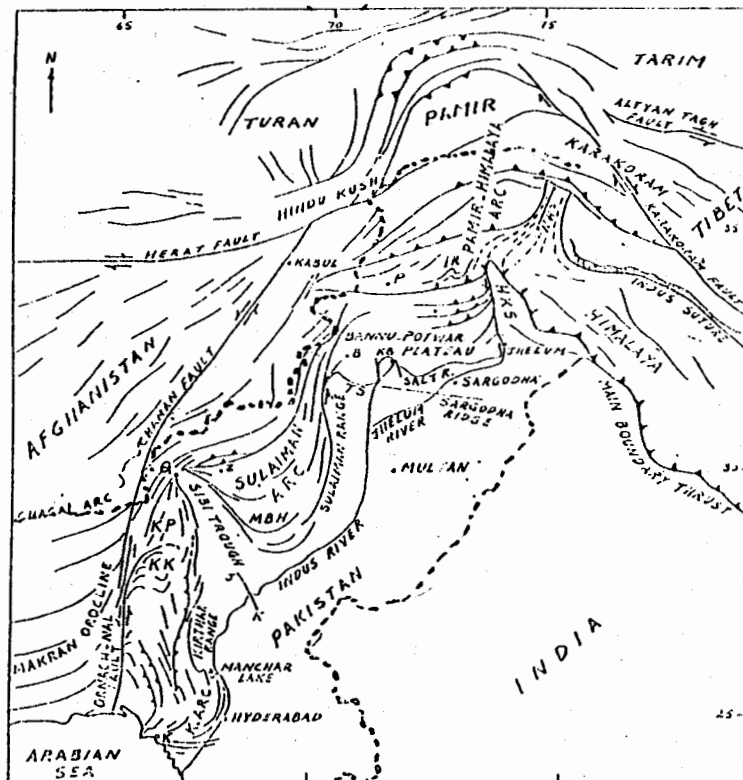


Fig. 4. Major tectonic trends and the documented earthquakes. (After Sarwar and Dejong 1979).

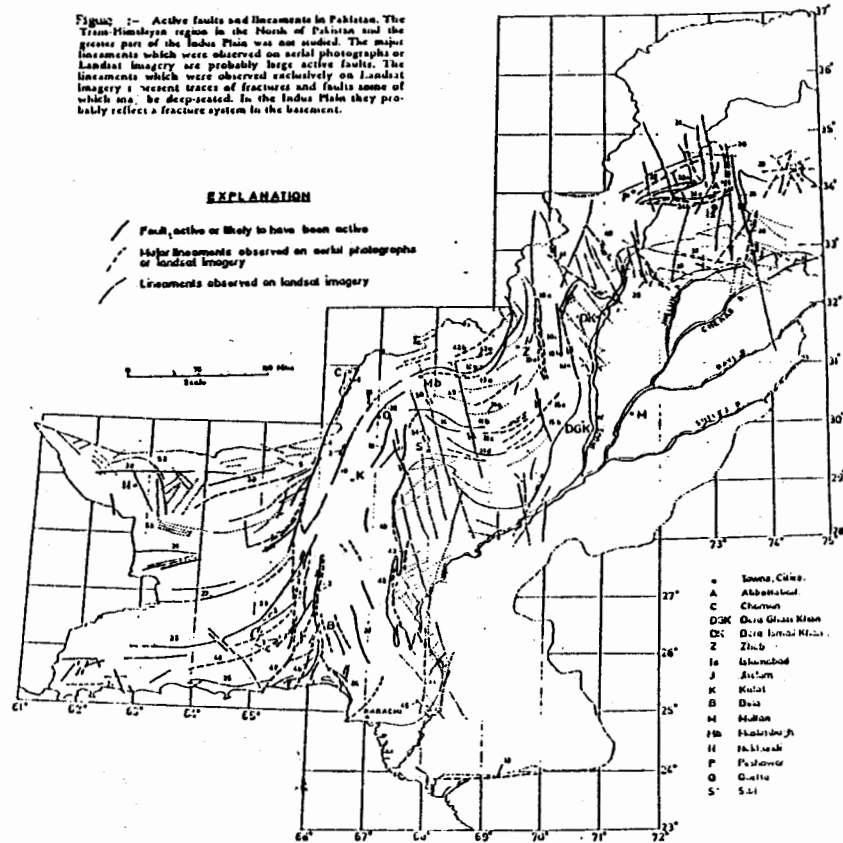


Fig. 5. Active faults and lineaments in Pakistan. (After Kazmi 1979).

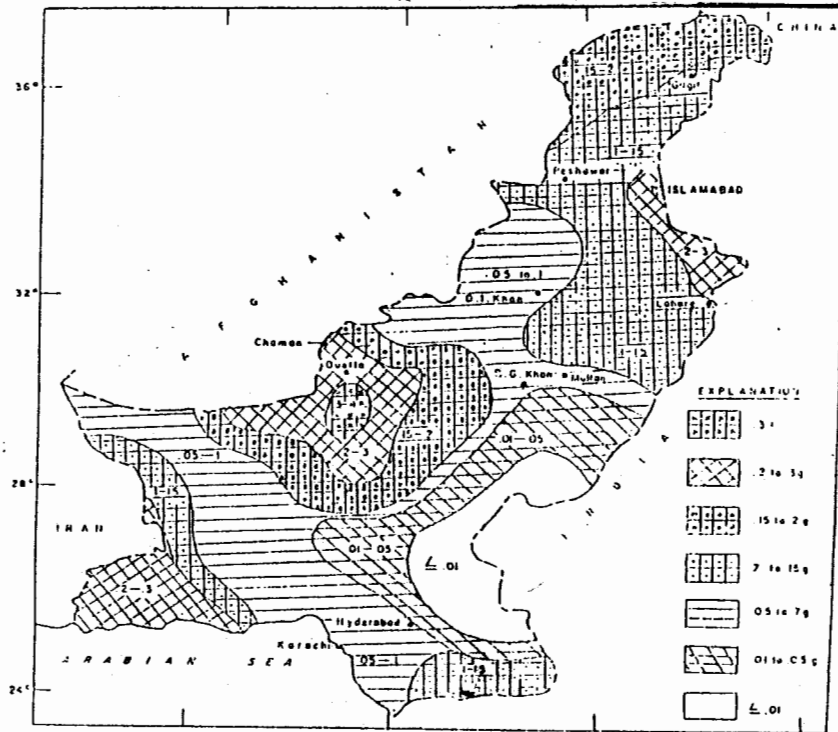


Fig. 6. Seismic Hazard Zones of Pakistan and their g Factors. (G.S.P. Record Vol. 47).

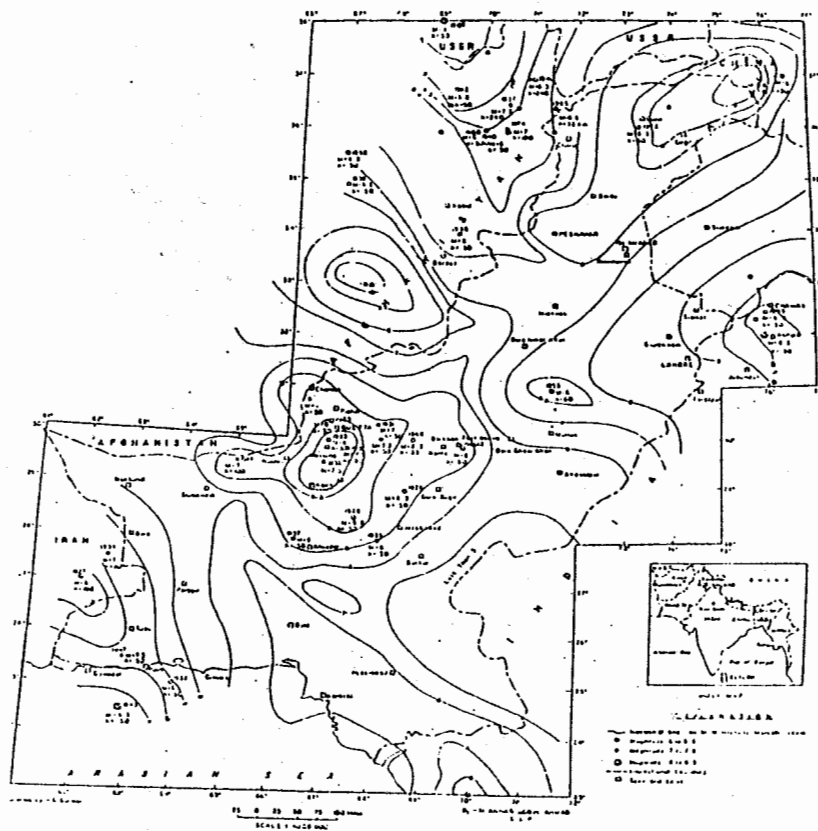


Fig. 7. Isoseismals of Pakistan on Modified Mercalli intensity scale. (G.S.P. Record Vol. 47).

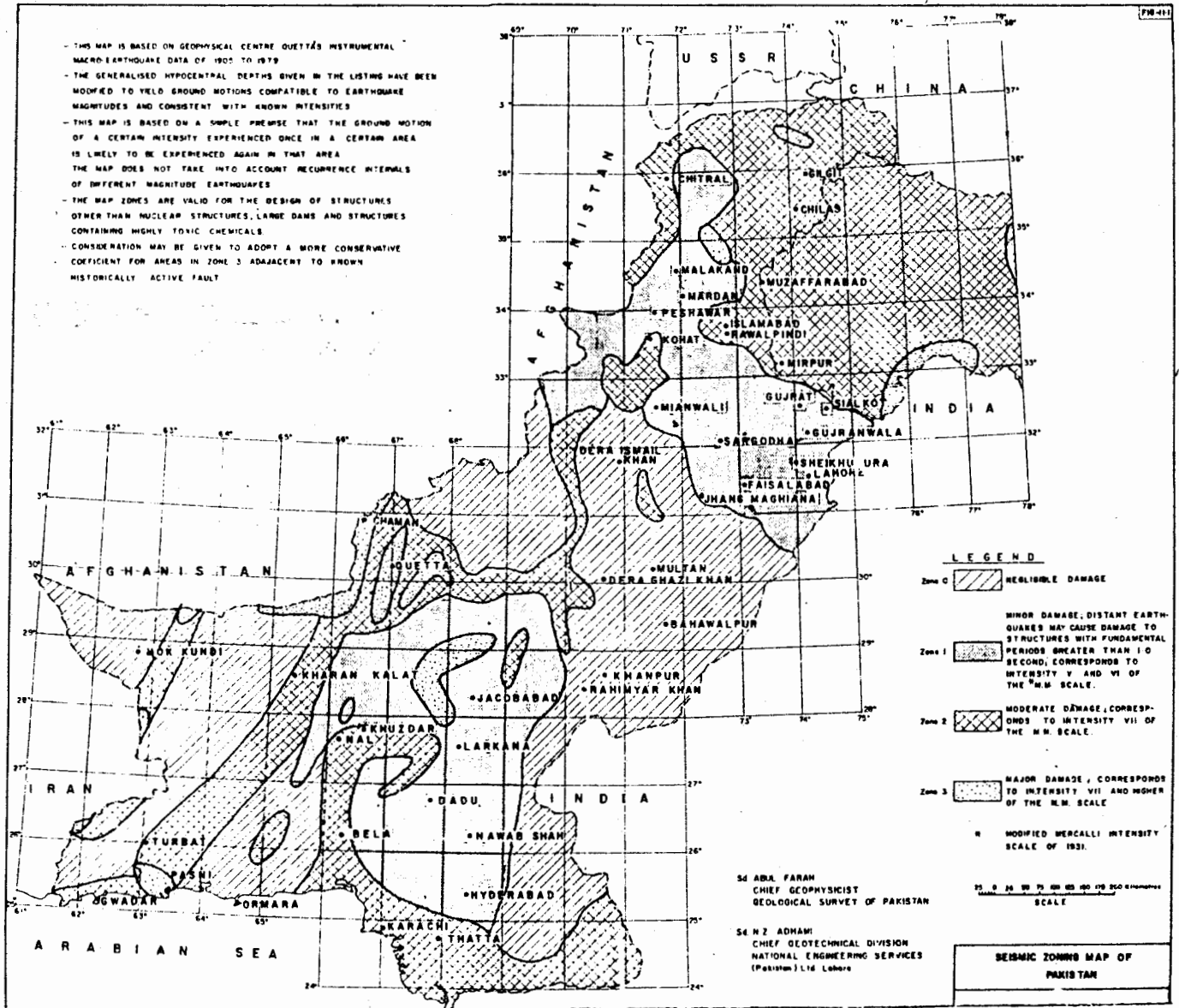


Fig. 8. Seismic risk zoning. (After Farah 1989).

al 1979), and the earthquake history clearly define the seismological sensitivity of Pakistan. In other words, high seismic risks are involved in our social life as can be in g-factor (Fig. 6). Isoseismal (Fig. 7), and the seismic risk zoning maps (Fig. 8) that are prepared by GSP using the seismicity data. Accordingly, areas of Pasni, Gowadar, Quetta, Chaman, north of Malakand, north of Gilgit and the eastern boundary of Sialkot pose major earthquake hazards. Islamabad like other areas fall in a zone that involves moderate seismic hazards.

Among the hazardous earthquake of the recent past, Quetta earthquake ($M = 7.5$) of May 30, 1935, is known to be the most disastrous as it destroyed the whole town and killed 50,000 people. Similarly, Pattan earthquake of December 28, 1974 and Gilgit earthquake of September 12, 1981, were quite sever. Rawalpindi earthquake of Feb. 14, 1977 though was minutely damaging, but the existence of its epicentre about 15 km east of Rawalpindi (Hakim 1991) may be a future threat to the public and sensitive structure in the area.

The effect of major earthquakes are not only confined to ground but may also extend to coastal sensitive structures due to tsunamis which are defined as seismic sea waves which may attain a height of 4 to 10 meters. The hazardous chain effect are summarized in figure 9 and are concerned with earthquakes: i) If its magnitude is 7 or more; ii) If its epicentral zone covers inhabitation and heavy structures such as dams; iii) If man-made structures are poorly constructed are nonresistant to ground vibrations; v) If soil liquifies or amplifies ground vibration during earthquakes.

Prediction and Prevention

Prediction of earthquakes is an attractive question. Extensive research work is in progress, several variables have been identified that vary before the occurrence of earthquake (Rikitake 1976). But there is still a long way to achieve success in predicting earthquake on short term

basis, the location, time and magnitude of the coming shock. However if prediction becomes possible, the critic's view is that off and on mass evacuation and interruption of socio-economic activities will become unbearable and uneconomic. So the best solution in the present circumstances is to adapt alternate strategy, i.e., prevention by preparedness as adapted by the developed word.

Earthquake hazards can be mitigated by preventing the failure or collapse of buildings and other man-made structures (Arya 1981). The prevention strategy is based on the following studies in any country, in the selected region or cities: 1) Seismic zoning and microzoning. 2) Seismic safety of structures. 3) Updating building codes and engineering practices. 4) Soil behavior during earthquakes. 5) Seismological education and public awareness.

Risk assessment in Pakistan

Risk assessment and the level of seismological studies in Pakistan in quite low. Widely spaced short-period three-stations network of Peshawar observatory works for the media to report the scale and location of earthquake, whereas the other two observatories (fully equipped) - one with Pakistan Atomic Energy Commission and the other with WAPDA (Tarbela) - are only site-study oriented. The seismic risk maps mentioned previously are based on moderate quality data and need to be revised in the light of recent earthquakes and the latest seismological knowledge.

By far the most important hazard is the ground vibration, which in turn shakes the buildings and causes the structures to collapse partially or completely. After the Quetta earthquake, a comprehensive building code known as the Quetta Building Code (QBC) was introduced in 1936 to allow only the earthquake resistant constructions. Later on, this code was replaced in 1986 by the Building Code which almost follows the Uniform Building Code for seismic design of ordinary buildings, while three

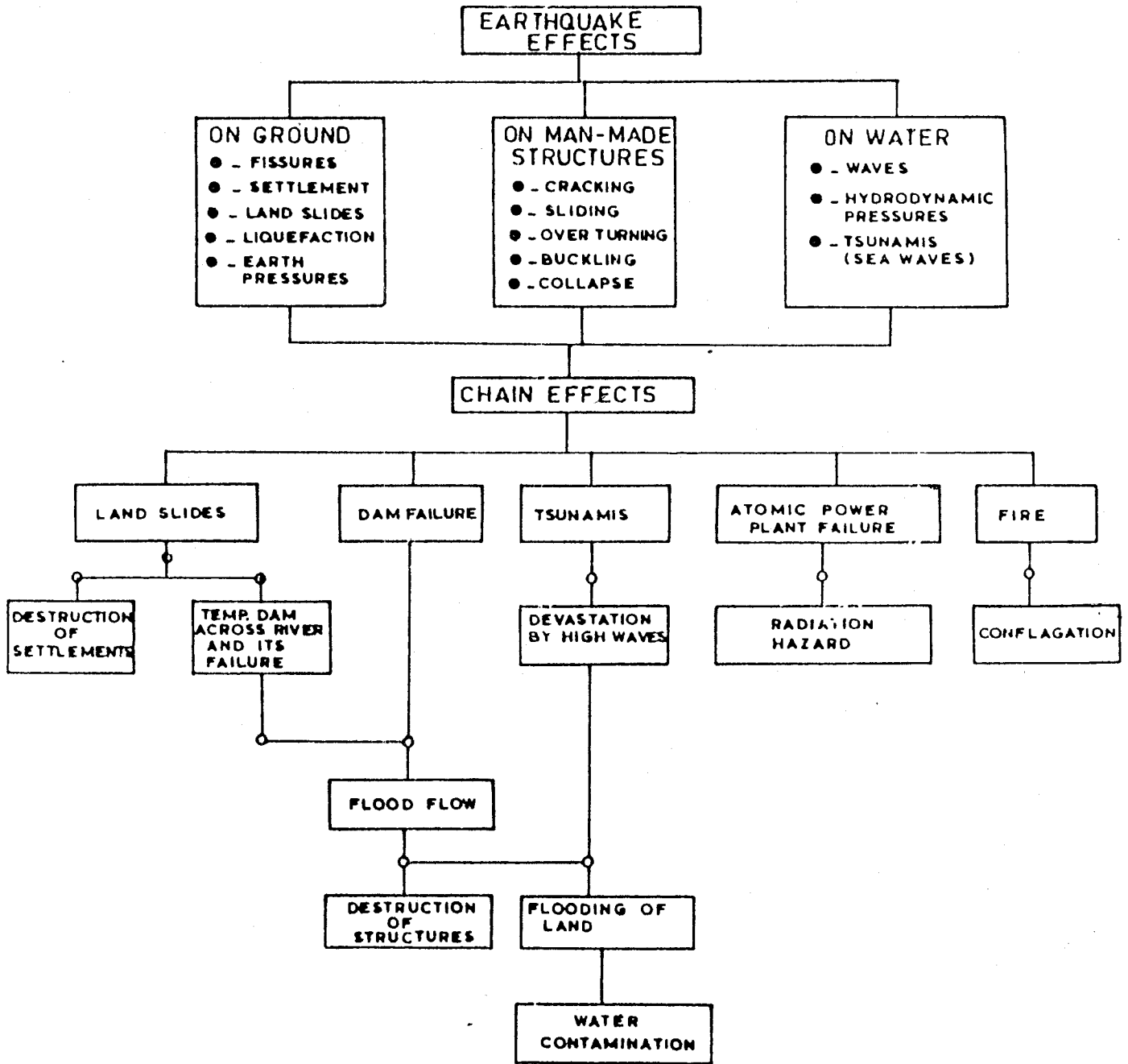


Fig. 9. Direct and chain effects of earthquakes, (After Arya, A.S. 1981).

dimensional dynamic analysis was adopted for special structures. As a matter of fact, Pakistan has so far not developed its own seismic code, but follows the American codes and IAEA guides for different types of civil structures (Hakim 1991). However, the enforced code except for a few public buildings/complexes, is not strictly observed in the private sector due to poor awareness of earthquake hazards masses, and weak legislation.

Similarly, the research on the influence of soils on the behavior of structures during earthquake needs special attention. Because the damage resulting from earthquake may be influenced in a number of ways by the characteristics of soil in the affected area (Seed 1982) as observed in Chilean earthquake of 1960, Niigatan earthquake of 1964, and even in Ziarat (1983) Khuzdar (1986) and Dasht-e-Goran (1990) shocks of Balochistan. Khan (1993) mentioned that the silt deposits on the valley flats of Balochistan amplify the seismic vibration, as damage to buildings of similar design and material on these deposits was greater than those on the piedmont deposits.

Further, the public education and awareness about the earthquake hazards is almost negligible, and consequently, the strategies for mitigating losses are not receiving due attention of the authorities. This issue gets place in the media only when the ground is shaken by the earthquakes or the damages exceed certain limit.

This just because that after the Quetta earthquake of 1935 we did not face the bitter consequences. However, the present environments of rapidly growing population, expanding urbanization and industrialization do not allow to wait any longer, and demand well defined plan and programme on the mitigation of earthquake hazards as precaution.

Planning

Prevention strategies could be developed effectively with the establishment of Centre for

Seismological Studies and Earthquake Engineering. Necessarily the Centre should be equipped with needed facilities of strong motion network, computer system, soil/material studies, and the trained personnel to carry out independent research and to design training and education programmes for the public, engineers/architects, and for the government officials to promote awareness and follow/implement the building code and property insurance schemes. Effective prevention strategy is to include all the five components, i.e., government, public, engineers/architects, seismologists, and the geologists/geographers.

- i) Government is supposed to enforce the regulations of building code and property insurance.
- ii) Engineers/architects should develop economically feasible earthquake resistant construction.
- iii) Seismologists are required to revise seismic zoning and micro-zoning of the country.
- iv) Geologists should demarcate active faults and slide zones.
- v) Geographers should work on land use and physical planning.
- vi) Scientists should study the soil behavior during earthquakes.
- vii) Public should have awareness and follow guidelines.

CONCLUSION

High seismic risks are involved in our social life. Rapidly growing population and expanding urbanization strongly demand and effective implementation on national level of the strategies for prevention and mitigation of earthquake hazards.

REFERENCES

- ARYA, A.S. (1981) Earthquake are avoidable disasters. In Symposium on Earthquake disaster mitigation, University of Roorkee, India. vol.2 pp. 1-7.

- BARAZANGI, M., & DORERMAN, J.** (1969) World seismicity maps compiled from ESSA, Coast and Geodetic Survey, epicentre data 1961-1967. *Bull. Seis. Soc. Am.* vol. 59 pp. 369-380.
- BATH, M.** (1979) *Introduction to seismology.* Birkhauser Verlag, Germany.
- BENIOFF, H.** (1964) Earthquake source mechanism. *Science, N.Y.* No. 143, pp. 1399-1406.
- FARAH, A., LAWRENCE, R.D., & DEJONG, K.A.** (1984) An overview of the tectonics of Pakistan. In *Marine geology and oceanography of Arabian Sea and coastal Pakistan*, eds. Haq, B.U. and Milliman, J.D., New York, Von Nostrand Reinhold. pp. 161-176.
- FARAH, A.** (1989) Earthquake risk. *Nature* vol. 338, 196 p.
- HAKIM, A.** (1991) Damages and counter-measures of masonry in Pakistan. IISE Country Report Nos. 1,2,3.
- JACOB, K.H. & QUITTEYER, R. I.** (1979) The Makran region of Pakistan and Iran: Trench-arc system with active plate subduction. In *Geodynamics of Pakistan*, editors: Farah, A., and Dejong, K.A., pp. 305-317.
- KAZMI, A.H.** (1979) Active fault system in Pakistan. In *Geodynamics of Pakistan*. Editors: Farah. A., and Dejong, K.A., pp. 285-294.
- KHAN, S.N.** (1993) Seismic risk assessment and mitigation in Pakistan with special reference to soil conditions and building types in Balochistan. *Bull. Int. Inst. Seis., and earthquake eng.* vol. 27 pp. 137-154.
- MOLNAR, P., & TAPPONNIER, P.** (1975) *Cenozoic tectonics of Asia: effects of continental collision.* *Science*, vol. 189, pp. 419-426.
- QUITMEYER, R.C., FARAH, A., & JOCOB, K.H.** (1979) The Seismicity of Pakistan and its relation to surface faults. In *Geodynamics of Pakistan*. Editor: Farah, A., and Dejang, A.K., pp. 271-284.
- RIKITAKE, G.** (1976) *Earthquake prediction.* Elsevier Scientific Pub. Co. New York.
- SARWAR, G. & DEJONG, K.A.** (1979) Arcs, oroclines, syntaxes: The curvatures of mountain belts in Pakistan. In *Geodynamics of Pakistan*, Editors: Farah, A., and Dejong, K.A., pp. 341-349.
- SEEBER, L., ARMBRUSTER, J.G., & QUITMEYER, R.C.** (1981) Seismicity and continental subduction in the Himalayan arc. In *Zagros-Hindukush-Himalayan geodynamic evolution.* *Geodynamics Ser. 1.* Editors: Gupta, H., and Denalany, F. *Am. Geophy. Union Washington D.C.*, pp. 215-242.
- SEED, B.H., & IDRIASS, I.M.** (1982) Ground motion and soil liquefaction during earthquakes. *Earthquakes Engg. Res. Inst. California.*
- Seismic risks prevention and mitigation programme in Islamic Republic of Iran, Report No. IIES 69-90-4.
- Manuscript received on 5.6.1994
Accepted for publication on 15.12.1994.

PREPARATION OF ORIENTED CLAY MINERAL SAMPLES FOR X-RAY DIFFRACTION ANALYSIS

JAWED AHMAD

Centre of Excellence in Mineralogy, University of Balochistan
P.O. Box 43 Quetta, Pakistan.

ABDUL HAQUE

Centre of Excellence in Mineralogy, University of Balochistan
P.O. Box 43 Quetta, Pakistan.

ABSTRACT: Good oriented clay mineral sample requires separation and removal of non-clay and non platy minerals in suspension, must be dispersed as individual colloidal particles, because in the flocculated condition they produce submicroscopic to polymineralic aggregates within which the orientation is poor to random. All of this preparation must be accomplished with a minimum use of chemical in order to protect the physical damage of clay minerals.

METHODOLOGY

The following process should have to be taken into account during the preparation of oriented samples for X-ray diffraction (Brindley, 1980; Dixon & Weed, 1977). They are:-

SEPARATING OF CLAY MINERALS FROM CLASTIC ROCKS.

Most common non-clay minerals are feldspar, zeolite, gypsum, quartz, carbonate, pyrite and iron-oxide. The first three from the above list can be often separated from the clay minerals by taking finer portion of the sample, leaving them in the coarser residue.

The X-ray diffraction tracing obtained through these samples will have a rough idea of the proportion of clay and non-clay minerals. Such idea would further make the basis for taking subsequent steps.

10 grams of shale sample was crushed in a porcelain mortar and loaded it into sample holder with emphasis on crushing by impact rather than grinding which can cause phase

changes.

For removal of carbonates, acetic acid digestion is used. Within 250 ml buffered solution, add 10 grams of crushed sample. Stir it at room temperature upto that moment when there is absence of CO₂ bubbles which evidence that either the acid is neutralized or carbonate fraction is gone. Immediately rinse the sample, and the procedure may be repeated till no reaction occurs on adding acid.

When using Cu α target X-Ray, fluorescent X-Ray forms, iron is a problem-producing element showing a high background which can mask peaks. Iron oxide also cements particles together and, thus, to overcome this situation a monochromator may be used in the beam path to short cut the iron radiation. The most commonly used "chemical treatment" is the citrate-bicarbonate-dithionate (CBD) method proposed by Jackson (1969).

Organic material in the samples by using a strong oxidizing agents, such as commercial bleach (MILTON-2): sodium hypochloride (NaOCl), and hydrogen peroxide. NaOCl is quicker, cheaper and

safer than hydrogen peroxide. Each sample of crushed clastic rocks was treated with 10-20 ml. NaOCl and each mixture was then heated in a boiling water bath for about 15 minutes. This was then centrifuge at about 800 r.p.m. for a duration of 5 minutes and decanted. The procedure was repeated until organic material was sufficiently removed with the evidence of sample's color changing to white, grey or red.

IONS IN EXCHANGEABLE POSITIONS

Clay minerals can absorb anions and cations and hold them in an exchangeable state. These ions are exchanged when the clay minerals holding them come in contact with solution rich in other ions (Brindly, 1980; Carroll, 1970).

There is a simple test for this; prepare 10 ml Ag NO₃ and keep it in a light proof dropper bottle. One or two drops of AgNO₃ will cause the precipitation of AgCl, even if there is small amount of Cl ions present. If all Cl ions cannot be removed in this way, final washing should be done by dialysis through which clay can be put into suspension in a dialysis tube, and immersed large volume of warm deionized water. Gentle stirring is helpful and water should be changed four to five times a day until no more ions are detected.

DISPERSION OF CLAY SIZED MATERIAL LESS THAN 2_{μm}.

Dispersion of a sample was carried out in distilled water by crushing the sample to 1 mm size pieces and short soaking for 24 hours followed by 5 minute in a blender or centrifuge having 750 r.p.m. for particle size dia of less than 2_{μm} (after Jackson, 1969).

The removal of soluble salts is the first step. Such salts produce flocculation phenomenon which means opposite charged attract each other and the particles lump together to form a layer of particles within the solution. Thus, with the help of flocculation, clay material can stay at the bottom of container with a

centrifuge. After decantation, refill the container with distilled water. By this way soluble salts can be removed. In case where the dispersion was not achieved after first or second try, then sodium meta-hexaphosphate is added to the solution in order to get the dispersion. The flocculation will help firstly to produce lumps, these lumps settle easily at the bottom of container than the smaller individual particles.

After having got stable dispersion (identified by homogenous appearance from top to bottom of the container) then, slides from these solution can be prepared for X-ray diffraction.

PROCEDURE FOR SAMPLES LESS THAN 0.5_{μm}.

10 grams of sample crushed in a porcelain mortar and pretreatment was carried out for non clay fraction or impurities. After this treatment the sample placed in 125ml beaker with distilled water for duration of 24 hours. If the sample is not properly dispersed, then add 5mg of sodium meta-hexaphosphate as dispersion agent and stir with glass rod, after an hour one mg enough to see the sample is uniformly dispersed in 125ml beaker. Now divide the dispersed solution in three test tube and put it to centrifuge at 4500 r.p.m.

In order to find the required time to centrifuge it at 4500 r.p.m. the given formula has been used by Jackson, 1969.

$$t = \frac{n \log_{10} \frac{R}{S}}{3.81 N^2 r^2 (s)}$$

where t = Required time; n = Diameter of particle; R = Length of titled axis; S = Length of centrifuge tube; N = Revolution/minute; r = Radius in centimeter of R; s = Difference between sp. gravity.

After centrifuging, pour separate/suspended material into another breaker and immediately

prepare slide to run into X-ray diffractometer.

Amer. Spec. Paper, 126 p.80

Generally three slides were prepared from each sample (Brindley, 1980; Drewer, 1973; Kinter & Diamond, 1939).

- a) ADOA- Air Dried Oriented Aggregate, dry in oven at 60-80°C overnight, then store it in a desiccator until ready to run. This means running of sample at zero percent relative humidity.
- b) GOA- Glycolated Oriented Aggregate. This glass slide size (2.7 x 4.6 cm) placed in ethylene glycol in desiccator, let it rest for 1 to 2 days in glycol run.
- c) FOA- Fired Oriented Aggregate. This glass slide put into electric furnace at 550°C for duration of one hour.

DIXON, J.B. WEED, S.B (1977) Minerals in soil environments. Soil. Sci. Soc. Amer, p.948.

DREWER, J.I (1973) The preparation of oriented clay mineral specimen for X-ray diffraction analysis by a filter membrane peel techniques. Amer. Mineral. 58, p. 533-554.

JACKSON, M.L (1969) Soil Chemical Analysis, Advanced Course, 2nd ed. Univ. Wisconsin, Soil. Macl. Soc, 895p.

KINTER, E.G. & DIAMOND, S. (1939) A new method for preparation and treatment of oriented aggregate specimens of soil clays for X-ray diffraction analysis. Soil. Sci. 81, pp. 111-120.

CONCLUSION

Oriented clay mineral sample slides were prepared for less than 2_{μm}, after crushing the sample and pretreatment was carried out for non clay fractions or any other impurities. After this treatment, the dispersion of sample achieved with the help of sodium meta-hexaphosphate. When dispersion achieved the sample is distributed in three test tubes and put it to centrifuge. After this process the glass slides of oriented clay mineral sample is ready to run for X-ray diffraction for treated, glycolated and fired pattern. (Jawed, 1987).

JAWED, A (1987) Clay mineralogy of the Ghazij shale formation of Balochistan, M.Phil. Report, C.E.M. Univ. Baln. Quetta, 9-16pp. (unpublished).

Manuscript received on 2.2.1994

Accepted for publication on 5.3.1994

REFERENCES

- BRINDLEY, G. W** (1980) Crystal structure of clay minerals and their X-ray identification, Monograph. Mineralogical Society London p. 495.
- CARROLL, D** (1970) Clay minerals: A guide to their X-Ray identification. Geol. Soc. Amer. Spec. paper, 126 p.80.
- CARROLL, D** (1970) Clay minerals: A guide to their X-Ray identification. Geol, Soc.

PETROGRAPHIC COMMENTS ON KHEWRA TRAP, THE SALT RANGE, PAKISTAN.

S. M. SHUAIB, SHAMIM A. SHEIKH & SHAHID NASEEM

Department of Geology, University of Karachi, Karachi.

ABSTRACT: The Khewra Trap samples were obtained from two outcrops about 400 meters apart, that are the only igneous rocks occurring in the Pre-cambrian Saline Series sedimentary succession of the Salt Range,. Samples were studied both as hand specimen under the microscope. Khawra Trap is a hard, compact, non-calcareous, porphyritic, and very rough to touch volcanic rock. Phenocrysts, consist of dirty white to gray needles and prismatic crystals which are radiating and also occur random directions; whereas the ground mass is microcrystalline to cryptocrystalline, cherry red and brown to black in colours. No flow structure is observed either from the orientation of the phenocrysts or through colouring of the groundmass. Microscopically Khewra Trap is composed of phenocryst minerals which are partially altered idiomorphic tremolite and completely altered enstatite (antigorite pseudomorphs after enstatite) embedded in the groundmass which is microcrystalline to cryptocrystalline and even glassy (isotropic) at places. The laths and needles are mainly altered alkali feldspars (orthoclase to albite). The rock belongs to trachytic series which was subjected to hydrothermal solutions.

INTRODUCTION

Khewra Trap crops out at a number of locations along the eastern part of the Salt Range in association with the Pre-Cambrian Punjab Saline Series (Fatmi, 1984 & Goe, 1989). Samples were collected from two exposures about 400 meters apart for petrographic examination (Figure 1). Previous investigations on Khewra Trap were made by Fleming (1853), Theobald (1854), Wynne (1978), Pascoe (1920), Chhibber (1944), Gee (1944 & 1989), Mosebach (1956) and Martin (1956; 1962). However, detailed petrographic investigations on Khewra Trap were carried out by Mosebach and Martin. Mosebach considered Khewra Trap as a volcanic rock lying between alkali-trachyte and lusitanite on the basis of microscopic, X-ray and chemical analyses. He calculated from the chemical analysis of fresh portion of Khewra Trap the normative minerals as potash feldspar 66.0%, enstatite (Fe-poor) 30.8%, ilmenite 1.2%, hematite 1.8% and apatite 0.2%. Martin (1956 & 1962) investigated the Khewra Trap rock samples obtained from the outcrops and the cores from Dhariala well drilled in the eastern part of the Salt Range (Figure 1). He called the rock variolitic basalt. He mentioned about the flow texture in Khewra Trap, total

absence of ferromagnesian minerals, and phenocrysts being completely replaced by fibrous gypseous material, the ideas with which the authors of the present paper do not agree.

STRATIGRPHY

The Salt Range consists of slightly curved, east-west oriented mountain range south of the Potwar plateau (Fig. 1). Generally it has been assumed that the salt Range resulted from an uplift along a fault at its southern margin, allowing for minor southward (Gee 1989). The exposed formations of the range are all unmetamorphosed sediments with the exception of the local occurrences of Khewra Trap, a much weathered lava flow occurring sporadically. The Trap in Khewra gorge (Fig. 2) is gently dipping, and shows layering parallel to the overlying beds of marl and gypsum, and underlying beds of laminated carbonaceous dolomite having a maximum thickness of about seven meters (Martin, 1956). In the eastern Salt Range, the Saline Series is the oldest exposed rocks of Pre-Cambrian age, followed by thick Cambrian sequence (Jehlum Group), which is unconformably overlain by rocks of Permian age as shown in the table below.

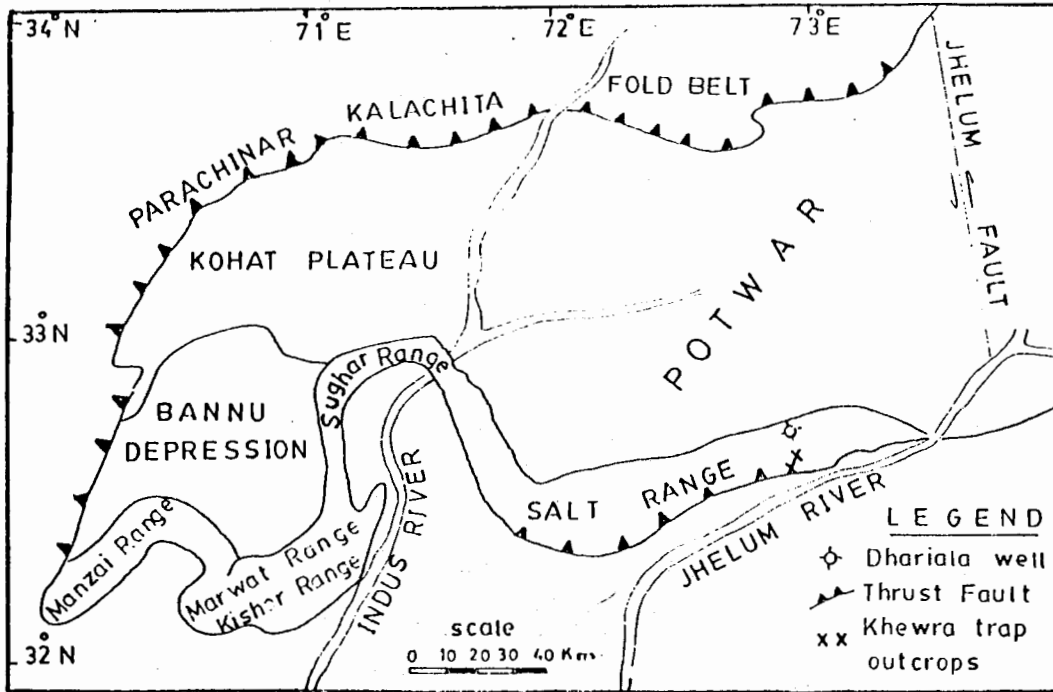


Fig. 1. Potwar - Kohat - Bannu Geological Province of Pakistan showing position of the Khewra Trap outcrops and Dhariatala well in the eastern part of Salt Range.

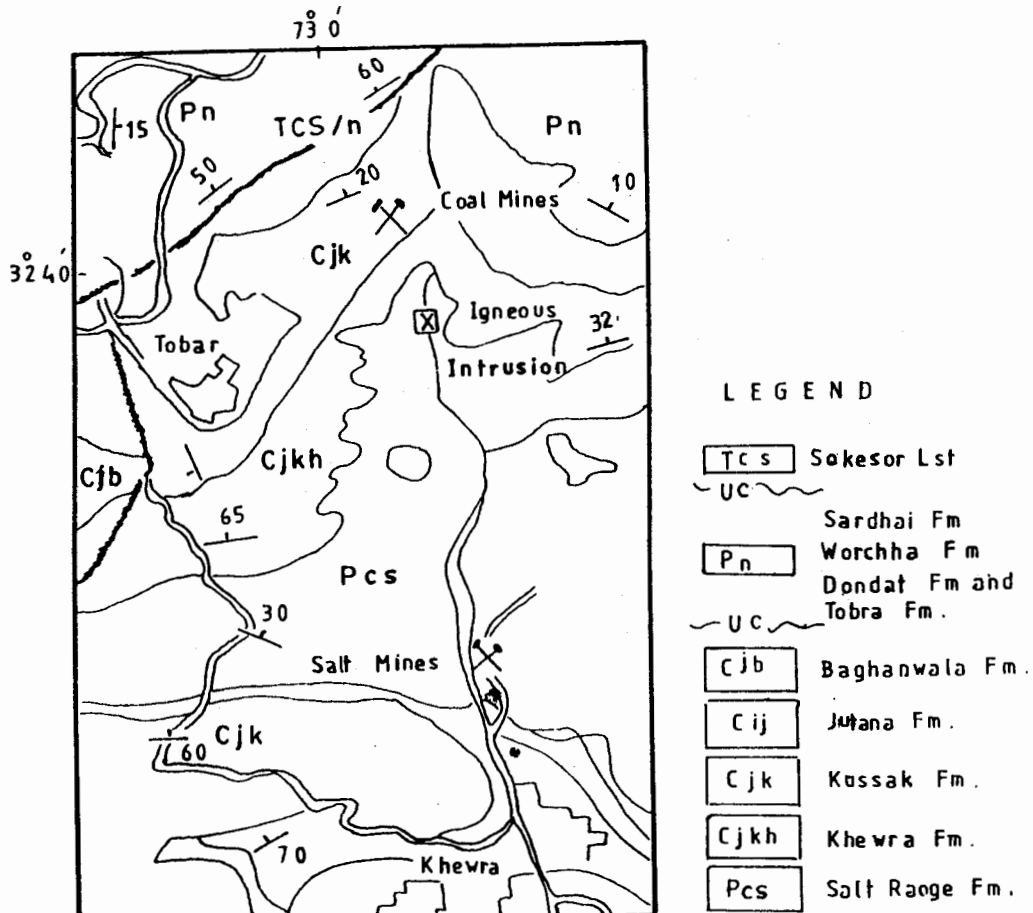


Fig. 2. Geological map of Khewra Gorge showing location of igneous intrusion (after Fatmi, 1984).



Plate 1. Photograph of a Khewra Trap sample showing phenocrysts of radiating prismatic crystals which also lie in random directions in microcrystalline to cryptocrystalline groundmass having patches of cherry red, brown and black.



Plate 2. Radiating idiomorphic prismatic crystals of partially altered tremolite with brownish relics in brownish microcrystalline to cryptocrystalline groundmass in which laths of feldspars (F) are embedded at random direction. C. Empty space formed during slide making. Polarized light (X 50).



Plate 3. Phenocrysts of idiomorphic, prismatic and rhombic crystals of partially altered tremolite (T) with brown relics and altered brown enstatite (P) (antigorite) are embedded in microcrystalline to cryptocrystalline groundmass. Polarized light (X 50).

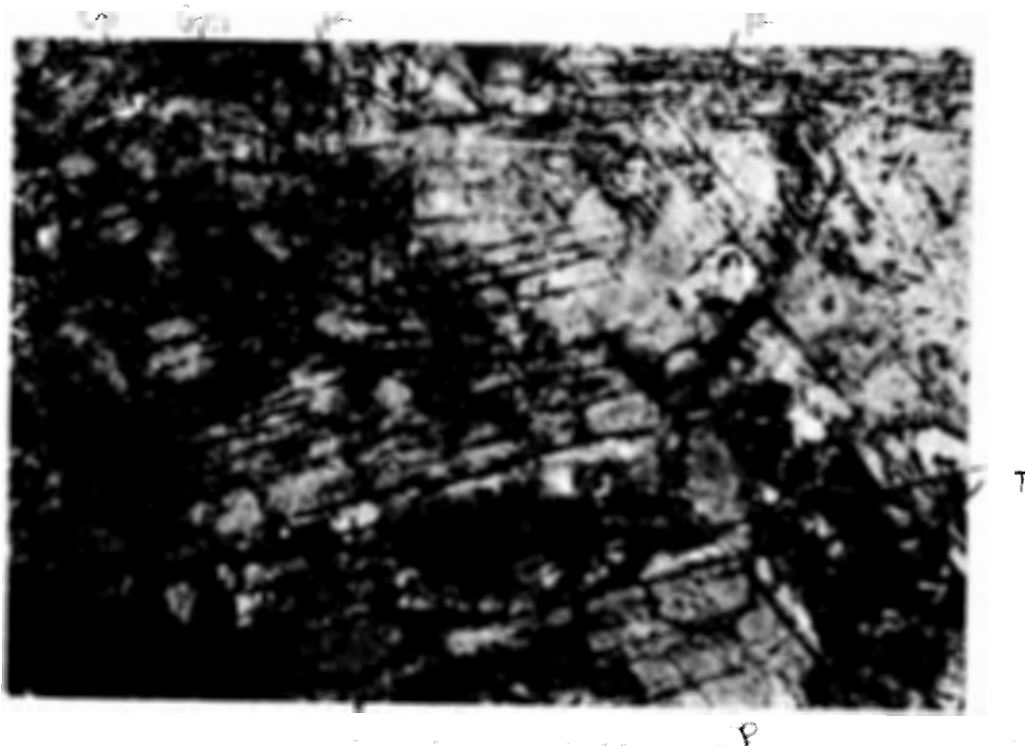


Plate 4. Phenocrysts of partially altered, idiomorphic prismatic tremolite with brown relics in the central portions, and brown rectangular altered enstatite preserving cleavage traces at about right angle (antigorite) in microcrystalline to cryptocrystalline groundmass. Polarized light (X 50).



Plate 5. Feldspars microlites, radiating and in random directions. A small idiomorphic, prismatic and partially altered tremolite. A cavity with highly irregular rims filled with secondary siliceous (cq) and ferruginous materials(cs). Polarized light (X -50)

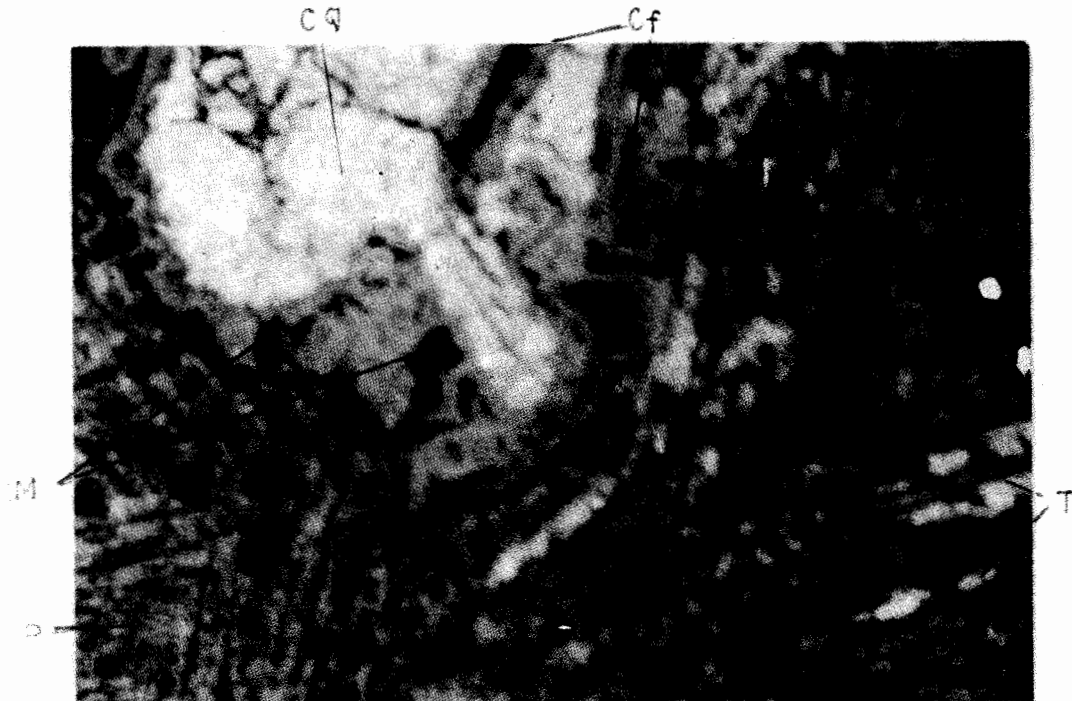


Plate 6. Phenocrysts of partially altered small prismatic tremolite and brownish altered enstatite preserving zoning (antigorite) in microcrystalline to cryptocrystalline groundmass in which laths of altered feldspars are present. A cavity filled with secondary quartz grains having highly irregular siliceous and ferruginous rims with development of magnetite grains. Polarized light (X 50).

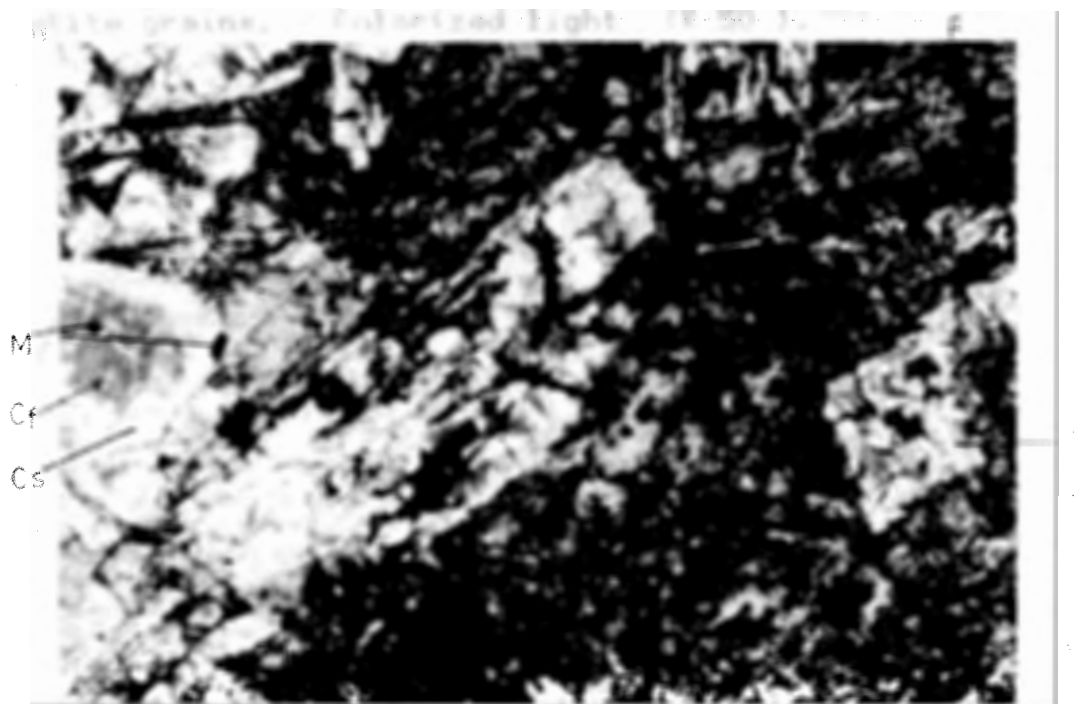


Plate 7. Phenocrysts of idiomorphic cracked rhombic and prismatic tremolite with brownish relics in the central areas and rhombic cleavage traces embedded in brownish microcrystalline to cryptocrystalline groundmass, in which laths of microlitic altered feldspars are present. An irregular cavity is filled with secondary siliceous and ferruginous materials and a few small magnetite crystals (M). Polarized light (X 50)

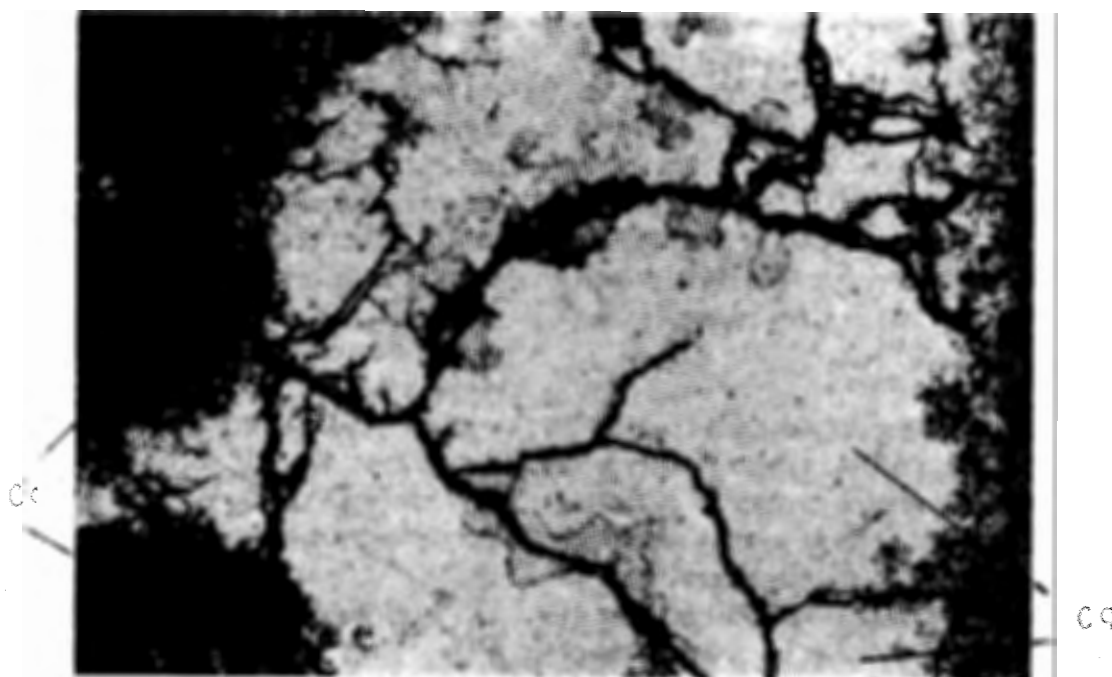


Plate 8. Cavity is filled with secondary irregular quartz grains which are surrounded by ferruginous(Cf) and calcareous (Cc) highly irregular rims. Polarized light (X 50).

Age	Group	Formations	Thick- ness (metres)	Rock Type
PERMIAN SEDIMENTS				
----- MAJOR UNCONFORMITY -----				
Cambrian	Jhelum	Baghanwala (Salt pseudomorph beds)	35-100	Blood red shales and flaggy sandstone with salt pseudomorphs.
		Jutana (Magnesian Sandstone)	80-100	Massive light coloured dolomite & dolomitic sandstones, subordinate shales.
		Kussak (Neobolus shales)	40-80	Grey and purplish shales & glauconitic sandstones, pebbly bed at base.
		Khewra sandstone (Purple sandstone)	160-200	Massive maroon fine-textured sandstones, & maroon, shales.
Pre-Cambrian		Salt Range Formation (Punjab Saline Series)	+ 800	Red gypseous marl with rock-salt; gypsum-dolomite above; occasional oil shale & Khewra Trap

PETROGRAPHY

Khewra Trap in the hand specimen is a hard, compact, non-calcareous, porphyritic, rough to touch volcanic rock, in which the microcrystalline to cryptocrystalline groundmass varies in colour from cherry red, brown to black in the form of patches of different sizes. Prismatic phenocrysts are either radiating, spherulitic or in random directions having an average dimension 10:2:1 (Plate 1). Microscopically, the constituents of Khewra Trap may be divided into three characteristic groups, namely: Phenocrysts; Groundmass, and Amygdales.

Phenocrysts: Phenocrysts form about 35% of the section and are of two types. First type is partially altered, idiomorphic, mostly euhedral, prismatic and rhombic in form, mainly radiating, spherulitic, colourless to slightly greenish, with fairly high relief. Cleavage is not clear because of alteration but in a few rhombic sections, traces of two directions of rhombic cleavages are observed. Brown relics resembling groundmass are present in most of this type of phenocrysts which are generally present in their central portions. This phenocryst mineral belongs to amphibole group

and seems to be tremolite. The presence of relics mostly in the central areas and resembling groundmass indicates the formation of tremolite from the composition of solidified lava with the introduction of hydrothermal solutions (Harkor, 1950, p.37 - 39). Relics are the remainings of the lava which the idiomorphic tremolite crystals had not been able to utilize, throw or remove during crystal formation (Plates 2-7). The second type of phenocryst mineral in thin sections has the same brown colour as the groundmass and seems to be part of it, but is has a definite rectangular outline and traces of two directions of cleavage at about right angles. Relief is low and refractive index is greater than canada-balsam but less than tremolite phenocrysts. It is mostly euhedral in form. The mineral belonged to pyroxene group but was completely altered with the introduction of hydrothermal solutions, and now seems to be antigorite pseudomorphs after enstatite.

Groundmass: Groundmass forms about 60% of the thin section, brownish in colour, microcrystalline to cryptocrystalline and even glassy (isotropic) at certain places. Brownish colour in groundmass is due to the presence of hematitic and limonitic dust. A few microscopic magnetite grains are presents. Altered brownish

needles and laths of feldspars are embedded in the groundmass and look part of the groundmass but are distinguished by their outlines. Relief and refractive index of feldspars are difficult to determine as they are part of groundmass but a few of them occurring cracks seem to be alkali feldspars (orthoclase to albite).

Amygdales: Amygdales are not very common and difficult to recognize in hand specimen. They may form about 5% of the thin section. They are the cavities /vesicles of the rock filled by secondary materials. The secondary fillings consist of ferruginous, calcareous and siliceous constituents. Amygdales are highly irregular in shape and in most cases the central parts are composed of angular quartz having calcareous, ferruginous and siliceous rims often containing grains of magnetite (Plates 5-8).

CONCLUSION

Khewra Trap is porphyritic volcanic rock exposed in the eastern part of the Salt Range in association with the Saline Series of Pre-Cambrian age. It is the only igneous rock found in the Salt Range and has been under investigations since 1853. Detailed petrographic investigation on Khewra Trap were carried out by Mosebach (1956) and Martin (1956 & 1962). Mosebach described the rock as between alkaline trachyte and lusitanite in composition based on mainly X-Ray and chemical analyses of Khewra Trap samples. Martin termed the rocks as variolitic basalt based on megascopic and microscopic examination of the Khewra Trap samples from the outcrop, and these from the cores of Dharia well in the eastern Salt Range (Fig. 1). He observed flow texture and noted absence of ferromagnesian minerals and phenocrysts completely replaced by fibrous gypseous materials. But our petrographic investigations, both megascopic and microscopic, prove the presence of ferromagnesian phenocrysts belonging to both amphibole and pyroxene groups, though they are partially to completely altered but generally preserve their original forms and cleavage traces. Altered feldspars are mostly microlites which occur radiating and at random

laths and needles embedded in the brownish crystalline to cryptocrystalline, and in parts glassy groundmass. Feldspars seem to be the alkali variety. Flow structures are not observed either from the orientation of the phenocrysts or in the directional colouring of the groundmass.

Cavities are present which were formed due to escaping gases from lava under rapid cooling. These cavities are highly irregular in shape and are filled by secondary ferruginous, calcareous and siliceous are composed of angular and irregular quarts. The rock seems to belong to trachyte series which had undergone alteration through hydrothermal solutions.

REFERENCES

- CHIBBER, H.L.** (1944) The age of the Saline Series of the Salt Range, Punjab: Proc. Nat. Acad. Sc. India, 14, pt. 6, pp. 244-248
- FLEMING, A.** (1853) On the Salt Range of the Punjab: Quant. Jour. Geol. Soc. IX, pt. 3, pp. 189-200.
- FATIMI, A. N. ET AL.** (1984) Geology of Salt Range: First Pakistan Geological Congress, Lahore. pp. 1-14.
- GEE, E. R.** (1944) The age of the Saline Series of the Punjab and of Kohat: Proc. Nat. Acad. Sc. India, 14, pt 6, pp. 269-312.
- _____ (1989) Overview of the geology and structure of the Salt Range with observations on related areas of northern Pakistan. Geol. Sur. of Amer. Special paper 232, pp. 95-112.
- HARKER, A.** (1950) Metamorphism: Methuen & Co. Ltd. London. pp. 37-39 & 86-87
- MARTIN, N. R.** (1956) The Petrography of Khewra Trap rock, Salt Range, West Pajistan. Rec. Geol. Sur. Pak. vol VIII, part 2, pp. 45-48

_____(1962) Mosebach on the Khewra Trap
The Geol. Bull. Punjab Univer. No. 2.
pp. 57-58

MOSEBACH, R. (1956) Khewrait Vom Khewra
Gorge, Pakistan: ein neues Typus
kalireicher, Effusivgesteine Neues JB,
Abh. 89, pt. 2, pp. 182-209.

PASCOE, E. H. (1920) Petroleum in the Punjab
and North West Frontier Provinve: Mem.
Geol. Surv. India. XI. pt. 3, pp. 331-493.

THEOBALD, W. (1854) Notes on the geology
of the Punjab Salt Range: Jour, Asiat.
Soc. Beng. XXXIII, 651 p.

WYNNE, A. B. (1978) On the geology of the
Salt Range in the Punjab: Mem. Geol.
Surv. India, XIV, pp. 1-305.

Manuscript received on 30.5.1994

Accepted for publication on 15.10.1994.

DOLOMITE RESERVES WITHIN CHILTAN RANGE, SOUTH OF QUETTA DISTRICT, BALOCHISTAN, PAKISTAN.

ABDUL HAQUE

Centre of Excellence in Mineralogy, University of Balochistan,
P.O. Box 43, Quetta, Pakistan.

JAWED AHMAD

Centre of Excellence in Mineralogy, University of Balochistan,
P.O. Box 43, Quetta, Pakistan.

MIAN HASSAN AHMAD

Geological Survey of Pakistan, P.O. Box 15 Quetta, Pakistan.

ABSTRACT: Estimated reserves of dolomite have been discovered at least in two localities around Quetta valley within Chiltan Range. At Zierat nala approximately 2555 million long tons, and at Gwani nala 1010 million long tons reserves of dolomite, associated with Chiltan Limestone of Jurassic have been estimated.

INTRODUCTION

Dolomite reserves have been discovered at large scale in two localities around Quetta valley in Chiltan Range, namely: at Ziarat nala, and Gwani nala, which are easily accessible upto the deposits of dolomite. Ziarat Nala 17 Km., S-W of Quetta near RDC highway, is lying on the southern edge of Survey of Pakistan toposheet No. 34 J/16 with Lat: 30° 00" to 30° 02' 01" and with long: 66° 49' 28" to 66° 51' 38". Gwani nala on the other hand, 27 Km., S-E of Quetta, near Sukkur highway, occupies southeast corner of Survey of Pakistan toposheet No. 34

N/4 with Lat: 30° 00' 00" to 30° 01' 50" and with long: 67° 00' 00" to 67° 03' 03".

Previously, dolomites had been reported in the area, by Bagwa and Ahmad (1981); but Ahmad (1974) claimed that dolomite deposited were reported initially by him at Ziarat Nala. His arguments were based only one sample of dolomite, but he did not publish any exclusive reported on dolomite. The present paper is based on the discovery of different localities of dolomite in Quetta region from where sample have been collected; their chemical analyses has been shown in Table. 1.

Table: 1 CHEMICAL ANALYSIS OF DOLOMITE FROM ZIARAT NALA SW OF QUETTA & GWANI NALA SE OF QUETTA.

SAMPLE NO.	INSOL %	Fe _{2O3} %	Al _{2O3} %	CaO %	Mg ^o %	H ₂ O %	H ₂ O ⁺ %	L.O.I. %
CNZ 20	0.82	0.43	0.67	39.25	15.32	0.02	0.12	43.12
CNZ 20 A	2.60	0.32	0.18	38.19	15.32	0.08	0.11	43.10
CNG 6	1.28	0.32	0.68	35.89	17.75	0.07	0.12	43.99
CNZ 20 B	0.21	0.20	0.30	33.65	18.55	0.05	0.15	46.58
CNZ 20 C	0.36	0.28	0.70	32.77	19.16	0.14	0.16	46.82
CNZ 208	0.18	0.22	0.08	31.73	20.27	0.10	0.21	47.01
CNZ 4	0.21	0.20	0.30	33.65	18.55	0.05	0.15	46.58

CALCULATION OF DOLOMITE RESERVES

The average specific gravity of dolomite is 2.85 lbs., the average weight of one cubic foot of water when its specific gravity is one, is equal to 62.4 lbs. The constant for dolomite is 2240. Thus, calculation of reserves of dolomite in tonnage by the formula.

$$\frac{\text{Volume of dolomite in cubic feet} \times 2.85 \times 62.4}{2240} = \text{Million long tons}$$

Where volume of dolomite in feet is equal to average length (L) x average width (W) x average height (H)

At Ziarat Nala

Volume of dolomite is 13124 x 459.35 x 5338.187 equal to 3.218060992 cubic feet.

Tonnage at Ziarat nala is 2554.91 million long tons.

At Gwani Nala

Volume of dolomite is 10827 x 9.84 x 1200 equal to 127845216 cubic feet.

Tonnage at Gwani Nala is 1010 million long tons.

USES

Dolomite rock has three important industrial applications

- i) As refractory bricks after calcining and dead burning.
- ii) As fluxing material to blast furnace and steel melting shop and in ferromanganese furnace.
- iii) As manufacturer of mineral wool and as an extender in paints.

Other minor, but important, uses of dolomite are that it is used as a powder used for dusting the faces of coal mine working to prevent coal seam from catching fire; as carrier to fertilizer mixture and in the manufacture of floor tile.

CONCLUSION

In the region of Quetta Valley economic deposit of valuable and workable reserves of dolomite rock, associated with Chilton Limestone of middle Jurassic, have been discovered at two localities viz: Ziarat and Gwani Nalas. The estimated reserves are respectively 2555 and 1010 million long tons, which can be excavated and used in industries surrounding Quetta Valley, both for the welfare of the region and for the industrial growth of Pakistan.

REFERENCES

- AHMED H.** (1974) Interim Report on Dolomite Deposits of Chilton Range, Quetta Pishin District, Balochistan, Pakistan. Geol. Surv. Pak. Inf. R.T.L. 85.
- AHMED Z.** (1975) Geology of Mineral deposits of Balochistan. Geol. Surv. Pak. Rec. Vol.36, PP. 111-115.
- BAGWA, S.K. & AHMED, H.** (1981) Geology of Chiltan (Quadrangle 34 J/16), Quetta District Balochistan. Geol. Surv. Pak. Inf. R.T.L. 161.
- SINHA, R.K.** (1986) Industrial Minerals, 11nd Edition OXFORD PRESS, PP. 157 - 163.

Manuscript received on 6.2.1994

Accepted for publication on 24.3.1994

MEASUREMENT OF SPECTRAL INDUCED POLARIZATION ON ROCK SAMPLES CONTAINING SULPHIDE MINERALS

SYED WAQAR HAIDER NAQVI

Geological Survey of Pakistan, P.O. Box 15, Quetta, Pakistan.

ABSTRACT: Spectral induced polarization (SIP) method is recently introduced in mining and petroleum exploration. Physical and electrical parameters that influence the induced polarization (IP) phenomena of sulphide bearing rock have been studied. Laboratory SIP measurement were done on rock samples which were collected from Hokuroku and other parts of Japan.

Analyses and interpretation of the data discriminate the host rocks in to three classes which are highly polarizable, moderately polarizable and unpolarizable.

INTRODUCTION

The induced polarization (IP) method has become increasingly used in mining exploration during the last few decades. This method provides diagnostic information regarding the presence of a particular type of minerals, such as a sulphide, oxide, and graphite. It is difficult to identify them by other geophysical methods. IP study is presented to prove the worth.

I.P. METHOD

There are two conventional ways to measure IP phenomena. The first is time domain measurement and the second is frequency domain measurement.

In the time domain measurement, we measure the decay curve of residual voltage with some time windows (Fig. 1.d,f). Square wave current which has off-time parts is usually used. IP parameters, such as chargeability, are calculated from the shape of the curve.

In frequency domain measurement, impedance between output voltage and input current is measured as a function of frequency at two or more frequencies (Fig. 1-c,e). We used square wave current, and amplitude and phase of

basic frequency signals are measured. Percent frequency effect (PFE) is defined as follows. Madden T.R., T. Cant Well (1967).

$$PFE = 100 (p_{dc} - p_{ac}) / p_{ac}$$

Where P_{dc} and P_{ac} are apparent resistivities at d.c. and high frequency, respectively. Usually P_{dc} is measured at about 0.1 Hz and P_{ac} is at about 1 HZ.

Recently, (SIP) method has been introduced. In this method impedance is measured over a wide range of frequency by using sophisticated equipment, which is controlled by microprocessors that are installed inside. Nowadays the SIP technique has been used worldwide for wide variety of application: for example, hydrocarbon exploration, disseminated and massive sulphide exploration, ground water, and geothermal exploration.

The purpose of SIP method is to discriminate rock types by classifying characteristics of IP responsible of subsurface medium over a wide frequency range. It is important to distinguish IP responses due to desired sulphide mineralization from those due to various uneconomic geologic materials. The latter includes both sulphide and non-sulphide:

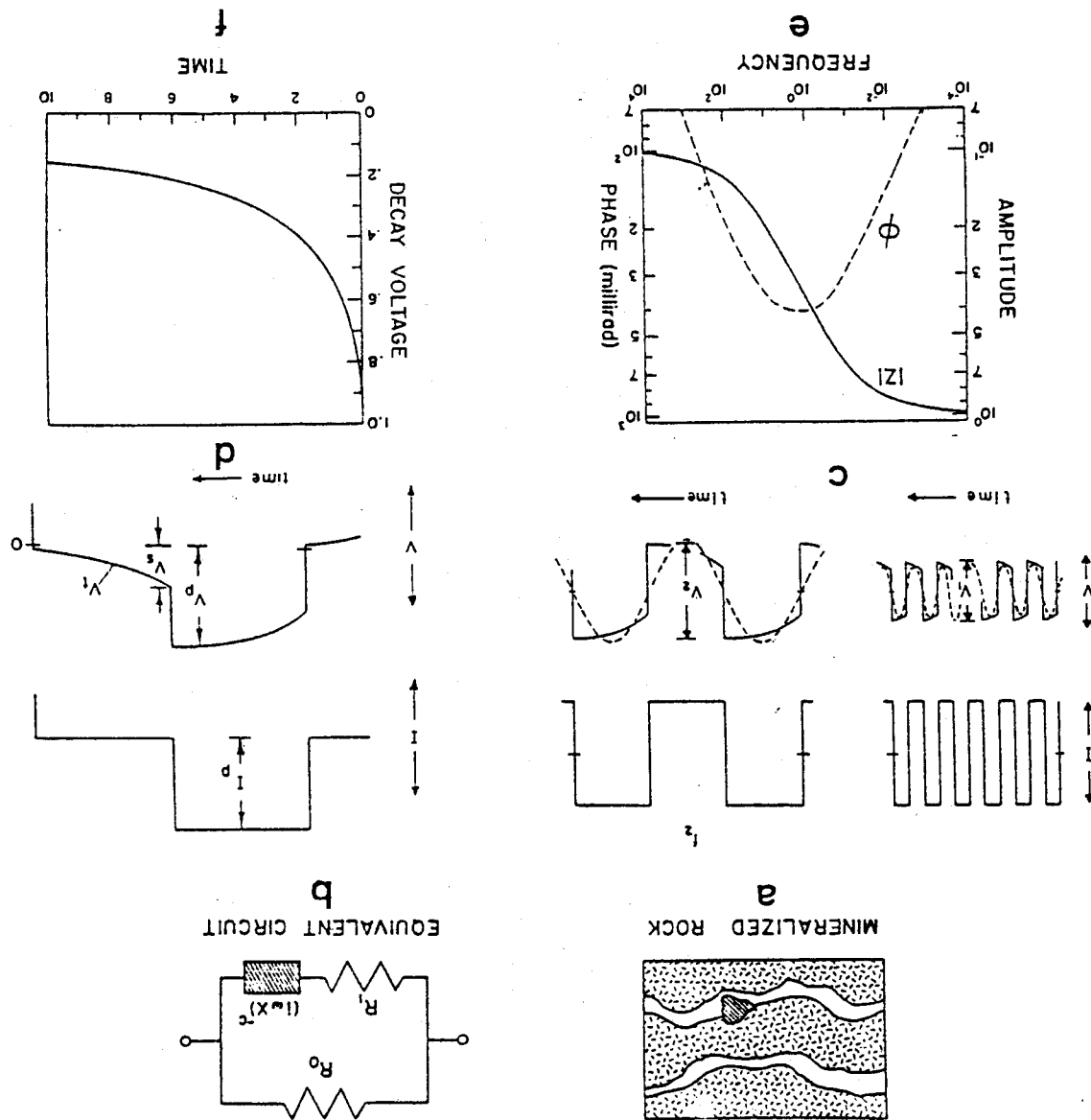


Fig. 1. Basic concept of IP phenomena and typical record signals. (a) and (b) are a schematic model and equivalent circuit of mineralized rock, respectively. (c) and (e) are wave form and spectrum of frequency domain.

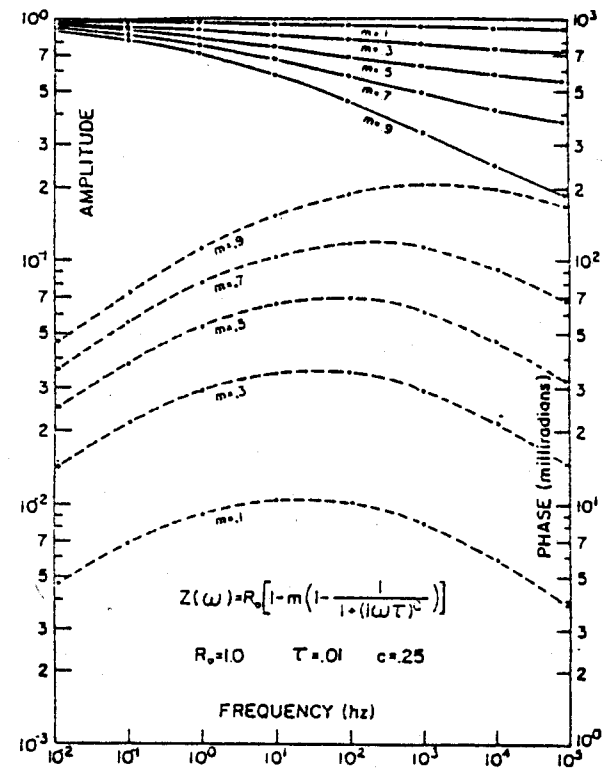


Fig. 2. Amplitude and phase curves for a Cole-Cole relaxation model with $R_0 = 1.0$, $\tau = .01$, $c = .25$, and m varying from 0.1 to 0.9.

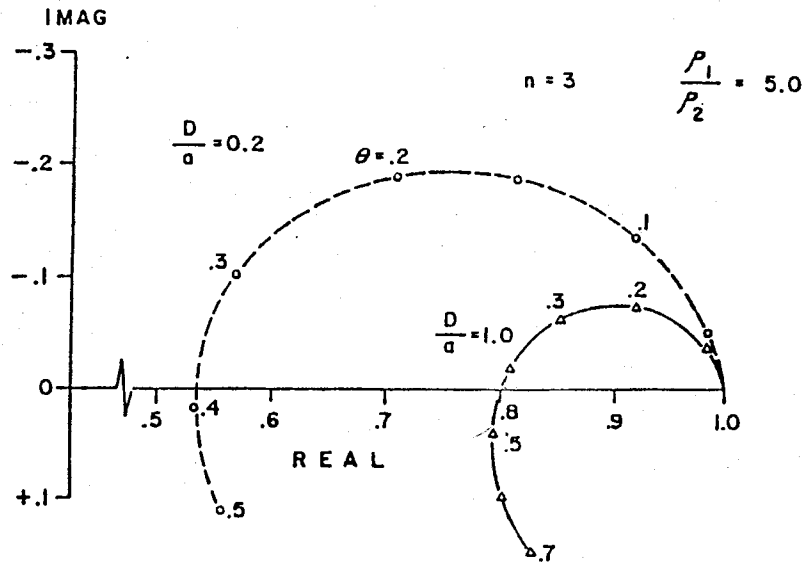


Fig. 3. Theoretical inductive coupling effects of dipole-dipole configuration over a two-layered earth. Resistivity contrast of overburden and basement is 5, -n-spacing is 3, and ratios of the thickness of overburden and a-spacing are set as 0.2 and 1.

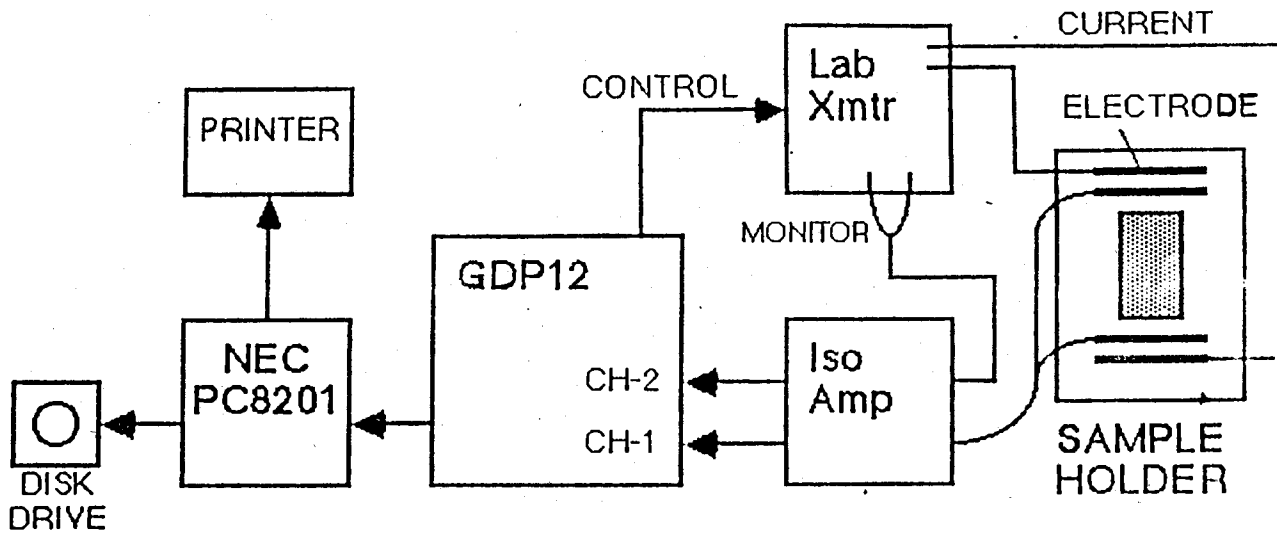


Fig. 4. Block diagram of the measurement system.

for example, pyrite, graphite, magnetite, hematite, and clay. Since resistivities are similar among these materials, electrical methods which deal resistivity distribution can not distinguish them. However, if we carry out SIP over a wide frequency range, we can distinguish them by observing difference of their frequency responses.

Numerous researchers have examined the relationship between specific types of mineralization and their IP responses by laboratory measurements on small rock samples. Madden and Marshalls (1959) studied membrane effect on IP by using manufactured clay and synthetic ion exchange samples. Fraser and Sill (1964) examined polarization responses of clay bearing sandstone. Elliot and Guilber (1974) reported on the responses caused by magnetite, which has intergrowth of hematite and ilmennite. Sumner (1976) summarized the procedure of laboratory work on IP. The identification of fine sediments was discussed by Iliceto, et.al (1982). Complex resistivity of synthetic sulphide bearing rock was studied by mahan, et al. (1986).

However, the impedance of field IP data contains both IP effect and inductive coupling. The inductive coupling is due to electromagnetic interaction of the currents flowing in the wires. The magnitude of this effect increases with electrode spacing and with the increase of frequency (Hohmann 1973, 1975; Dey and Morrison, 1973). The removal of inductive coupling becomes a great problem in the analysis of field IP data.

In the case of dipole-dipole electrode configuration on a uniform earth, phase-shifts due to the inductive coupling are in the same direction as IP effect of subsurface polarizable materials. It is called normal coupling. If the geometry is more complex, the inductive coupling causes great distortion of the IP effect.

Removal of the normal coupling from field data was discussed by Pelton et al. (1978), and Hallof and Pelton (1980). In their method, the field data were analysed by using two Cole-

Cole dispersion equation. Impedance $Z(\omega)$ is written as follows

$$Z(\omega) = R_0 \left\{ 1 - m_1 \left[1 - \frac{1}{1 + (i\omega\tau_1)^{C_1}} \right] - m_2 \left[1 - \frac{1}{1 + (i\omega\tau_2)^{C_2}} \right] \right\}$$

The exponent of the frequency is less for the IP effect than for the normal coupling. Hallof and Pelton (1980) stressed two points which represented their technique to remove inductive coupling. (1) The phase curve of Cole-Cole dispersion is symmetric about the peak value (Fig. 2), whereas the normal inductive coupling is not. Therefore field data only up to peak phase-shift should be considered in the inversion. (2) If some IP effect is present, it is easy to determine the deviation of the observed curve from the predicated curve of inductive coupling at lower frequencies.

Wynn and Zonge (1975) described a different way of removal of inductive coupling and they applied their method to field data. They calculated inductive coupling over horizontally stratified earth (Fig. 3), and applied these calculated value to observed data.

SAMPLE MEASUREMENT

Samples: Induced Polarization Measurement was carried out on 34 rock samples which were collected from some parts of Japan (Hokuroku, Sazare, Hitachi, and Shimokawa) by the Geological Survey of Japan and the Metal Mining Agency of Japan. these samples were divided into seven groups for measurement (Table1).

Preparation: The samples were put into an electric oven and dried at 107°C for about 24 hours, then dry weight (W3) of the samples were measured. After that, they were dipped into water for 24 hours in room pressure and for 24 hours in a vacuum chamber to reintroduce water into them. One container was used for each group. Two kinds of water were used. Processed water was used for all samples and tap water was for seven samples in group 8 (H, MA17) and group 9 (C, F,O, MA2, MA4).

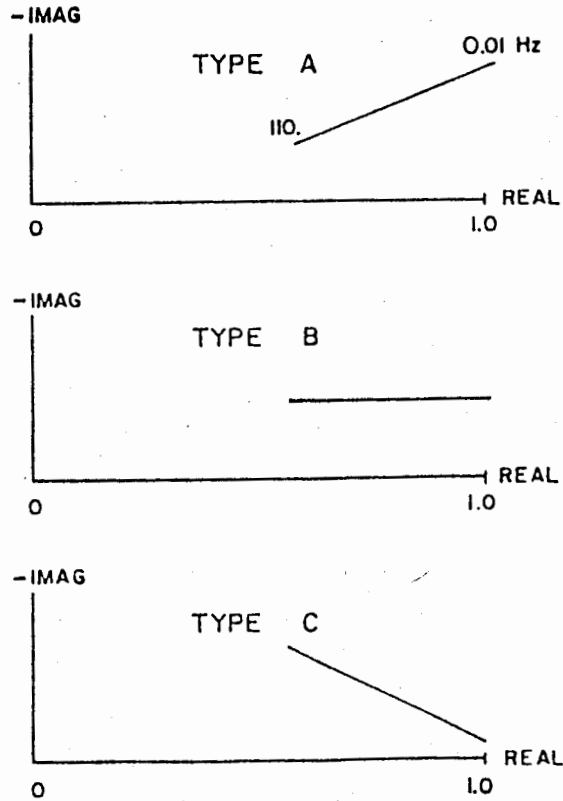


Fig. 5. Basic signatures of IP spectrum.

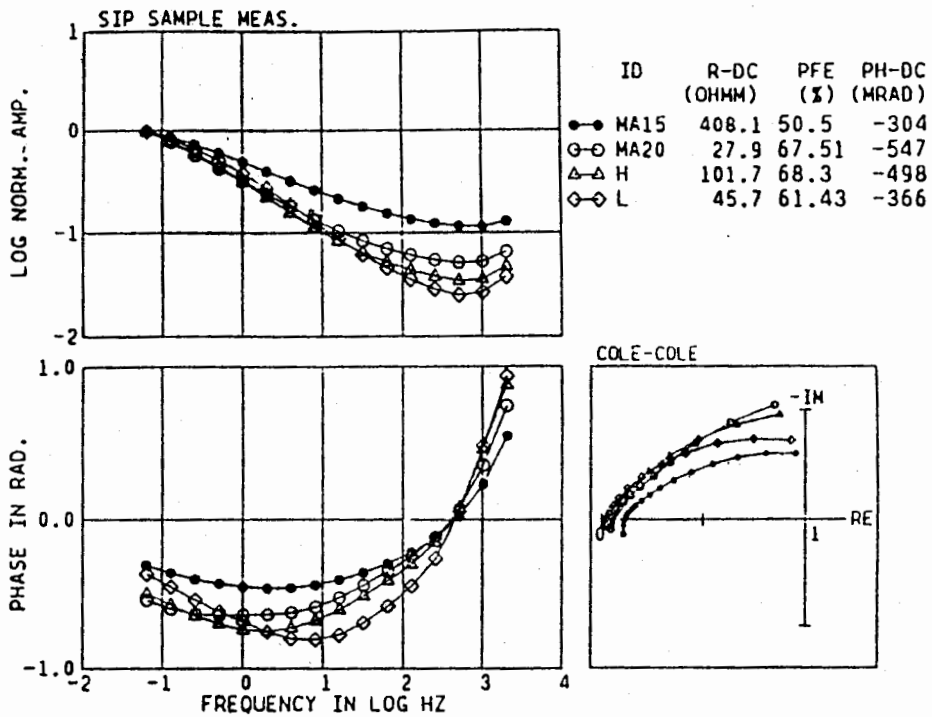


Fig. 6. Spectrum of highly polarizable rocks (type A). Amplitudes are normalized by the value of .0625 Hz. R-DC and PH-DC are values at .0625 Hz.

Wet weight (W_1) and weight in water (W_2) were measured to determine physical properties of the samples such as density and porosity. Effective porosity (Φ), dry density (D_d), and wet density (D_w) were obtained by [$D_w = W_1/(W_1 - W_2)$] [$D_d = W_3/(W_1 - W_2)$] [and $\Phi = (W_1 - W_3)/(W_1 - W_2)$].

These values are listed in Table 2. The conductivity and pH of the water in the container are measured before and after the dipping (Table 3).

IP Measurement: The measuring system consisted of two channel receiver (Zonge, GD - 12 system), laboratory transmitter, isolation amplifier, sample holder, oscilloscope, personal computer, and printer (Fig. 4).

Water-saturated rock samples were clamped between four electrode pass in the sample holder. The lab-transmitter supplied a square wave current. The switching time of the current was controlled by GSP -12. Current monitor signal of the lab-transmitter and potential difference between the opposite surfaces of samples were introduced into the isolation amplifier. The output of the isolation amplifier was introduced into GDP - 12. Channel 1 was for potential difference and channel 2 was for current monitor. The isolation amplifier was used to avoid that the electric grounds of GDP - 12 and lab-transmitter become common to negative side of the input signal of GDP -12.

The measuring program, which was installed in GDP -12, automatically digitized two input signals, and calculated Fourier transform and transfer function (impedance) between current strength and potential difference. Impedance was sent to the personal computer and the printer. The measurement was done as frequency domain measurement. Frequency changes from .0625 Hz to 2048 Hz with a binary step. Therefore the number of frequencies is 16. Current strength is 2 microamperes in usual measurement, except the examination of the effect of current density.

The given factor were also considered in the measurement: as i) Effect of current density, ii) Effect of water type, iii) and effect of lamination.

INTERPRETATION

Classification of IP effects: The rock sample can be visually divided into three types according to the characteristics of IP responses. This classification bases on the content of metallic particles, as i) Highly polarizable (metallic), ii) moderately polarizable, and iii) Unpolarizable (non metallic).

For the presentation of the complex resistivity at frequencies from .0625 to 2048 Hz, the following quantities are used: real and imaginary components, and magnitude and phase of the complex resistivity.

The classification scheme used in the study describes the basic ground or host rock signature. They are refereed as type A, B, and C (Fig. 5). Type A response is characterized by an out of phase component which decreases with increasing frequency and it is usually associated with strong alteration, sulphide mineralization including pyrite, graphite, and stone clays. Type B is characterized by an out of phase component which is constant for all frequencies. It is associated with moderate alteration, low pyrite mixed mineral environments, and transition zones between type A and C. Type C describes an out of phase component which increase with increasing frequency or small PFE and is usually associated with weak alteration such as chloritization, and it has been found in alluvial area, fresh volcanic rocks, and limestone.

It is evident from previous experimental researches that IP phenomena should depend upon current density, size of the sulphide particles, resistivity of the matrix, and the distribution of the sulphide grains as well as the total sulphide content.

Sample which are classified to these three

types are listed in Table 4. Also, typical spectra of classes A, B and C are illustrated in figures 6, 7, and 8, respectively. PFE, phase shift at .0625 Hz, and resistivity at .0625 Hz as well as the shape of Cole-Cole expression are used for the classification.

Curves of figure 6 show large PFE (greater than 50%) and large phase-shift (larger than 300 milliradians at .0625 Hz). They belong to type A, and sample MA20, H and L are copper ores. Although resistivity varies from 27 to 408 ohm meter, shapes of normalized amplitude are similar to each other. Sample MA15 contains a lot of small dykes of sulphide, which causes a great IP effect, although the total amount of metallic minerals is much less than the ore sample MA20 which contain about 7.4% copper. While resistivity of MA15 is one decade larger than MA20, their PFEs are almost same.

Figure 7 shows IP spectra of moderately polarizable samples. Curves of Cole-Cole expression show flat shapes at lower frequencies. Phase shifts at 0.0625 Hz are from about 50 to 110 milliradians, and PFE is around 10 to 15%.

Samples A, B, C, and F, which are andesties of the green tuff region, have large porosity. However, resistivities are medium and small amount of disseminated sulphide causes moderate polarization. On the other hand, porosities of samples No. MA4, MA5, MA7, and MA16 (phyllite and breccia) are small. The amount of sulphide in these samples must be larger than those of sample A, B, and F, because they all show almost same IP effect.

Figure 8 shows example of unpolarizable samples. PFE and phase-shift are small for samples, the curves of Cole-Cole expression tend to concentrate to the position of (1,0). Also, porosity is low and therefore resistivity becomes high. This group include granite, diabase, andesite of Kuroko area which have little mineralization. Although MA6 contains some amount of pyrite, IP effect is small. It is caused by the fine texture of diabase and low porosity.

Effect of Current Density: The effect of current density on IP phenomena was examined with sample G (Fig. 9). Current strength of 1, 2, 5, 10 and 100 microamperes was used in the experiment. When the current density increase, resistivity at .0625 Hz decreases, PFE increases, and phase shift at .0625 Hz decreases. However these changes are rather smaller as compared with drastic changes of the phase spectra at higher frequencies than 100 Hz. This great change is due to the inductive coupling.

Effect of Water Type: Measurement was carried out on seven sample of group 8 and 9 with tap water as well as processed water to examine the effect of water. Significant changes were not found in phase and amplitude spectra. In metallic rock (MA17) it was observed that PFE and resistivity increased due to change of conductivity and pH of the water, although the moderately polarizable rock (MA4) did not show significant change (Fig. 10-a). However, the unpolarizable rock (O) gave the change in resistivity (Fig. 10-b). Perhaps this is due to conductivity of the water and porosity of the sample.

Effect of Lamination: Sample I had a lamination, and effect of the lamination on IP phenomena were observed. Measurement was done in a direction parallel to the lamination (I-a), and perpendicular to it (I-b) (Fig. 11). Significant change was noticed. Resistivity at .0625 Hz, PFE, and phase shift were higher in the parallel case than the perpendicular case.

CONCLUSION

Based on IP measurement studied samples were divided them into three groups according to their IP spectra. It is confirmed that spectrum changes with respect to mineralization, lithology, porosity. It is clearly found that the content of metallic minerals is the most important factor which affects the IP response, Following facts are found.

- i) Since sample measurement provides

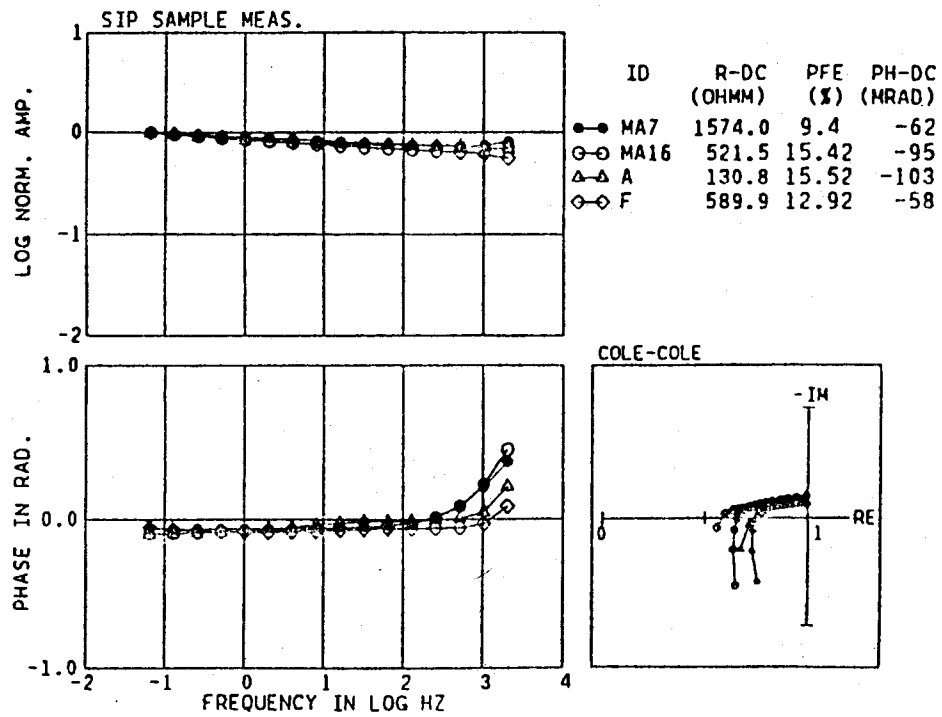


Fig. 7. Spectrum of moderately polarizable rocks (type B).

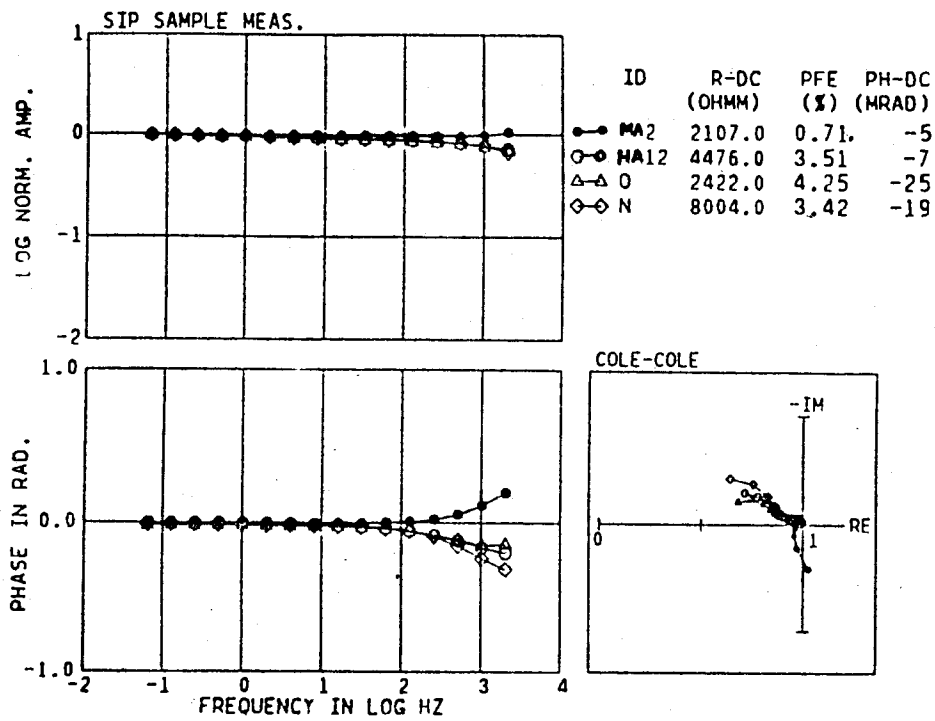


Fig. 8. Spectrum of unpolarizable rocks (type C).

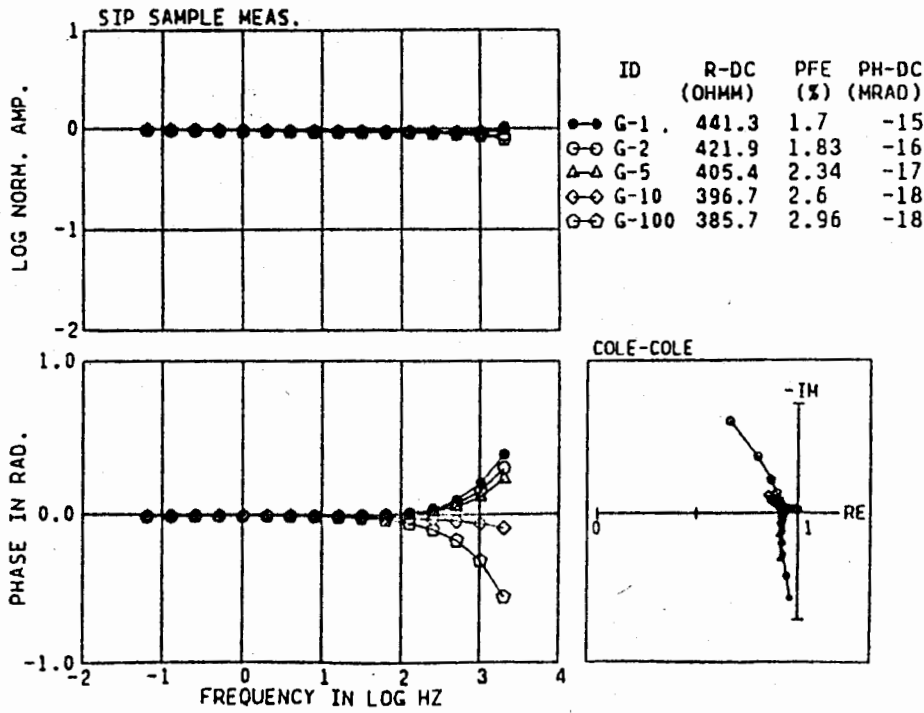


Fig. 9. Effect of current density on IP phenomena. Current strength is 1, 2, 5, 10, and 100 microamperes. "G-1" corresponds to 1 microampere, for example.

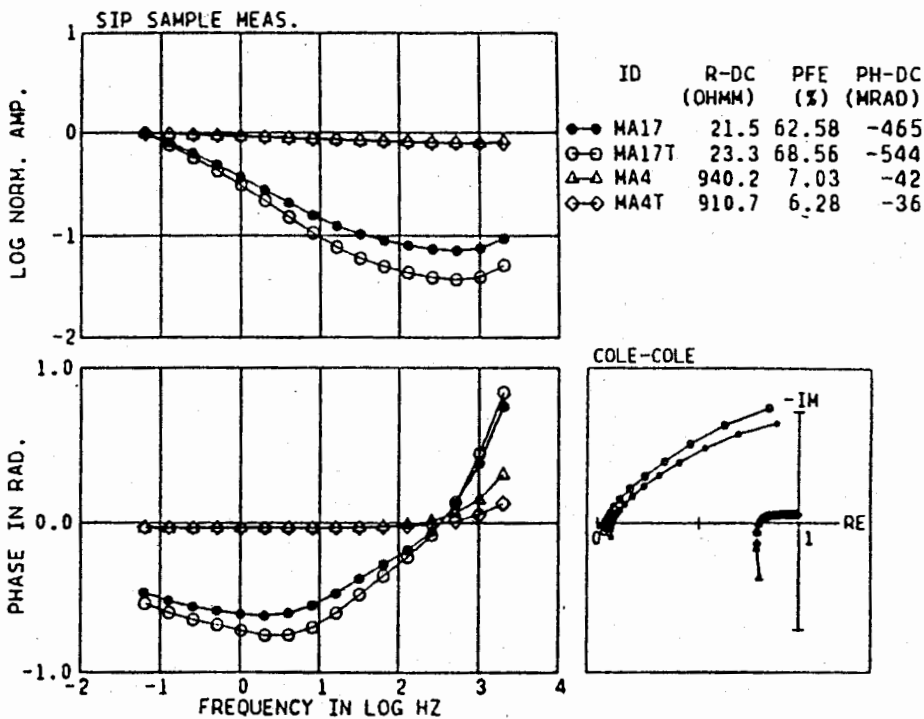


Fig. 10-a. Effect of water type on IP phenomena. "T", the right-most letter of the ID, means tap water.

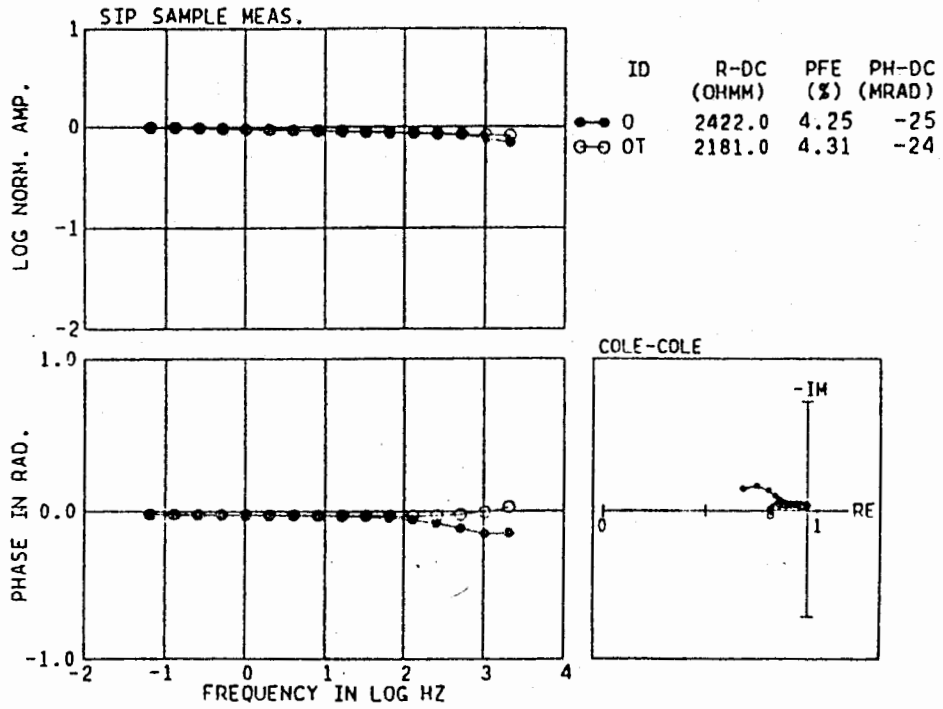


Fig. 10-b. Effect of water type on IP phenomena.

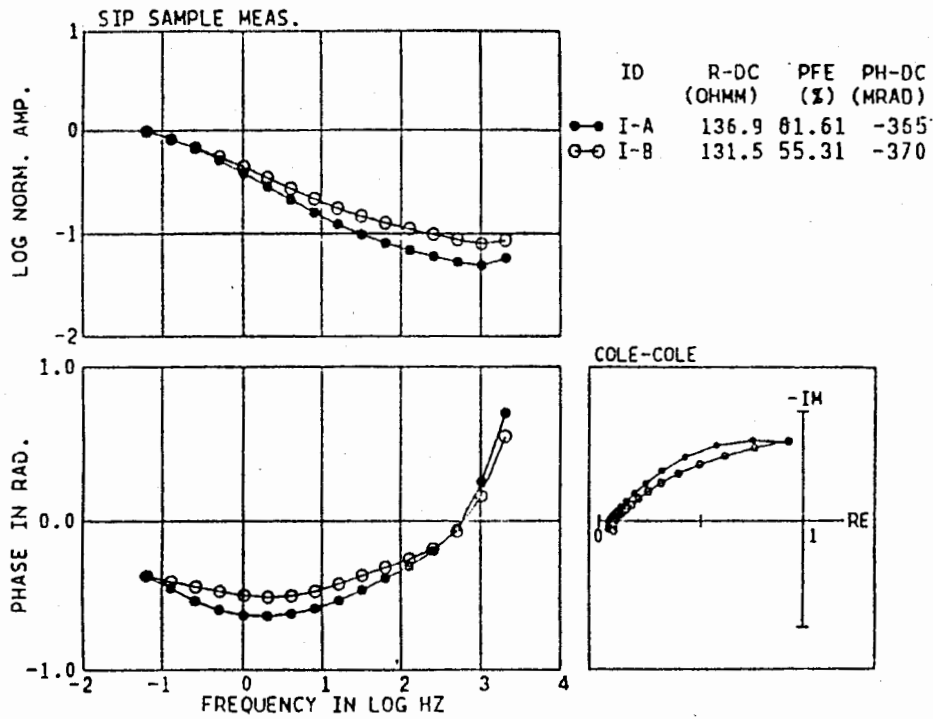


Fig. 11. Effect of lamination on IP effect. Current was applied in parallel (I-a) and perpendicular (I-b) direction to the lamination.

Table 1. Sample with their dimensions and lithology. Group means container number which was used for dipping.

No	Sample no.	Cylinder			Cube				Group	Remarks (Lithology, place, etc)
		Diam (cm)	Area (cm ²)	Height (cm)	Width (cm)	Depth (cm)	Area (cm ²)	Height (cm)		
1	MA1	6.32	31.37	3.52					1	Diabase, Shimokawa, (MASK1, 148m)
2	MA2	4.76	17.79	10.05					1	" " (" 261m)
3	MA3	4.76	17.79	7.18					1	Breccia, " (" 308m)
4	MA4	4.76	17.79	5.31					2	" " (" 313m)
5	MA5	3.64	10.40	5.58					2	" " (" 358m)
6	MA6	3.64	10.40	8.15					2	Fine diabase, " (" 360m)
7	MA7	6.32	31.37	10.21					2	Phyllite, " (MASK2, 225m)
8	MA10	4.90	18.83	2.76					2	" " (" 366m)
9	MA11	4.76	19.79	10.00					1	Diabase, " (" 432m)
10	MA12	4.76	17.64	10.20					1	" " (" 440m)
11	MA14	4.76	17.64	7.08					1	Brecciated tuff, " (" 525m)
12	MA15	4.76	17.64	3.80					2	Phyllite, " (" 665m)
13	MA16	4.76	17.64	6.96					2	" " (" 753m)
14	MA17			10.08					3	Copper ore, " "
15	MA18			10.10					3	" " "
16	MA19			10.08					3	" " "
17	MA20			10.08					3	" " "
18	A	8.20	52.87	6.28					4	Agglomerate, Hokuroku (GSM1 330m)
19	B	6.55	33.69	6.73					4	Andesitic Tuff, " (" 540m)
20	C	5.97	27.94	6.27					4	Green Andesite, " (" 770m)
21	D	5.97	27.94	7.02					4	" " (" 910m)
22	F	4.74	17.64	8.69					5	" " (W7)
23	G	4.30	14.58	8.74					5	Andesite, " (W5)
24	O	4.75	17.64	8.77					5	" " (W7)
25	P	4.75	17.64	8.86					5	" " (W7)
26	Q	4.75	17.64	8.78					5	Agglomerate, " (W7)
27	H				5.52	4.20	23.20	5.53	6	Copper ore, Sazare (Shikoku)
28	I-a				7.27	6.67	48.49	7.44	6	" " "
29	I-b				6.67	7.44	49.49	7.27	6	" " "
30	J				5.30	4.92	26.10	5.12	6	Copper ore, Hitachi (Ibaraki)
31	K				3.03	3.03	9.18	5.3	6	" " "
32	L				3.05	3.05	9.30	5.07	6	" " "
33	M				4.23	4.78	20.21	5.42	7	Granite
34	N				4.77	4.57	21.82	5.34	7	Granodiorite

Table 2. Weight, density, and porosity of the samples.

No	Sample no.	Weight			Density		Porosity ϕ (%)
		Wet (gr) V1	In Water (gr) V2	Dry (gr) V3	Dry (g/cm ³) Dd	Wet (g/cm ³) Dw	
1	MA1	351.1	205.6	313.9	2.866	2.877	1.0959
2	MA2	497.6	320.3	495.9	2.7969	2.8065	0.9591
3	MA3	351.0	226.3	349.4	2.8019	2.8147	-1.2831
4	MA4	260.0	166.2	259.1	2.762	2.771	0.9594
5	MA5	156.4	98.9	155.6	2.706	2.72	1.3912
6	MA6	229.5	146.1	228.0	2.733	2.7518	1.7985
7	MA7	863.0	546.7	858.3	2.713	2.728	1.485
8	MA10	144.2	91.7	143.7	2.737	2.746	0.95
9	MA11	449.9	275.6	430.8	2.4716	2.5811	10.958
10	MA12	504.3	327.2	502.9	2.839	2.847	0.790
11	MA14	319.8	197.9	315.5	2.588	2.623	3.527
12	MA15	197.6	130.6	196.9	2.938	2.949	1.044
13	MA16	329.4	207.2	326.9	2.675	2.695	2.045
14	MA17	299.1	219.3	298.8	3.744	3.748	0.3759
15	MA18	302.15	219.15	301.6	3.633	3.640	0.662
16	MA19	301.05	217.35	300.4	3.589	3.596	0.776
17	MA20	284.4	207.75	284.0	3.705	3.710	0.521
18	A	789.6	464.4	729.8	2.244	2.428	18.388
19	B	552.0	326.7	525.5	2.332	2.450	11.762
20	C	438.1	265.1	422.2	2.440	2.532	9.190
21	D	520.5	326.1	514.7	2.647	2.677	2.983
22	F	371.9	219.9	354.7	2.333	2.446	11.315
23	G	305.1	179.6	292.6	2.331	2.431	9.960
24	O	394.6	240.8	387.5	2.519	2.566	4.616
25	P	400.1	244.4	394.9	2.536	2.569	3.339
26	Q	367.0	212.9	354.1	2.297	2.381	8.371
27	H	581.7	458.3	581.3	4.710	4.713	0.324
28	I-a						
29	I-b						
30	J	548.3	424.4	546.9	4.414	4.425	1.129
31	K	197.4	151.9	197.0	4.329	4.338	0.879
32	L	182.1	135.7	178.9	3.855	3.924	6.896
33	M	288.1	180.4	286.8	2.662	2.675	1.207
34	N	311.7	198.1	310.9	2.738	2.743	0.7042

Table 3. Conductivity, pH, and temperature of water where sample were dipped.

Group	Conductivity ($\mu\text{s/cm}$)	pH	Temperature ($^{\circ}\text{C}$)	Remarks
1	36.5	6.25	18.5	Processed Water Cond. $3.50\ \mu\text{s/cm}$ pH 4.8
2	52.8	6.65	18.5	
3	101.9	6.9	18.5	
4	52.9	7.26	18.5	
5	108.9	4.05	18.5	
6	244.0	4.05	19.5	
7	9.1	6.3	18.5	
8	335.0	7.3	18.5	Tap Water Cond. $299\ \mu\text{s/cm}$ pH 7.1
9	405.0	6.9	18.5	

Table 4. Grouping of samples according to the IP responses. Classification is done with PFE, phase shift at .0625 Hz, and shape of Cole-Cole curves.

Type	Sample	PFE .0625-1 (%)	Resist .0625Hz ($\Omega\ \text{m}$)	Phase .0625Hz (mRad)	
A	MA15	50.5	408.1	-304	
	MA17	62.58	21.5	-465	
	MA18	64.0	27.9	-525	
	MA19	55.35	32.6	-461	
	MA20	67.51	27.9	-547	
	H	68.3	101.7	-498	
	J	65.46	110.7	-429	
	K	57.26	53.4	-324	
	L	61.43	45.7	-366	
	I-a	61.61	136.9	-365	
	I-b	55.31	131.5	-370	
	B	A	15.52	130.8	-103
B		14.5	297.3	-107	
C		14.02	637.7	-89	
F		12.92	589.9	-58	
MA4		7.03	940.2	-42	
MA5		6.67	1469.0	-33	
MA7		9.4	1574.0	-62	
MA16		15.52	521.5	-95	
C		MA1	0.95	3478.0	-7
		MA2	0.71	2107.0	-5
	MA3	1.77	1074.0	-10	
	MA6	3.5	506.4	-26	
	MA10	4.82	2840.0	-24	
	MA11	2.08	403.0	-12	
	MA12	3.51	4476.0	-7	
	MA14	1.22	473.8	-12	
	D	5.68	1391.0	-40	
	O	4.25	2422.0	-25	
	P	2.43	1771.0	-16	
	Q	4.43	1309.0	-28	
	G	1.83	421.9	-16	
	M	2.02	2622.0	-17	
N	3.42	8004.0	-19		

direct information of rock properties, it is observed that PFE and phase shift have value than what we usually obtain in the field IP measurement. The resistivities of the samples are much higher than those of field measurement. This caused by changes of the environment, such as water content, ionic solution and, temperature.

ii) Current density affects IP phenomena. Although the effect is visually small at frequencies less than 100 Hz, PFE and phase changes systematically according to the current strength. The changes at higher frequencies are very large.

iii) Lamination also affects resistivity and PFE.

iv) Effect of water type was not checked completely. Tap water increase IP effect on some samples, and decreases on other ones. Further observation and precise control of sample preparation are needed to obtain schematic changes.

v) Sample A, B, and C from the green tuff area have large porosity and little amount of metallic content. However their IP effects are rather higher than expected. Perhaps the clay minerals increase the IP effects.

vi) Although sample MA6 contains some amount of pyrite, its resistivity is higher, and PFE and phase shift are small. Therefore it is grouped into C type. MA6 is diabase of a very fine texture and its porosity is less than 2%. It overcome the effect of pyrite and causes high resistivity and low IP effect.

ACKNOWLEDGEMENT

I would like to thank the Japanese Government through its organization JICA and GSJ for providing all the support and facilities which are necessary for the Offshore Prospecting Course.

I wish to express my sincere appreciation and thanks to my advisor, Mr. T. Uchida for his invaluable guidance and all forms of support during the individual study, and also thanks Mr. M. Nishikawa of MMAJ who provided the instrument and the rock samples.

REFERENCES

DEY, A & MORRISON, H.F. (1973)

Electromagnetic coupling in frequency and time domain induced polarization surveys over a multilayered earth. *Geophysics*, vol. 38, No. 2, pp. 380-405

ELLIOT, C.L. & GUILBERT, J.M. (1974) Induced polarization response attributed to magnetite and certain Fe-Ti oxide minerals. Presented at 44th SEG Annual International Meeting. November 12, in Dallas.

FRASER, D.S. (1964) Electrical properties of clay-containing sandstone, electrical polarization. Report, MT-64-4, Inst. of Eng. Res. Univ. of California, Berkeley.

HALLOF, P.G. & PELTON, W.H. (1980) The removal of inductive coupling effect from spectral data. Presented at the 50th SEG Annual International Meeting Houston, Texas.

HOHMANN, G.W. (1973) Electromagnetic coupling between ground wires at the surface of a two layer earth. *Geophysics*, vol. 38, pp. 854-863.

_____ (1975) Three-dimensional induced polarization and electromagnetic coupling. *Geophysics*, vol. 40, pp. 309-329.

ILICETO, V., STARATO, G., & VERONESE, S., (1982) An approach to the identification of fine sediments by induced polarization laboratory measurements. *Geophysical Prospecting*, vol. 30, pp. 331-347

MADDEN, T.R. & MARSHALL, D.J., (1959) Induced polarization, a study of its causes. *Geophysics*, vol. 24, pp. 790-816.

MADDEN, T.R. & CANTWELL, T. (1967) Induced polarization, mining *Geophysics*, vol. 2, Society of Exploration Geophysicists, pp. 373-400.

MAHAN, M.K., REDMAN, J.D., & STRANGWAY, D.W. (1986) Complex sivity of synthetic sulphide bearing rock. *Geophysical Prospecting*, vol. 34, pp. 743-768.

PELTON, W.H., WARD, S.HHALLOF, P.G., SILL, W.R., & NELSON, P.H. (1978) Mineral discrimination and removal of inductive coupling with multifrequency IP. *Geophysics*, vol. 43, pp. 588-609.

SILL, W.R. (1964) Induced Polarization in clay-bearing sandstones and the effects of oil saturation. Ref. Rep. Inst. of Geophys. and planet. Sci., Univ. of California, Snadiego.

SUMMER, J.S., (1976) Principales of induced polarization for geophysical exploration. Elsevier Scientific Publishing Company, 277p.

WYNN, J.C. & ZONGE, K.L.(1975) E.M. coupling its intrinsic value, its removal and the cultural coupling problem. *Geophysics*, vol. 40, pp. 831-850.

Manuscript received on 9.6.1994

Accepted for publication on 27.10.1994.

CLAY MINERALS OF GHAZIJ FORMATION FROM A SECTION TAKEN IN DEGHARI VALLEY, MASTUNG DISTRICT, BALOCHISTAN, PAKISTAN.

JAWED AHMED

Centre of Excellence in Mineralogy, University of Balochistan,
P.O. Box 43, Quetta, Pakistan.

ABDUL HAQUE

Centre of Excellence in Mineralogy, University of Balochistan,
P.O. Box 43, Quetta, Pakistan

ABSTRACT: Across a section of Ghazij Shale (middle Eocene) exposed in the Deghari Valley, Mastung District, twenty samples have been collected. By means of X-Ray diffraction (XRD) method, clay minerals have been identified, viz: illitic clay (20%); kaolinite (35%); mixed layer clay (15%), and species of chlorite (thuringite = 30%).

INTRODUCTION

Deghari Valley (latitude 30° 4, 20" to 34° 4' 25" N; longitude 67° 14' 50" to 67° 16' 06", toposheets No. 34 N/4 and 34 N/8) lies 40 miles to south-east of Quetta. The measured stratigraphic thickness of Ghazij shale at Deghari Valley section is 4800 feet (146404m) which was systematically sampled at an interval of 240 feet by using Abney level.

The purpose of present study is to characterize the clay minerals content of Ghazij Shale, because very little mineralogical data exists so far, on the clay minerals of this locality.

Ghazij Formation (middle Eocene) exposed both in the Kirther Range and part of Sulaiman Range, consists dominantly of shale with subordinate claystones, sandstones, limestones, alabaster and coal at Deghari Valley. The outcrops color is pale greenish grey, brown and light grey.

Shale is light grey to dark green soft, friable, fissible, earthy and blocky in appearance. Base of the formation is well exposed because the underlying strata of early Eocene, Dunghan

Limestone is dip 30.SW and has shown an excellent escarpment.

Twenty samples were collected across the strike at a regular interval of 5% of the total thickness. Offset but stratigraphically equivalent samples were collected 100-200 feet in both directions from the main sampling line. The samples were taken from an average depth of one foot below the surface.

ANALYTICAL METHOD

X-Ray diffractogram patterns were obtained for the clay size (0.5_u m) fraction of each sample. About 10 gram material from each sample was crushed in the porcelain mortar and kept in distilled water for 24 hours. This was treated with 5 mg of sodium meta-hexaphosphate as dispersion agent. Then, after one hour, this dispersed sample was split into three fractions for centrifuging. Glass slides were then prepared from each separate suspended material a) air dried oriented aggregates b) ethylene glycolated oriented aggregates and finally c) fired oriented aggregates. These slides were run on XRD units. All samples were treated for removal of organic material and iron oxide. Several samples

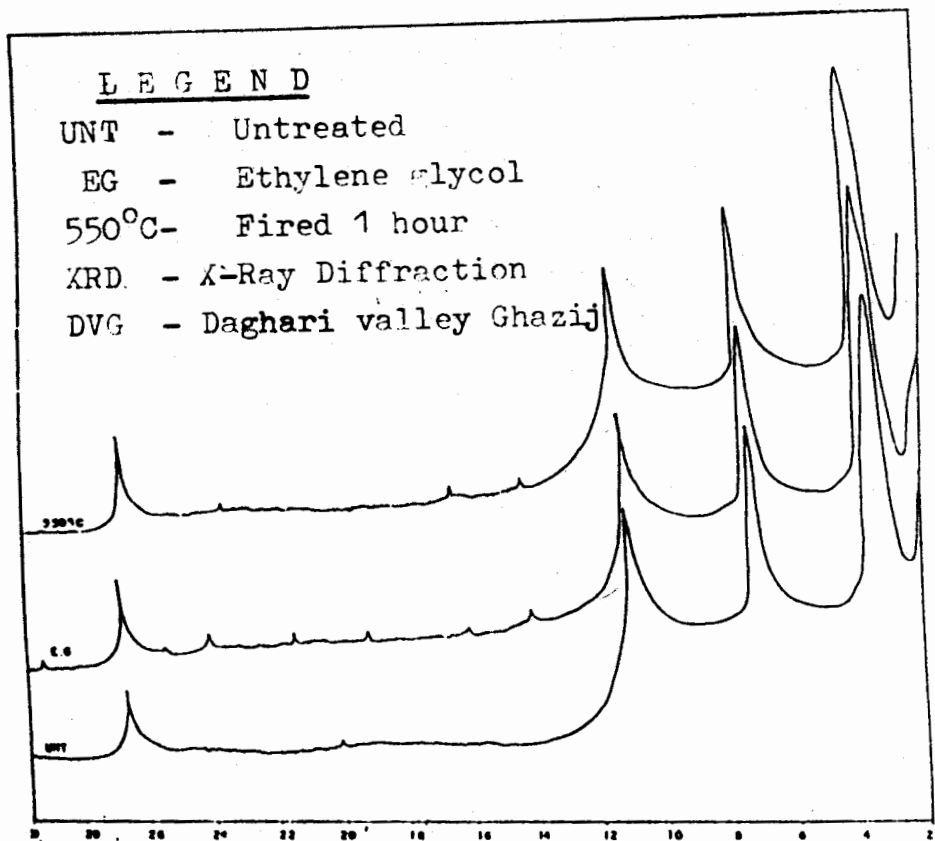


Fig. 1. XRD-DVG Illite-chlorite.

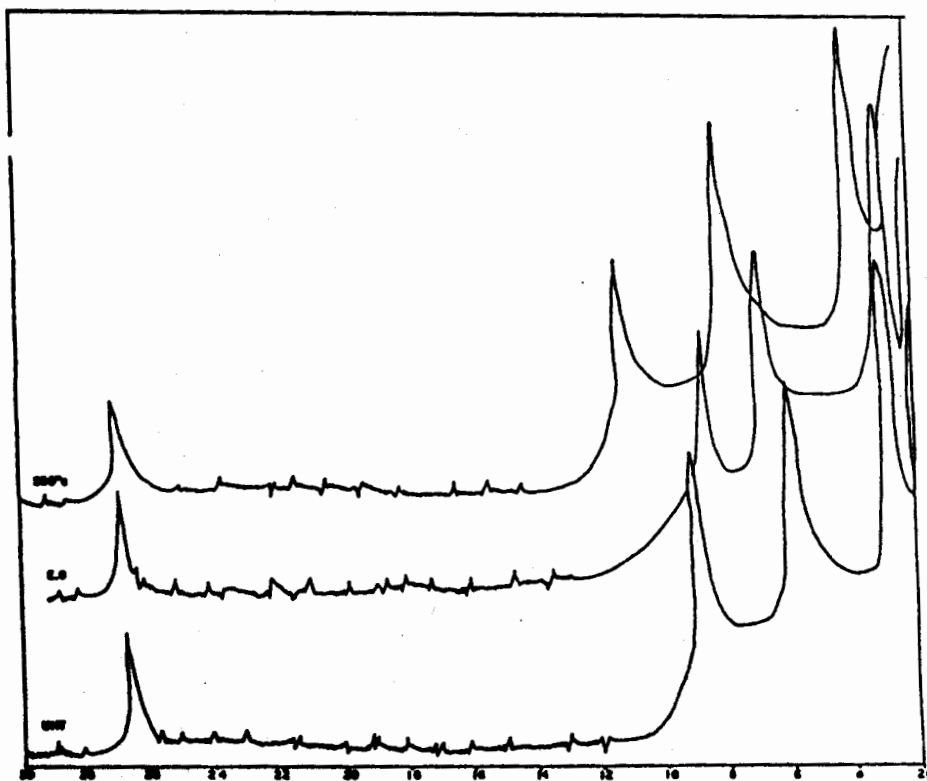


Fig. 2. XRD-DVG Smectite-chlorite.

contained chlorite which was removed by heating for one hour in dilute HCl at 80°C.

DISCUSSION & RESULT

X-Ray diffraction pattern gives strong intense, broad first basal order reflection of illite 10\AA at 8.8 spacing; second basal order reflection of illite 5\AA at 17.3 spacing. No change is observed in pattern when treated with ethylene glycol and there is no shift of "d" spacing when treated with heat. Integrated intensity of illite was 83% percent and measured crystallinity of illite was 18mm.

Regular mixed layer illite-chlorite as shown in figure 1, give strong (001), (002) and (003) reflections relatively at 3.60, 7.34 and 11.18 "d" spacing. There is no change in shape or shift on position of peak when treated with ethylene glycol or heated. Mixed layer illite-chlorite (001) is 35.5, (002) 22.8 and (003) is 31.3 percent where as quartz is 10 percent.

Mixed layer smectite-chlorite is identified by X-ray pattern as shown in figure 2, wherein intense (001) reflection at 29.6\AA with 3.06 "d" spacing and (002) reflection at 6.28 "d" spacing. The natural material is made up of 15\AA (smectite) and 14.1\AA (chlorite) which upon further treatment with ethylene glycol gives strong (001) reflection at 31\AA ($17 + 14$) and (002) reflection at 15.5\AA with 5.52 "d" spacing. The material is heated upto 550°C, give collapsed 24\AA ($10 + 14$) spacing and (002) reflection at 11.6\AA with 7.62 "d" spacing. The shape of the peak is sharp, intense and asymmetrical. Quartz peaks are identified at 3.34\AA . The relative intensity of smectite chlorite is (001) 35.5 (002) 22 and of (003) is 32 percent. The relative intensity of quartz is 10 percent.

Kaolinite is characterized by intense (001) reflection at 7.41\AA and (002) 3.57\AA respectively at 12.34 and 24.9 "d" spacing. There is no change upon glycolation in the "d" spacing of peak as observed in the untreated

pattern. When specimen heated for half an hour upto 550°C the result was complete destruction of the pattern.

To distinguish between kaolinite and chlorite structure the samples were heated between 550 and 600°C for one hour. This should decompose kaolin minerals but not chlorite. Another method is to use warm dilute HCL to dissolve chlorite and leave kaolinite.

In this diffractogram pattern special kind of chlorite species thuringite is identified 6.4, 12.8 and 19.14 "d" spacing. Whereas, quartz at 26.64 "d" spacing. No change is observed when the sample is treated with ethylene glycol or fixed for one hour at 550°C.

CONCLUSION

In Deghari valley, clay minerals of Ghazij Formation are illitic clay, mixed layer clay, kaolinite and thuringite. The rock is generally composed of illitic clay (20%), kaolinite (35%), thuringite (30%) and mixed layer clay (15%).

REFERENCES CITED

- BAILEY, S.W.** (1972) Determination of chlorite composition by X-ray spacing and intensities. *Clays and clay minerals*, vol.20 pp.318-88.
- BODINE, M.W. Jr. & STANDAERT, R.R.** (1977) Chlorite and illite compositions from upper Silurian Rock Salt, Rets of New York. *Clays and clay minerals* vol.25 pp.57-71.
- BRADLEY, W.F.** (1953) Interpretation of mixed layers minerals. *Analyt. Chem.* vol.25 pp.727-730.
- BRINDLAHEY, G. W. & BROWN, G.** (1980) Crystal structures of clay minerals and their X-ray identification. *Min. Soc.* 2nd 495p.

KODAMA, H & OINUMA, K (1963)

Identification of kaolin minerals in the presence of chlorite by X-ray diffraction and infrared absorption spectra. *Clays and clay Minerals*, vol. 13. pp. 236-349.

SRODON, J (1980) Present identification of illite-smectite interstratification by X-ray powder-diffraction. *Clay and clay minerals*. vol.28 pp.401-411.

Manuscript received on 20.2.1994

Accepted for publication on 10.3.1994

SKARNIZATION OF THE MASSIVE SULFIDE ORES AND ASSOCIATED ROCKS OF THE PAZANG GROUP IN BESHAM AREA AT THE NORTHERN MARGIN OF INDO-PAKISTAN PLATE.

MOHAMMAD TAHIR SHAH

National Centre of Excellence in Geology, University of Peshawar, Pakistan.

ABSTRACT: Proterozoic sediment-hosted massive sulfide ores occur in the highly deformed and metamorphosed rocks of the Pazang group in the Besham area, District Kohistan. The massive sulfide ores and associated rocks of the Pazang group were subjected to skarnization after their deposition. Both magnesian and calcic skarns were formed. As a result, the Mn-rich skarn minerals (i.e. clinopyroxenes, pyroxenoids, garnet, olivine, and serpentine) have been developed within these rocks. The chemistry of these minerals suggest that the protoliths for both calcic and magnesian skarn were probably impure limestone and dolomite respective with intercalations of umber, chert and clays.

INTRODUCTION

The rocks of the Indo-Pakistan Plate, south of Main mantle Thrust (MMT), have a complex tectono-metamorphic history with polyphase deformation and metamorphism (Fletcher et al. 1986; Baig et al. 1987; Baig et al. 1988; Baig et al. 1989; Treloar et al., 1989; La Fortune et al. 1992). These rocks have been divided into Besham, Pazang and Karora groups. The first two groups are a part of the basement complex and the third one is composed of a cover of metasediments that unconformably overlie the basement complex (Fletcher et al., 1986; Treloar et al., 1989).

The stratiform sediment-hosted massive sulfide (Zn-Pb) ores of Proterozoic age (Pb isotope age of 2120-2199 Ma; Shah et al., 1992) occurs in the rocks of the Indo-Pakistan Plate along its northern margin in the footwall of the MMT around Besham and are confined to the Pazang group. This group was proposed by Fletcher et al., (1986) for the group of metasediments with a type locality near Pazang village. The Two areas, Lahor and Pazang, which have prime importance regarding the base metal mineralization are situated on west and east

side of the river Indus respectively (Fig. 1). The stratigraphy established for the Pazang rocks is more or less the same at both Lahor and Pazang mineral prospects.

The rocks of the Pazang group occur as tectonic pods within the basement gneiss of the basham group (Fig. 1) and are differentiated into three formations from top to bottom: the metaquartzite/meta-arkose formation; the sulfide formation, and the pelitic formation (Fletcher et al., 1986, Shah, 1991). The sulfide formation having Zn-Pb mineralization, constitutes the distinct portion of the Pazang group and has further been divided from bottom to top into magnetite-rich carbonates, sulfide-rich calcisilicate rocks, massive sulfide ores, sulfide-bearing clinopyroxenites, sulfide-rich quartzofeldspathic rocks, and sulfide-poor quartzofeldspathic rocks (Shah, 1991). The metasediments of the Pazang group are intruded by pegmatite dikes in both Pazang and Lahor mineral prospects. These dikes have dislocated the Zn-Pb mineralized zones in both areas and made the underground survey much difficult.

The massive sulfide ores are considered to be of skarn type (Ashraf et al., 1980). derived

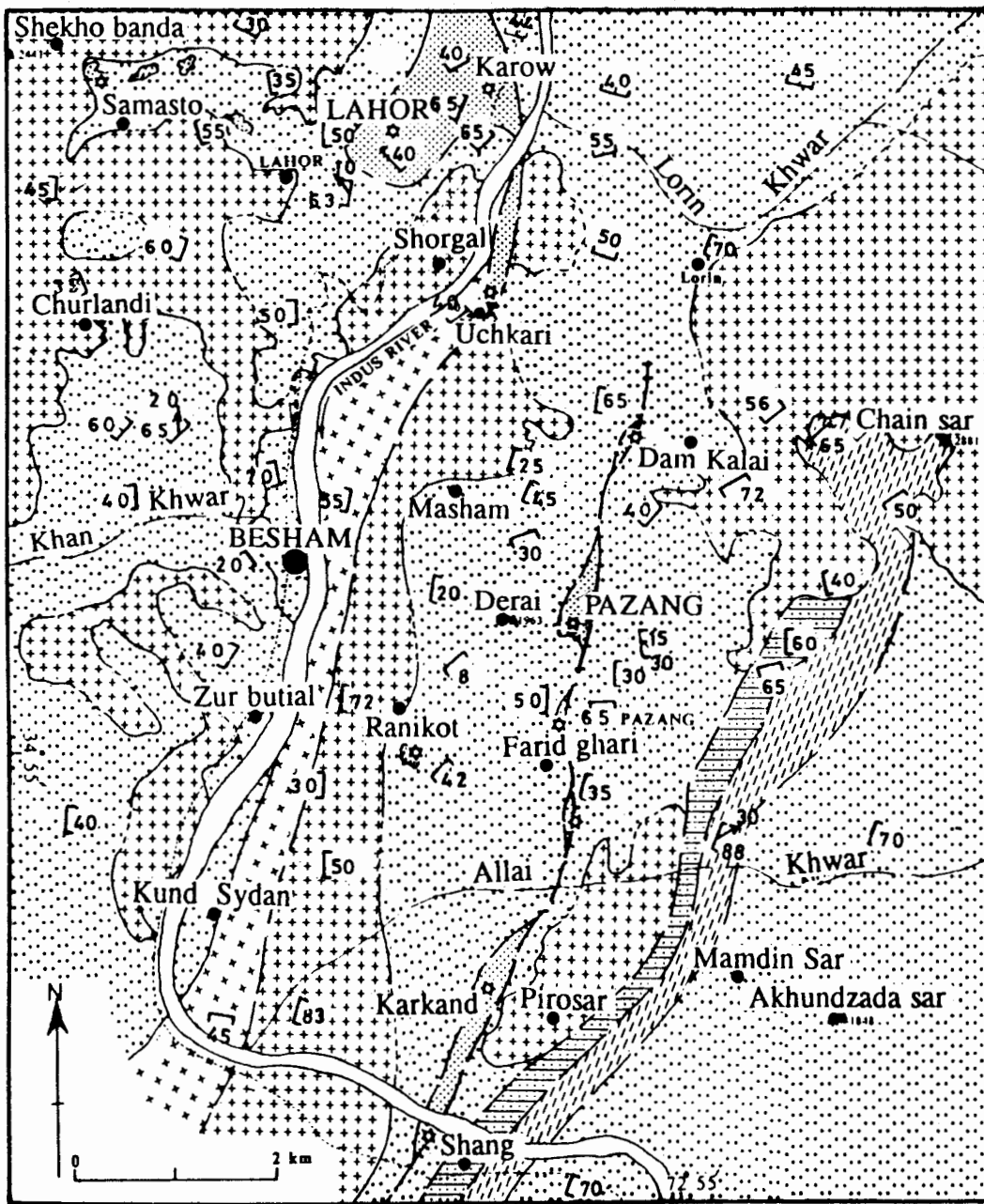

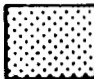
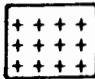



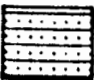
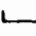










Fig. 1. Geological map of the area around Besham, northern Pakistan.

EXPLANATION

Besham Group	Pazang Group	Lahor Granitic Complex
 Pelitic, Psammitic calcareous, Graphitic schist and Gneisses	 Sulfide-rich Quartzite, Carbonate, Calc-silicate Clinopyroxenite and Quartzo-feldspathic rocks	 Metagranites and Pegmatites
 Banded Gneiss	 Pb, Zn & Fe sulfide mineralization	 Fault
 Mica schist with quartz nodules	 Foliation	 Contacts
 Graphite augen gneiss and pegmatite gneiss	 Compositional layering	 Inferred contacts
	 Lination crenulation	 Karakoram highway
	 Village, Peak in meters	 Streams

from metamorphic rocks and remobilized during the process of anatexis (Butt, 1983), and stratiform exhalative type (Fletcher et al., 1986, Shah, 1991). The lead isotope studies and other evidence strongly favour the exhalative origin for these ores (Shah, 1991; Shah, 1992; Shah, et al., 1992). As these ores occur in a highly deformed and metamorphosed terrane, most of the textural features suggest that the mineralization predates the deformation and metamorphism. Both metamorphism and pegmatite intrusions may have caused the skarnization of the rocks of the Pazang group, especially the sulfide formation after their deposition.

This paper present mineral chemistry of some of the skarn minerals (i.e. clinopyroxenes, pyroxenoids, garnet, olivine, serpentine) developed during skarnization of the massive sulfide ores and associated rocks of the sulfide formation. On the basis of the chemistry of the these minerals the protolith composition has also been established.

CHEMISTRY OF SKARN MINERALS

Sample from the skarns have been examined petrographically, and the electron micro-probe analyses (Table 1 two pages) of some of the calc-silicate constituents have been determined by using the Cameca SX-50 electron microprobe at the University of South Carolina, Columbia (USA). The operating conditions were 15 Kv accelerating potential and beam current of 25 nA. Natural and synthetic standards were used, with counting times of 20-30 seconds for each element.

CLINOPYROXENES: The selected clinopyroxene analyses from various rock units of the Pazang group are presented in Table 1. The formulae have been normalized to 6 oxygen and mole percentages of end members hedenbergite (Hd), diopside (Di) and johannsenite (Jo) were calculated. These end members vary widely (Di = 19-73 mole %, Hd = 17-50 mole %, and Jo = 7-62 mole %) in these clinopyroxenes. These clinopyroxenes also show wide range of

composition with regard to the MnO, FeO, and MgO but have small variations in SiO₂ and CaO. Other components are present with concentration below 1.4 weight percent. The core to rim analyses of a single crystal or even of different grains of the same type of clinopyroxene, show no significant variation in composition. Compositionally, these clinopyroxenes are manganoan ferrosalite, manganoan salite and manganoan augite.

The Ca/Ca+Mg ratio is very close to 0.60 and only negligible or small amount of Al substitutes for Si in these clinopyroxenes. In addition, the content of Al and Ti is low. Published analyses of minerals of diopside-hedenbergite series (Deer et al., 1982, vol 2A, Table 14) indicate that the manganese content is low in Mg-rich members but increases in the more Fe-rich members (e.g. manganoan ferrosalite, Tilley, (1946), manganoan hedenbergite, Zharikov and Podlessky, (1955). As the clinopyroxenes from studied rocks are enriched in FeO and MnO, These (except manganoan augite) may be classed as member of diopside-hedenbergite series.

Triangular plot of Di-Jo-Hd indicates a compositional gap between the Mn-rich (towards johannsenite and Mn-poor (towards diopside-hedenbergite) clinopyroxenes (Fig.2). These pyroxenes form a general trend from diopside to hedenbergite apex with slight towards johannsenite apex and then sudden increase of Mn causes the trend to shift towards the johannsenite apex (Fig.2). This suggests that manganoan salite and manganoan augite have been replaced by manganoan ferrosalite due to the addition of various proportions of Fe and Mn in these clinopyroxenes.

PYROXENOIDS: Pyroxenoids in the form of rhodonite and pyroxmangite are found in sulfide-bearing clinopyroxenites, sulfide-rich calc-silicate rocks and massive sulfide ores of the Pazang group. The selected analyses of pyroxenoids are shown in the Table 1 along with their calculated end members, rhodonite (MnSiO₃), wollastonite

Fig. 2.

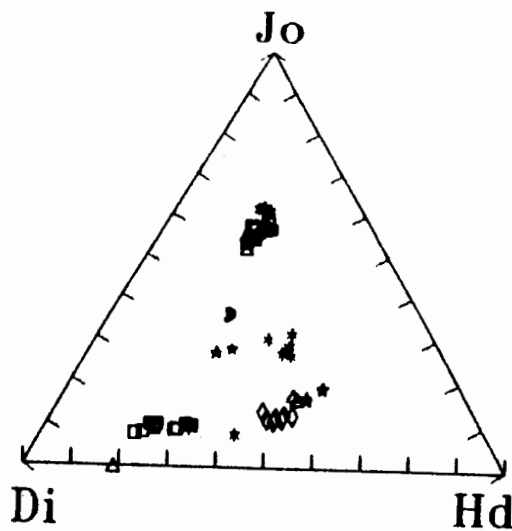


Fig. 2. Triangular plot of diopside (Di), hedenbergite (Hd), and johannsenite (Jo) molecular proportion in clinopyroxenes from the rocks of the Pazang group. Symbols are : ■ = sulfidebearing clinopyroxenite, ▲ = sulfide-rich quartzofeldspathic rocks, ◆ = sulfide-poor quartzofeldspathic rocks * = sulfide-rich calc-silicate rocks, * = massive sulfide ores.

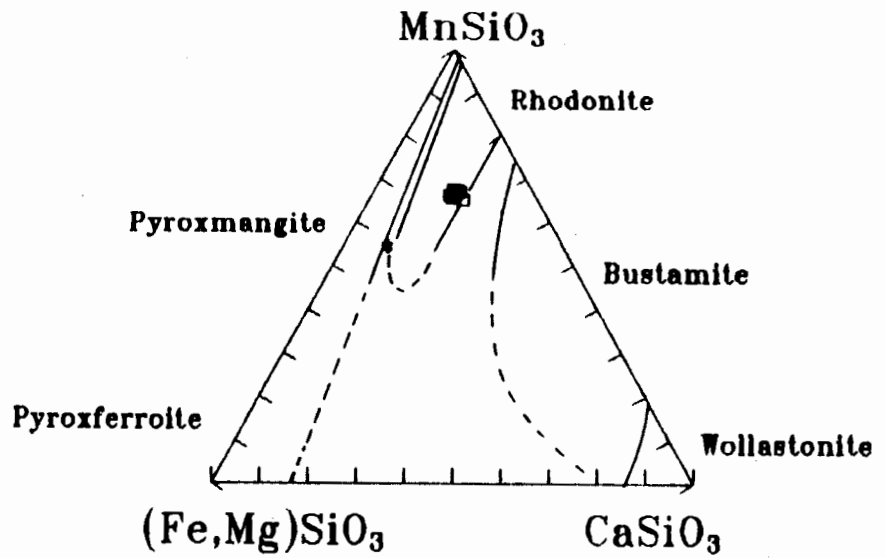


Fig. 3.

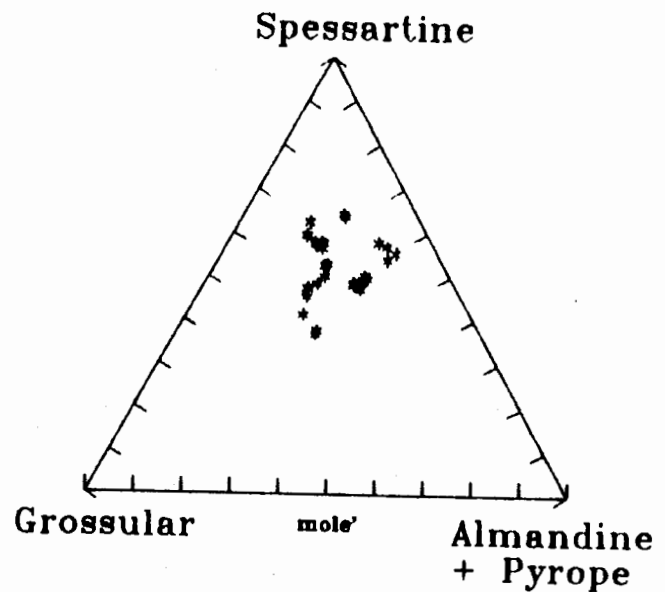


Fig. 4.

Fig. 3. Traingular plot of ferrosilite (Fe, Mg)SiO₃ and wollastonite (CaSiO₃), and rhodonite (MnSiO₃) molecular proportion in the rocks of Pazang group. Various field are after Peacor et al., (1981). Symbols as for Fig. 2.

Fig. 4. Plot of electron microprobe analyses of garnet from the rocks of the Pazang group on Besham area.

Table 1. Selected microprobe analyses of skarn type calc-silicate minerals in various rocks of the Pazang group in Besham area.

CLINOPYROXENE

Mangnoan salite			Manganoan ferrosalite								Manganoan Augite					
S.No	BP109		BL4		BL3		BP190		BL47		BP149		BP232		BL34	
	rim	core	rim	core	rim	core	rim	core	rim	core	rim	core	rim	core	rim	core
SiO ₂	51.13	51.47	49.49	49.63	49.42	49.60	51.09	49.38	51.02	50.74	48.65	49.08	50.49	50.05	55.58	55.67
TiO	0.08	0.05	0.01	0.00	0.01	0.00	0.00	0.03	0.00	0.02	0.02	0.01	0.00	0.02	0.00	0.00
Al ₂ O ₃	1.32	0.74	0.43	0.38	0.27	0.64	0.44	1.19	0.19	0.21	0.07	0.08	0.13	0.13	0.38	0.40
FeO	9.50	9.14	12.99	13.19	14.02	12.85	19.00	19.61	14.01	16.07	12.83	13.04	17.81	17.40	12.86	12.96
MnO	3.09	3.32	9.00	8.66	7.81	9.67	6.61	6.33	3.52	3.87	8.09	9.08	5.42	5.52	3.80	3.86
MgO	10.75	10.84	6.75	6.84	6.17	5.65	8.00	7.95	7.66	6.87	5.68	5.01	6.56	6.41	14.62	14.50
CaO	22.49	22.59	19.71	19.78	19.73	20.08	10.66	10.03	23.10	22.37	22.81	22.23	20.48	20.26	10.40	10.44
Na ₂ O	0.47	0.47	0.71	0.66	0.55	0.82	0.40	0.71	0.13	0.11	0.20	0.24	0.13	0.17	0.57	0.51
K ₂ O	0.00	0.00	0.00	99.00	0.24	0.02	0.06	0.26	0.02	0.01	0.01	0.00	0.01	0.02	0.44	0.42
TOTA	98.82	98.64	99.10	99.13	98.21	99.34	96.25	95.48	99.67	100.25	98.35	98.78	101.03	99.70	98.65	98.76
Numbers of ions on the basis of six (O)																
Si	1.97	1.98	1.98	1.98	1.99	1.98	2.07	2.03	2.00	1.99	1.97	1.98	1.99	1.99	2.08	2.09
Al	0.06	0.03	0.02	0.02	0.01	0.03	0.02	0.06	0.01	0.01	0.00	0.00	0.01	0.01	0.12	0.12
Ti	0.00	0.00	0.00	0.00	0.00	0.00	0.00	0.00	0.00	0.00	0.00	0.00	0.00	0.00	0.00	0.00
Fe	0.31	0.29	0.31	0.29	0.27	0.33	0.64	0.67	0.46	0.53	0.28	0.31	0.59	0.58	0.40	0.40
Mn	0.10	0.10	0.85	0.85	0.85	0.86	0.23	0.22	0.12	0.13	0.99	0.96	0.18	0.19	0.12	0.12
Mg	0.62	0.62	0.40	0.41	0.37	0.34	0.48	0.49	0.45	0.40	0.34	0.30	0.39	0.38	0.82	0.82
Ca	0.93	0.93	0.85	0.85	0.85	0.86	0.46	0.44	0.97	0.94	0.99	0.96	0.86	0.86	0.42	0.42
Na	0.03	0.03	0.44	0.44	0.47	0.43	0.03	0.06	0.01	0.01	0.43	0.44	0.01	0.01	0.04	0.04
K	0.00	0.00	0.06	0.05	0.04	0.06	0.00	0.01	0.00	0.00	0.02	0.02	0.00	0.00	0.02	0.02
Mole percent end members																
Di	60.19	61.39	25.93	26.33	24.88	22.09	35.69	35.33	43.87	38.15	21.30	19.15	33.48	33.26	61.19	61.19
Hd	30.10	28.71	19.65	18.93	17.90	21.48	47.57	48.73	44.85	49.76	17.23	19.74	50.87	50.55	29.85	29.85
Jo	9.71	9.90	54.43	54.74	57.22	56.44	16.74	15.94	11.27	12.09	61.47	61.11	15.65	16.19	8.96	8.96
Ca/Ca+	0.60	0.60	0.68	0.68	0.70	0.72	0.49	0.48	0.68	0.70	0.74	0.76	0.69	0.69	0.34	0.34

(continued table 1)

GARNET

S.No	BP109		BL4		BL43		BP190	BP125	BL47	BL34	BP232	
	rim	core	rim	core	rim	core	GR1	GR2	GR1	GR1	rim	core
SiO ₂	36.83	36.68	35.87	35.96	34.23	35.19	36.35	35.19	36.83	36.18	36.75	36.94
TiO ₂	0.10	0.21	0.17	0.06	0.00	0.00	0.00	0.00	0.10	0.11	0.19	0.17
Al ₂ O ₃	18.70	18.32	13.88	14.92	15.87	14.84	20.25	14.84	18.70	17.81	20.03	19.72
FeO	12.54	13.05	10.68	9.35	10.56	11.68	15.04	11.68	12.54	11.30	14.73	15.27
MnO	17.67	17.87	29.91	29.90	27.06	24.97	24.79	24.97	17.67	25.78	23.55	23.30
MgO	0.70	0.66	0.07	0.06	0.03	0.03	0.72	0.03	0.70	0.07	0.30	0.31
CaO	12.76	13.20	9.77	9.93	10.77	12.84	4.03	12.84	12.76	9.29	6.51	6.42
Na ₂ O	0.01	0.02	0.10	0.00	0.01	0.01	0.01	0.01	0.01	0.01	0.03	0.01
K ₂ O	0.00	0.00	0.04	0.00	0.01	0.00	0.00	0.00	0.00	0.00	0.00	0.00
TOTA	99.32	100.03	100.50	100.18	98.54	99.56	101.22	99.56	99.32	100.55	102.10	102.14

Number of ions on the basis of 24 (O)

Si	6.00	5.96	6.08	6.07	5.87	5.98	5.92	5.98	6.00	5.97	5.92	5.96
Al	3.60	3.48	2.77	2.97	3.21	2.97	3.88	2.97	3.60	3.47	3.80	3.75
Ti	0.00	0.00	0.02	0.01	0.00	0.00	0.00	0.00	0.00	0.01	0.02	0.02
Fe	1.72	1.76	1.51	1.32	1.52	1.66	2.05	1.66	1.72	1.56	1.99	2.06
Mn	2.44	2.44	4.30	4.27	3.93	3.59	3.42	3.59	2.44	3.61	3.22	3.18
Mg	0.16	0.16	0.02	0.02	0.01	0.01	0.17	0.01	0.16	0.02	0.07	0.07
Ca	2.20	2.28	1.77	1.79	1.98	2.34	0.70	2.34	2.20	1.64	1.13	1.11
NA	0.00	0.00	0.03	0.01	0.00	0.00	0.00	0.00	0.00	0.00	0.01	0.00
K	0.00	0.00	0.00	0.00	0.00	0.00	0.00	0.00	0.00	0.00	0.00	0.00

Mole percent end members

Spessar	37.42	36.75	56.58	57.73	52.89	47.30	53.88	47.30	37.42	52.81	50.27	49.52
Grossul	33.74	34.34	23.29	24.24	26.64	30.77	11.09	30.77	33.74	24.07	17.59	17.28
Almand	26.38	26.51	19.87	17.82	20.37	21.84	32.29	21.84	26.38	22.87	31.04	32.05
Pyrope	2.45	2.41	0.26	0.22	0.09	0.09	2.74	0.09	2.45	0.25	1.11	1.15

OLIVINE

S.No	BP127		BL1	BL1	BP127	BL31
	Rim	Core	GR1	GR1	GR1	GR1
SiO ₂	36.96	36.06	35.70	31.85	32.03	31.88
TiO	0.00	0.00	0.00	0.01	0.03	0.06
Al ₂ O ₃	0.00	0.00	0.00	0.00	0.03	0.00
Cr ₂ O ₃	0.00	0.00	0.00	0.00	0.00	0.00
FeO	19.29	19.16	22.05	5.03	4.97	6.54
MnO	12.92	13.22	10.62	12.28	13.32	16.41
MgO	31.24	31.43	31.02	44.55	43.84	40.42
CaO	0.05	0.02	0.00	0.06	0.12	0.09
TOTA	100.47	99.93	99.41	93.82	94.34	95.42

Numbers of ions on the basis of 4 (O)

Si	1.00	0.99	0.99	1.32	1.32	1.33
Al	0.00	0.00	0.00	0.00	0.00	0.00
Ti	0.00	0.00	0.00	0.00	0.00	0.00
Cr	0.00	0.00	0.00	0.00	0.00	0.00
Fe	0.43	0.43	0.51	0.17	0.17	0.22
Mn	0.29	0.31	0.25	0.43	0.47	0.58
Mg	1.26	1.29	1.27	2.74	2.70	2.52
Ca	0.00	0.00	0.00	0.00	0.00	0.00

Mole percent end members

Fo	63.42	63.59	62.83	82.04	80.84	75.90
Fa	21.81	21.25	25.00	5.09	5.09	6.63
Te	14.77	15.16	12.17	12.87	14.07	17.47
Mg/Mg	0.74	0.75	0.72	0.94	0.94	0.92

SKARNIZATION OF MASSIVE SULFIDE ORES & ASSOCIATED ROCKS

Sulfide-bearing clinopyroxenes = BL3,BL4,BP109

Sulfide-rich quartz-feldspathic rocks = BP190,BL43

Sulfide-poor quartz-feldspathic rocks = BP125,BL47

Sulfide-rich calc-silicate rocks = BP149,BL34

Massive sulfide ores = BP232

Magmatite-bearing carbonates = BP127,BL1,BL31

(CaSiO₃), and ferrosillite (Fe,Mg)SiO₃. Two distinct groups of pyroxenoids are distinguished and massive sulfide ores fall in the field of rhodonite while that of sulfide-rich calc-silicate rocks fall near the field of pyroxmangite. The samples containing pyroxenoids are enriched in the bulk Mn contents (>6 wt %) and, therefore, are suggestive of the fact that the whole rock chemistry has controlled the formation of pyroxenoids in the rocks.

Rim to core analyses of both rhodonite and pyroxmangite were carried out in order to check, whether or not any of these two minerals replace each other. These analyses showed homogeneity within single crystal and, therefore, does not suggest any sign of transformation of either pyroxmangite to rhodonite or vice versa during the metasomatic reactions in these rocks. The pyroxenoids-rhodonite transformation for the MnSiO₃ composition has been discussed by various workers (Ito, 1972; Peters et al. 1973; Maresch & Mottana, 1976).

Rhodonite: Rhodonite is colorless, and often shows blue interference color and occurs as subhedral grains of 1-2 mm in size. Both rhodonite and pyroxmangite are optically so similar that they can not be distinguished from other easily. It is not the pure MnSiO₃ composition but has 7-9 weight % of CaO and 7-8.50 weight % of FeO. The rhodonites has a narrow range of composition with 65-67 mole% of MnSiO₃ and 15-18 mole% of (Fe,Mg)SiO₃.

Pyroxmangite: Pyroxmangite is mostly present in the sulfide-rich calc-silicate rocks. In thin section it is colorless and occurs as subhedral grains (1-2 mm in size) having parting and undulose extinction. Chemically the pyroxmangite represents the pure (Mn,Fe)SiO₃ with small amount of Ca and Mg and is more or less homogenous in composition.

GARNET: Garnet in the studied rocks is pale pink to pale brown in thin section. Chemical analyses (Table. 1) represent that it is predominantly spessartine rich with spessartine

content ranging from 36.75 - 64.37 mole%. The almandine content ranges from 14.42-33.23 mole% and grossular from 8.59-34.75 mole %. All garnet analyses have low to insignificant pyrope contents (<4 mole%). No Calderite contents are calculated, as Fe₂O₃ of these garnets could not be determined on the electron microprobe. The enrichment of spessartine molecule with respect to grossular, almandine plus pyrope molecules is also reflected in Fig. 4. The appreciable amount of grossular and almandine molecules and very low pyrope molecule reflect geochemical association of Mn with Fe⁺² rather than Mg in these garnets.

The average composition of garnet, with respect to mole% spessartine (spes), almandine (alm), grossular (Grs) and pyrope (Pyp), in various rock types of the Pazang group is:

1). sulfide-bearing clinopyroxenite = Spes_{54.81}Alm_{22.64}Grs_{28.70}Pyp_{1.33}, 2). sulfide-rich quartzo-feldspathic rock = Spes_{54.81}Alm_{24.91}Grs_{20.68}Pyp_{1.20}; 3). sulfide-poor quartzo-feldspathic rock = Spes_{40.49}Alm_{24.91}Grs_{32.95}Pyp_{1.67}; 4). sulfide-rich calc-silicate rock = Spes_{55.42}Alm_{19.57}Grs_{24.48}Pyp_{0.11}; and 5). massive sulfide ores = Spes_{49.28}alm_{31.16}Grs_{18.33}Pyp_{1.23}.

No significant compositional variation from core to rim has been noticed in a single crystal of garnet. However, considerable variation in Mn, Fe, Ca, and Al is observed in different grains of garnet with the sulfide-bearing clinopyroxenite, sulfide-rich quartzo-feldspathic and sulfide-rich calc-silicate rocks. The chemistry of garnet within the massive sulfide ores is more less similar in both the single crystals and also among different grains. This can be attributed to the equal partitioning of various elements, especially Mn, Fe, Ca, Al, and Si, in the garnet with the massive sulfide ores. Mn contents of garnet were plotted against Fe, Mg and Ca (plot not shown). Mn shows scatter against Mg and Ca while it has negative correlation with Fe. This suggests that Mn may have been substituted for Fe in these garnets.

The studied garnets having spessartine as principal molecule, and their association with the other Mn-rich clinopyroxene and pyroxenoids, are the characteristic features of Mn-rich assemblages in skarn type mineralization (Deer et al., 1982).

OLIVINE: Olivine is usually present as anhedral grains embedded in calcite and serpentine mass within the magnetite-rich carbonate rocks. The outline of original large olivine grain (2-3mm) can be observed by optical continuity of small olivine grains separated by secondary serpentine minerals.

Selected olivine analyses are given in Table 1. Olivine is characterized by major forsterite ($\text{Fo}_{61.54-63.69}$) and subordinate fayalite ($\text{Fa}_{21.25-26.29}$) and tephroite ($\text{Te}_{12.37-15.16}$). The olivine is of Mn-rich variety having MnO in the range of 10.62 to 13.22 wt%. This type of Mn-rich olivine with tephroite 13 to 24 mole % has been described as iron knebelite which contains no nickel and only insignificant amount of chromium (Rozendaal & Stumpf, 1984). This olivine therefore, distinguished from the magmatic olivine which contains an average of 0.2-0.4% nickel (Rozendaal and Stumpf, 1984). Rim to core relationship of olivine suggests no significant variation in composition within single grain. The Mn shows positive correlation with Mg and negative correlation with Fe in this type of olivine (plot not shown). It appears that Mn has been substituted for Fe in the structure of olivine and, therefore, it reduces the fayalite contents of these olivines. The CaO concentration with olivine 0.00 to 0.05 weight %.

SERPENTINE: Serpentine occurs as alteration product of olivine in the magnetite-rich carbonates. Mesh texture after olivine is observed in serpentine mass, at places pseudomorphs after olivine are distinct but mostly the olivine has been completely replaced by serpentine with fine grained magnetite distributed throughout serpentine mass.

Selected serpentine analyses are presented

in Table 1. these analyses show that SiO_2 and MgO in most of the samples are more or less similar. The MnO and FeO show greater variation among individual grains of serpentine. Three of the analyses show relatively high SiO_2 (43-44 wt %) and low MgO (38-40 wt %) with very low FeO (<3 wt %) contents. The serpentine analyses have high ratio of Mg/Mg+Fe (0.91 to 0.97) as compared to the coexisting olivine (0.70 to 0.75). This increase can be attributed to the oxidation of iron (originally bound in olivine) during serpentinization with the formation of magnetite. This inference is supported by the distribution of magnetite in the serpentine mass. It seems that there is also the release of SiO_2 and addition of MgO during serpentinization of olivine in these rocks.

DISCUSSION

The rocks of Pazang group, due to metasomatism, metamorphism and deformation, have a complex history. One of the more contentious aspects of skarn studies involve distinction between metamorphic and metasomatic formation of calc-silicate minerals in the complex metamorphic environment (Einaudi et al. 1981). The composition of the skarn silicate assemblage depends, to considerable degree, on the composition of replaced protolith. The calcic (limestone-replacing) skarn and the magnesian (dolomite-replacing) skarn are the most common varieties. The rocks of the Pazang group are characterized by both magnesian and calcic skarns. The magnesian skarn developed olivine and serpentine in the magnetite-rich carbonate rocks whereas calcic skarn formed clinopyroxenes, pyroxenoids and garnet in the massive sulfide ores and associated metasediments. Most of the skarn minerals in both Pazang and Lahor massive sulfide ores and associated sulfide-rich rocks are enriched in manganese. Mn-rich clinopyroxenes (manganosalite, manganosalite, manganosalite), Mn-rich pyroxenoids (pyroxmangite, rhodonite) and Mn-rich garnet (spessartine) are the most diagnostic minerals whereas, olivine, serpentine

and phlogopite are locally enriched in manganese. A Mn-rich Titanium phase (manganian pyrophanite) was also found in two samples.

The protolith for the sulfide-rich calc-silicate rocks and the sulfide-bearing clinopyroxenites was probably impure limestone with intercalations of number (naturally occurring earth containing oxides of manganese and iron), cherts and clays in which the calcic-skarn has yielded the calc-silicate phases (e.g., clinopyroxene, pyroxenoids and garnet) by reaction of manganese, iron, silica, aluminum and other components (contributed by umbers, cherts and clays) with limestone during the reaction skarn. The pyroxenoids always formed after clinopyroxene in these rocks. This may be due to an enrichment of Mn more likely due to the increasing depletion of Mg and Fe accumulated in the early formed clinopyroxene (i.e., manganian salite and manganian ferrosalite).

The mineralogy of magnetite-rich carbonates, especially endiopside, olivine, serpentine and phlogopite, suggests that the protolith was Mg-rich carbonates/dolomite having cherty nodules and umbers. This type of mineralogy can be termed as magnesian skarn (Einaudi and Burt, 1982) which may have formed due to the reaction of silica, manganese and iron (leached out from cherts and umber) with dolomites. The development of olivine in the magnetite-rich carbonate of Pazang group is unlikely because of lack of proper chemical composition required for its formation. However, the present of chert and umber within the protolith of dolomite composition can better explain the development of olivine in these rocks. The reactions involved during skarnization may have been facilitated generally by regional metamorphism and to some extent by intrusion of pegmatites within the rocks of the Pazang group.

The replacement of dolomite and

carbonate and the growth of prismatic silicates and remobilization of ore phase have developed various zones. No significant compositional gradient seems to occur in a single zone (except in banded cal-silicate rocks), however, various zones are separated by sharp boundaries from each other. The zones which are nearer to the massive sulfide ores are rich in calc-silicate and sulfide minerals as compared to those away from the massive sulfide ores. The occurrence of rhodonite and pyroxmangite is restricted to the sulfide ores, clinopyroxenites and calc-silicate rocks. This suggests that the protolith for the massive sulfide ores was enriched in manganese, which is true in the case of exhalative sediment-hosted base metal mineralization (Oen and DeMaesschalck, 1986).

Well developed stratification of the massive ores and the host skarn of the Pazang group in Besham area can be distinguished as "stratiform skarn" which is considered to be a common characteristic of many stratiform submarine exhalites. This type of skarn may have formed by the preservation of compositional layering often on fine scale even in high grade metamorphic rocks (Ashley and Plimer, 1989). Typical examples of this type of skarn have been demonstrated at a number of metamorphosed stratiform submarine exhalites constituting large base metal ore bodies e.g. Broken Hill area, N. S. W (Stanton, 1976; Barnes, 1983), Queensland (Stanton, 1982; Vaughan and Stanton, 1986), Alaska (Newberry et al. 1986).

ACKNOWLEDGEMENTS

This study was carried out as part of Ph.D dissertation under the USAID scholarship which is highly acknowledged. Thanks are due to John Shervais for valuable discussion and help during electron microprobe analyses at the University of South Carolina, Columbia (USA).

REFERENCES

- ASHLEY, P.M. & PLIMER, I.R.** (1989) "Stratiform skarns" A re-evaluation of three eastern Australian deposit Mineral. Deposita. 24, pp. 289-298.
- ASHRAF, M., CHAUDRY, M. N. & HUSSAIN, S. S.** (1980) General geology and economic significance of the Lahore granite and rocks of the southern opiolite belt in the Allai-Kohistan area Geol. Bu... Univ. Peshawar. '3, pp. 207-213.
- BAIG, M. S. & LAWRENCE, R. D.** (1987) Precambrian to early paleozoic orogenesis in the Himalaya Kashmir Jour Geol. 5, pp. 1-2.
- BAIG M. S. & LAWRENCE, R. D. & SNEE, L. W.** (1988) Evidence for late precambrian to early Cambrian orogeny in northwest Himalaya, Pakistan. Geol. Mag. 125, pp. 83-86.
- BAIG M. S., SNEE L. W., La FORTUNE, R. J. & LAWRENE, R. D.,** (1989) Timing of Pre-Himalayan Orogenic Events in the Northwest Himalaya: $^{40}\text{Ar}/^{39}\text{Ar}$ constraints. Kashmir Jour. Geol. 6 & 7, pp. 29-40.
- BARNES, R. G.** (1983) Stratiform tungsten mineralization in the Broken Hill block, N.S.W: Jour. Geol. Soc. Australia. 30, pp. 225-339.
- BUTT, K. A.** (1983) Petrology and geochemical evolution of Lahor pegmatite complex, northern Pakistan, and genesis of associated Pb-Zn-Mo- and U mineralization. In: Shams. F. A(ed.) GRANTS OF HIMALAYAS KARAKORAM AND HINDU KUSH. Institute of Geology, University of Punjab, Lahore, Pakistan, pp. 309-323.
- DEER, W. A., HOWIE, R. A. & ZUSSMAN, J.** (1982) Rock forming minerals, 2A Single-chain silicates (second ed). Longman, London.
- EINAUDI, M. T., MEINERT, L. D. & NEWBERRY, R. J.** (1981) Skarn deposits. Econ. Geol. 75th ANNIV. vol. pp. 317-391.
- EINAUDI, M. T. & BURT, D. M.** (1982) Introduction-terminology classification, and composition of skarn deposits, Econ. Geol. 77, pp. 745-754.
- FLETCHER, C. J. N., LEAKE, R. C. & HASLAM, H. W.** (1986) Tectonic setting, mineralogy, and chemistry of a metamorphosed stratiform base metal deposit within the Himalayas of Pakistan: Jour. Geol. Soc. London. 143, pp. 521-536.
- ITO, J.** (1972) Synthesis and crystal chemistry of Li-hydroxenoids, Mineral (Tokyo), 7, pp. 45-65.
- La FORTUNE, J. R., SNEE, L. W. & BAIG, M. S.** (1992) Geology and geochemistry of Indian plate rocks south of the Indus suture zone, Besham area. Kashmir. Jour. Geol. 10, pp. 27-52.
- MARESCH, W. V. & MOTTANA, A.** (1976) The pyroxmangite-rhodonite transformation for the MnSiO_3 composition. Contr. Mineral. Petrol. 55, pp. 69-79.

- NEWBERRY, R. J., DILLON, J. T. & ADAMS, D. D.** (1986) Regionally metamorphosed calcisilicate-hosted deposits of the Brooks range, northern Alaska: *Econ. Geol.* 81, pp. 1728-1752.
- OEN, I. S. & De MAESSCHALCK, A. A.** (1986) Mid-proterozoic exhalative-sedimentary Mn Skarns containing possible microbial fossils, Grythyttan, Bergslagen, Sweden, *Econ. Geol.* 81, pp. 1533-1543.
- PETERS, T. J., SCHWANDER, H. & TROMMSDORFF, V.** (1973) Assemblages among tephroite, pyromangite, rhodochrosite, quartz: experimental data occurrences in the Retic Alps. *Contr. Mineral. Petrol.* 42, pp. 325-332.
- ROZENDAAL, A. & STUMPFL, E. F.** (1984) Mineral chemistry and genesis of Gamsberg zinc deposit, south Africa. *Trans. Inst. Min. Metall. Sect. B., Appl. Earth Sci.* 94: Ba61-175.
- SHAH, M. T.** (1991) Geochemistry, Mineralogy, and petrology of the sulfide mineralization and associated rocks in the area around Besham and Dir, northern Pakistan. Unpubl. Ph.D thesis. University of south Carolina. Columbia (USA).
- _____ (1992) Tourmaline as an evidence of exhalative origin for Besham base metal deposits in northern Pakistan. *Geol. Bull. Univ. Peshawar.* 25, pp. 123-126.
- SHAH, M. T., THORPE, R. I. & SIDDIQUE, S. A.** (1992) Lead isotope signature of the Proterozoic sediment-hosted base metal deposits at the margin of the Indian plate in Besham area, northern Pakistan. *Geol. Bull. Univ. Peshawar.* 25, pp. 59-65.
- STANTON, R. L.** (1976) Petrochemical studies of the ore environment in Broken Hill, New South Wales: I-constitution of "banded iron formation"; Transactions of Institute of Mineral and Metallurgy Section, B., Applied Earth Science. 91. pp B47-46.
- _____ (1982) Metamorphism of stratiform sulfide orebody at Mount Misery, Einasleigh, Queensland, Australia: I-observations: Transactions of Institute of Mineral and Metallurgy Section B., Applied Earth Sciences. 91. pp. B47-71.
- TILLEY, C. E.** (1946) Bustamite from Treburland manganese mine, Cornwall, and its paragenesis. *Mineral Mag.* 27, pp. 236-244.
- TRELOAR, P. J., COWARD, M. P., WILLAMAS, M. P. & ASIF, KHAN, M. A.** (1989) Basement-cover imbrication south of the Main Mantle thrust, north Pakistan. *Geol. Soc. America, Special paper.* 232, pp. 137-152.
- VAUGHAN, J. P. & STANTON, R. L.** (1986) Sedimentary and metamorphic factors in the development of the pegmatite stratiform Pb-Zn deposit, Queensland, Australia. Transactions of Institute of Mineral and Metallurgy Section, B., Applied Earth Sciences. 95, pp. B94-121.
- ZHARIKO, V. A., & PODLESSKY K. V.,** (1955) On the behavior of pyroxene as a mineral of variable composition in infiltration skarn zones. *Dokl. Akad. Nauk S.S.S.R.* 105, pp. 1096-1099.

Manuscript received on 30.5.1994.

Accepted for publication on 31.1.1995.

PETROLOGY OF THE LAVA FLOW OF KOH-I-SULTAN CHAGAI DISTRICT, BALOCHISTAN PAKISTAN

MASOOD IQBAL

Geological Survey of Pakistan, P.O.Box 15, Quetta, Pakistan.

ABDUL HAQUE

Centre of Excellence in Mineralogy, University of Balochistan,
P.O. Box 43, Quetta, Pakistan.

KARAM KHAN

Geological Survey of Pakistan, P.O. Box 15, Quetta, Pakistan.

ABSTRACT: The rocks of Koh-i-Sultan constitute lava flow, subaerially accumulated pyroclasts, plugs, tuffs and agglomerates. Andesitic lava flow, andesitic and dacitic plugs as well as pyroclastic ejecta are the main constituents of the area wherein volcanic component has been later on, decomposed by solfataric and fumarolic activities. Moreover, minerals like sulphur, gypsum, alum and agate have also been found.

INTRODUCTION

Koh-i-Sultan (nearly 640sq. km. area) is situated about 37 km. in the north of Nokkundi Railway Station and is bounded between longitudes 62°45' and 63°0'E and latitudes 29°0' and 29°15'N. The area is easily accessible from Nokkundi.

A geological map of Koh-i-Sultan (toposheet No.30-K/16) has been carried out over a scale 1:50,000 and about 60 samples of the exposed rocks have been collected for the purpose of petrographic study.

The geological sketch of Koh-i-Sultan volcano had already been prepared by Vredenburg (1901). All other works carried out, were for the purpose to explore and evaluate sulphur deposits of Koh-i-Sultan (Gee 1964;

Ahmed, 1951; H.S.C., 1960; Muslim, 1971).

Koh-i-Sultan volcanic group consists of three centres viz: Mian Koh; Gamichah and Miri crater (the main crater) from which andesitic lava and pyroclastic debris were ejected, forming coalesced cones. A part from these centres, small satellite cones and plugs like Damodin, Chota Dilal, Mit Koh and Koh-i-Malik Shah represent also Koh-i-Sultan volcanic group.

Koh-i-Sultan volcanic group unconfirmably overlies the Sinjrani volcanic group, Chagai intrusions and Juzzak Formation of Paleocene age. Absence of folding and tilting in Koh-i-Sultan volcanic rocks and their well preserved forms indicate the younger age of the rocks. According to H.S.C. (1960), they are unlikely to be older than Pleistocene.

PETROLOGY

The oldest geological phase of Koh-i-Sultan volcanism is represented by basal agglomerates associated with lava flow. These agglomerates are further subdivided into lower and upper, on the basis of the size of the boulders and bombs. Thus, they are larger (upto one meter diameter) in the lower part and smaller in the upper ones. Solfataric and fumarolic activities are only observed in the upper agglomerates.

Coarse pyroclastic deposits are younger than the upper agglomerates and contain cinder debris and volcanic bombs mainly of andesitic composition as large as tens of meters in diameter.

TUFF: Reddish brown, greenish grey and maroon tuff mostly crystalline with crystals embedded in a glassy and devitrified matrix. The ground mass is mainly of glass argillic minerals, carbonate, quartz, plagioclase and opaque minerals. Phenocrysts are dominately plagioclase, hornblende, pyroxene and opaque minerals. Plagioclase is altered to sericite and kaolin. Tuff is fractured being occupied by minerals probably formed due to deuteritic action.

LAVA FLOW: Brown-grey andesitic lava flow is altered due to solfataric and fumarolic actions. Imperfect columnar structure, irregular jointing and spheroidal weathering is the characteristic features of these lava flow.

The petrographic study of these andesitic lava flow reveals that 60% of the ground mass is microlitic, and porphyritic. Phenocrysts are lithic plagioclase, hornblende, pyroxene and magnetite. The ground mass is composed of andesine along with minor quartz, hornblende, sericite, clay and opaque minerals. Twining and oscillatory zoning observed in plagioclase which has also corrosion on the margin. Its core is usually anorthite rich which is normally altered to sericite and clay minerals.

The hornblende is mainly oxy importing brownish red pleochroism having margin covered with magnetite and hematite grains. The cores of hornblende crystals have been affected by opaque minerals. Pseudomorphism is very conspicuous in hornblende and pyroxene by magnetite grains. Hornblende has been deeply oxidized giving a reddish brown colour to the andesites.

Magnetite or hematite also occurs as disseminated grains in the groundmass. Chlorite and secondary biotite, carbonate and limonite are found in trace amounts.

Augite and diopside are also observed in some andesitic rocks. The phenocrysts are as much as 40% of the total mass.

ASH FALL: The ash found in north, south and east of the Koh-i-Sultan and are assumed to have been deposited after weathering and decomposition of tuff or andesite washing down the slopes of the volcano. The ash is buff to light grey and mainly andesitic in composition. The ash also contains lapilli and andesitic lava.

REFERENCES

- AHMED, M.I.**, (1951) Volcanoes and sulphur of western Balochistan. Rec. Geol. Surv. Pak. vol. IV. Part-3.
- GEE, B.R.** (1964) Sulphur operations, Koh-i-Sultan, Balochistan. Jour. Sc. & Indus. Res. vol.5, No.1 pp.10-17.
- HUNTING SURVEY CORPORATION (Ltd)** (1960) Reconnaissance Geology of part of West Pakistan. A Canadian International Development Agency Project for Government of Pakistan.
- MUSLIM, M.** (1971) Evaluation of sulphur deposits, Koh-i-Sultan, District Chagai, Balochistan, Pakistan. Rec. Geol. Surv. Pak. vol.1 Part 3.

VREDENBURG, E. (1901) Geological sketch of Balochistan desert and part of eastern Persia. Mem. Geol. Surv. India. vol. XXXI, Part-2.

Manuscript received on 31.1.1994

Accepted for publication on 26.2.1994

A NOTE ON THE CHALCOPYRITE DISEASE IN SPHALERITE IN THE VOLCANIC-HOSTED COPPER MINERALIZATION IN DIR AREA, NORTHERN PAKISTAN.

MOHAMMAD TAHIR SHAH

National Centre of Excellence in Geology, University of Peshawar.

About three meter thick sphalerite-bearing copper-rich zone within the Dir metavolcanic sequence is exposed along a local fault in a stream section near Bikaria village north-west of Dir town. Sphalerite and chalcopyrite are the dominant ore phases with lesser amount of bornite, pyrite and magnetite. Sphalerite is yellowish brown to brown and forms isolated irregular shaped grains occasionally intergrown

scale blebs and rods in sphalerite have been termed as "chalcopyrite disease" by Barton (1978) and Eldridge et al, (1983). Various hypothesis are suggested in recent years for the origin of this disease and are summarized below in order to find out the possible origin for the similar type of texture observed in some of sphalerite grains from Dir area.

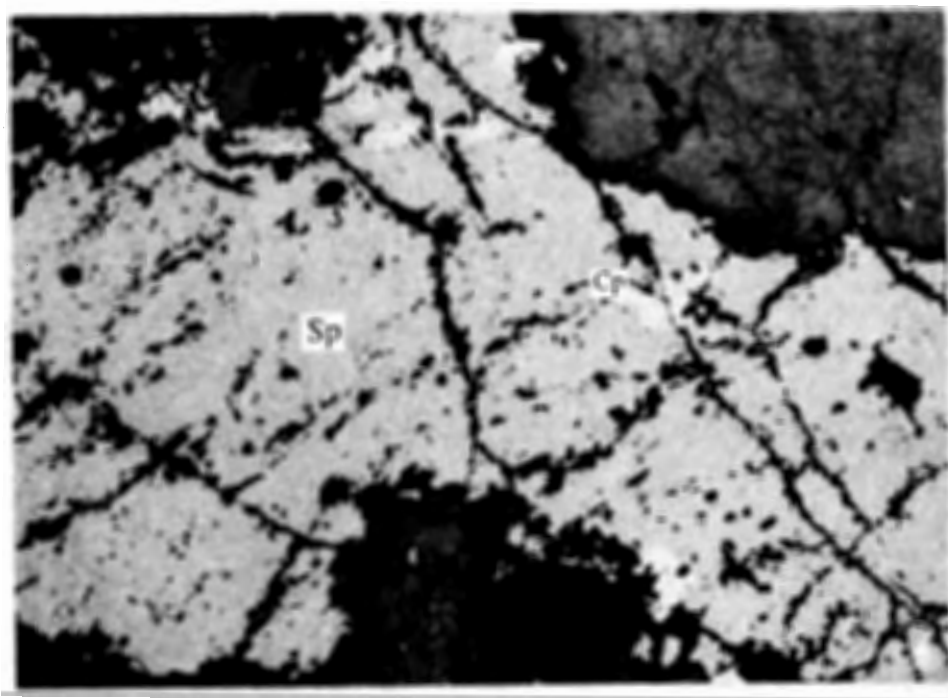


Plate. 1. Reflected-light photomicrography showing irregular grain of sphalerite (Sp). Fine-grained blebs and rods of chalcopyrite (Cp) are oriented within sphalerite causing chalcopyrite disease in sphalerite. (X50).

with chalcopyrite. Sphalerite often forms interconnected amoeboid masses which define laminae of several millimeter in thickness. Tiny ($< 1\mu\text{m}$) disseminated blebs and rods of chalcopyrite are common in sphalerite grains (Plate,1). These submicron to millimeter

It is generally believed that chalcopyrite blebs are the result of exsolution of chalcopyrite from the sphalerite lattice which was described by Ramdohr (1969) as "emulsion texture". Eldridge et al, (1983) have evaluated exsolution, coprecipitation, recrystallization and replacement

for the development of this type of texture while studying the Kuroko ore bodies. Barton (1978) described the chalcopyrite disease in sphalerite from Kuroko, Japan and Creede, Colorado. He suggested that this phenomenon may be the result of "a reaction of copper in solution with FeS in sphalerite and may be associated in time with the replacement of pyrite by chalcopyrite".

The idea of exsolution to the cause of chalcopyrite disease in sphalerite was disfavoured because of lack of enough copper in sphalerite to exsolve significant amount of chalcopyrite during cooling under the temperature condition (50-350°C) especially of Kuroko mineralization (Wiggins and Craig, 1980; Kojima and Sugaki, 1958). The exsolution phenomenon, however, is still favoured by various workers (i.e. Hanus, 1982; El-Bouseily 1985; Sillitoe et al., 1985). Eldridge et al. (1988) have concluded from their experimental work that the chalcopyrite disease in the sphalerite may be the product of interaction of hot copper-bearing fluid and the iron-bearing sphalerite which involve the replacement of FeS in sphalerite by chalcopyrite.

Both the chalcopyrite-bearing and chalcopyrite free grains of sphalerites were analyzed by electron microprobe at the University of South Carolina, Columbia (USA) and the mole% FeS (ranging from 4.12 to 12.21) in these sphalerites was determined. It is found that the chalcopyrite-bearing sphalerites have lower contents of mole% FeS (maximum 4.69%) compare to chalcopyrite-free sphalerite (maximum 12.21%). This suggest that those sphalerites which have the chalcopyrite disease may have formed earlier than chalcopyrite free sphalerites. The early-formed, iron-rich sphalerites, would have reacted with the hot copper-bearing fluid and replaced FeS to form the chalcopyrite inclusions. These sphalerites are, therefore, deficient in FeS contents (Eldridge et al., 1988). The chalcopyrite-free sphalerites either had no interaction with the copper-bearing fluid or they have formed at the late stage of precipitation of mineralizing fluid. The latter is

more likely because these sphalerite grains are in direct contact with or are intergrown with the chalcopyrite which occur as exsolution lamellae within bornite. This kind of texture suggest simultaneous crystallization of this type of chalcopyrite and chalcopyrite-free sphalerite in these rocks.

REFERENCES

- BARTON, P.B., JR.** (1978) Some ore texture involving sphalerite from the Furutobe mine, Akita Prefecture, Japan. *Min. Geol.* 28, pp. 293-300.
- EL-BOUSEILY, A.M., EL-DAHAR, M.A., AND ARSTLN, A.I.** (1958) Ore microscopic and geochemical characteristics of gold-bearing sulfide minerals, El Sid gold mine, Eastern Desert, Egypt. *Mineral. Depos.* 20, pp. 194-200.
- ELDRIDGE, C.S., BARTON, P.B., JR., & OHMOTO, H.** (1983) Mineral textures and their bearing on formation of the Kuroko ore bodies. *Economic Geology. Monograph*, 5, pp. 241-281.
- ELDRIDGE, C.S., BOURCIER, W.L., OHMOTO, H., & BARNES, H.L.** (1988) Hydrothermal Inoculation and Incubation of the Chalcopyrite Disease in Sphalerite; *Econ. Geol.* 83, pp. 978-989.
- HANUS, D.** (1982) The Colquiri tin deposit: A contribution to its genesis, in., Amstutz, G. C., El Gorse, A., Frenzel, G., Kluth, C., Moh, G., Wauschkuhn, A., and Zimmermann, R. A., eds., *Ore genesis the state of the art*: Berlin, Springer-Verlag, pp. 308-318.
- KOJIMA, S., & SUGAKI, A.** (1958) Phase relation in the Cu-Fe-Zn-S system between 500°C and 300°C under hydrothermal condition. *Econ. Geol.* pp. 158-171.

RAMDOHR, P. (1969) The ore minerals and their intergrowths: New York, Pergaman, pp. 1019.

SILLITOE, R. H., GRAUBERGER, G. L., & ELLIOTT, J. E. (1985) A diatreme-hosted deposit at Montana Tunnels, Montana Econ. Geol. 80, pp. 1707-1721.

WIGGINS, L. B., AND CRAIG, J. R. (1980) Reconnaissance of the Cu-Fe-Zn-S system: Sphalerite phase relationships. Econ. Geol. 75, pp. 742-751.

Manuscript received on 30.5.1994

Accepted for publication on 19.6.1994.

ANNUAL REPORT OF THE CENTRE OF EXCELLENCE IN MINERALOGY QUETTA

ACADEMIC STAFF

Date of Joining C.E.M.

*Associate Professor &
Acting Director*

1. **ABDUL HAQUE**
Dr. Troisieme Cycle (Caen, France)
M.Sc.(Balochistan) 21.11.1989

Assistant Professor

2. **JAWED AHMED**
M.Sc.(Karachi),
M.Phil.(CEM, Balochistan) 01.04.1980

*Lecturer-Cum-Research
Associates.*

3. **KHALID MAHMOOD**
Dr.Thesis of the
University (University
of Montpellier II,
France), M.Phil.(CEM,
Balochistan) 05.11.1989

4. **MOHAMMAD AHMED FAROOQI**
Ph.D.(Montana University USA),
M.Sc.(Balochistan). 05.11.1989

5. **MEHRAB KHAN BALOCH**
M.Phil.(CEM,Balochistan) 05.11.1989

GENERAL STAFF

Administrative Officer

1. **SHAHABUDDIN**
M.Sc.(Balochistan) 21.05.1977

Account Officer

2. **MIRZA MANZOOR AHMED**
B.Com.(Karachi)

Senior Technician

3. **KHUSHNOOD AHMED SIDDIQUI**
Dip.Assoc.Engr.(Hyderabad) 01.03.1976

Assistant Librarian

4. **ABDUL GHAFOOR**
M.L.S.(Balochistan) 02.05.1985

Superintendent (Office)

5. **LAL MOHAMMAD DURRANI** 12.05.1973

Photographer

6. **HUSSAINUDDIN** 16.06.1981

Stenotypists

7. **M.GHALIB SHAHEEN** 17.07.1985
8. **SAID RASOOL MAHJOOR** 06.06.1990

Assistants

9. **MOHAMMAD ANWAR** 18.09.1977
10. **JUMA KHAN** 12.06.1985

Storekeeper

11. **MUSA KHAN** 20.08.1977

Laboratory Assistant

12. **SHER HASSAN** 22.08.1977

Senior Clerk

13. **ABDUL MALIK** 28.04.1987

Driver

14. **ALI MOHAMMAD** 17.07.1984
15. **SALEH MOHAMMAD** 18.08.1990

Laboratory Attendant

16. **GHULAM RASOOL** 20.08.1977

Naib Qasid

17. **SIKANDAR KHAN** 30.04.1976
18. **MOHAMMAD RAFIQUE** 12.10.1978
19. **ATTA MOHAMMAD** 25.03.1986

Loader

20. **RAWAT KHAN** 02.07.1977

Chowkidar

21. **ABDUL WADOOD** 26.01.1992

Sweeper

22. **NAZIR MASIH** 01.04.1977

ACADEMIC ACTIVITIES

M.PHIL. STUDENTS

1. Din Mohammad

- Supervisor : Akhtar M. Kassi
(From Geology Deptt. U.O.B).
Dissertation Title : Structural and Sedimentological
studies of the coal-bearing Ghazij
Formation of Sor Range area.

Quetta District. Viva Voce

Examination is already conducted on 16.1.1995.

2. Mian Hassan Ahmed

Supervisor : Jawed Ahmed
Dissertation Title : Petrography and Stratigraphy of Chiltan Formation south of Quetta, Balochistan. In final stages.

3. Masood Iqbal

Supervisor : Abdul Haque
Dissertation Title : The ophiolitic rocks of Sra Salwat, south of Muslim Bagh, Balochistan. In final stages.

4. Qaiser Mahmood

Supervisor : Zulfiqar Ahmed
Dissertation Title : Geology of Wadh-Godh Haji Shakar area, Khuzdar District, Balochistan. Viva Voce Examination is already conducted on 3rd October, 1994.

5. Mohammad Ayub Baloch.

Supervisor : Abdul Haque
Dissertation Title : Petrography of ophiolitic rocks of Goth - Shafi Mohammad near Khuzdar District, Balochistan. In progress.

The University of Balochistan kept pending the registrations of the following five M.Phil. students who were accepted for admission by C.E.M. during 1994. The Centre has recommended their admissions though written and oral examination held on 22nd August, 1994, which were further endorsed by the meeting of the Academic Committee of the Centre held on 25.10.1994. However they cannot begin their classes until the meeting of University's Committee for Advanced Studies & Research approves their registrations.

1. Mr. Tahir Iqbal.
2. Mr. M.Yahya Khan Khwaja Khail.
3. Mohammad hanif.
4. Mr. Khawaja Saleem Mustafa.
5. Mr. Atif Saleem.

Ph.D. STUDENTS

1. Mehrab Khan Baloch.

Supervisor : Abdul Saleem Khan
(from Geology Deptt. U.O.B).
Co-Supervisor : Khalid Mahmood

Thesis Title : Petrological and Structural studies of igneous rocks of Baran Lak area, Bela, Khuzdar District, Balochistan. The candidate also waiting to get his registration through the meeting of Advanced Studies & Research, University of Balochistan, Quetta.

OTHER ACADEMIC ACTIVITIES

Dr. Khalid Mahmood, Lecturer-Cum-Research Associate has completed his Ph.D. programme in France and he has rejoined the Centre in 1994.

Dr. Mohammad Ahmed Farooqui has completed his Ph.D. Degree in States and he has taken his office in C.E.M. in 1994.

Dr. Edwin Gros, Professor and Geologist, Institute of Mineralogy and Petrology, University of Bern, Switzerland conducted joint collaborative field work with C.E.M. staff from 2nd to 28th February, 1995. Prof. E.Gros intends to continue his field work for further two months.

A computer Laboratory is being installed in 1994 by the personal best endeavours of Dr. M.A.Farooqui, Lecturer-cum-Research Associate, C.E.M.

INFORMATION FOR AUTHORS

ACTA MINERALOGICA PAKISTANICA Publishes in English annually the results of original multifaceted scientific research in the field of mineral sciences, covering mineralogy, petrology, crystallography, geochemistry, economic geology, isotope geoscience, petrography, petrogenesis, mineral chemistry and related disciplines. Review articles and short notes are also considered for publication. Priority is given to geoscientific papers with impact on Pakistani region.

In general, the manuscripts be organized in the following order; title; names(s) and institutional address(es) of the author(s); abstract; introduction; methods, techniques, material studied and area description; results; conclusions; acknowledgements; references; tables; figure captions. The abstract should not exceed 300 words. All tables and figures should be referred in the text and numbered according to their sequence in the text. All references to publications are given in the text by author's name and year of publication; and are listed at the end of text alphabetically by author's names and chronological per author.

Authors of the articles submitted for publication in ACTA MINERALOGICA PAKISTANICA should send three complete copies of the manuscript, typed double-spaced on one side of the paper only. Copies of tables should be in final format. As far as possible, tables and figures should be prepared for reduction to the single column size or to the page size (204mm x 278mm) or half page size. Use of mineral symbols by Kretz (The American Mineralogist, 1983, Volume 68, pp. 277-279) is recommended for superscripts, subscripts, equations, figures and tables. The Concise Oxford Dictionary is adopted for spelling. Underlining of text by a single line will mean printing in italics; that by a double line will mean printing in bold letters. The use of metric system and S.I. units is recommended. Bar scales should be used in all figures rather than numerical scales.

Only articles not previously published and not about to be published, wholly or in part, in either Pakistani or foreign journals, are considered for publication. Submission of an article is understood to imply that the article is original and unpublished and is not being considered for publication elsewhere. Publication is subject to the discretion of the referee(s)/Editor. All manuscripts are refereed before being accepted. Accepted papers become copyright of the Centre of Excellence in Mineralogy, Quetta. Authors alone are responsible for the accuracy of the contents and views expressed by referee(s) in their respective papers. Twenty five off-prints of each published paper will be sent to authors free of charge.

Manuscripts should be sent to: Acta Mineralogica Pakistanica C/o Centre of Excellence in Mineralogy, University of Balochistan, G.P.O. Box 43, Quetta, Pakistan. Phone Nos. are (081) 441974, 440500 & 447061.

CONTENTS

I. Strom generated turbidites of the lower Ludlow group (Late Silurian), Llangollen area, north Wales, United Kingdom.
ABDUL SALAM KHAN 3

II. Proposed lithostratigraphic subdivision of Chilton limestone, Quetta District, Balochistan, Pakistan.
JAWED AHMAD, ABDUL HAQUE & MIAN HASSAN AHMAD 11

III. Major metallic minerals of Sindh, Pakistan.
SYED AFZAL AHMAD 15

IV. Petrology of different dykes of Sra-Salwat area, Muslim Bagh, District Qila-saifullah, Balochistan, Pakistan.
ABDUL HAQUE & MASOOD AQBAL 20

V. Earthquakes and risks management in Pakistan.
MUBARAK ALI & ZULFIQAR AHMAD 24

VI. Preparation of oriented clay mineral samples for X-ray diffraction analyses.
JAWED AHMAD & ABDUL HAQUE 35

VII. Petrographic comments on Khewra trap, the Salt Range, Pakistan.
S. M. SHUAIB, SHAMIM A. SHEIKH & SHAHID NASEEM 38

VIII. Dolomite reservoirs within Chilton range, south of Quetta District, Balochistan, Pakistan.
ABDUL HAQUE, JAWED AHMAD & MIAN HASSAN AHMAD 47

IX. Measurement of spectral induced polarization on rock samples containing sulphide minerals.
S. W. H. NAQVI 49

X. Clay minerals of Ghazig Formation from a section taken in Deghari valley, Mastung District, Balochistan, Pakistan.
JAWED AHMAD & ABDUL HAQUE 64

XI. Skarization of the massive sulfide ores and associated rocks of the Pazang group in Besham area at the northern margin of Indo-Pakistan plate.
MUHAMMAD TAHIR SHAN 68

XII. Petrology of the lava flow of Koh-i-Sultan, Chagai District, Balochistan, Pakistan.
MASOOD IQBAL, ABDUL HAQUE & KARAM KHAN 79

XIII. A note on the chalcopyrite disease in sphalerite in the volcanic-hosted copper mineralization in Dir area, northern Pakistan.
MOHAMMAD TAHIR SHAH 82